MARTIN MARIETTA ENERGY SYSYEMS LIBRARIES
3 4456 0324845 7

ORNL/CSD/TM-272

ornl

OAK RIDGE NATIONAL LABORATORY

MARTIN MARIETTA

Benchmark Shielding Calculations for the NEACRP Working Group on Shielding Assessment of Transportation Packages

B. L. Broadhead
M. C. Brady
C. V. Parks

OAK RIDGE NATIONAL LABORATORY
CENTRAL RESEARCH LIBRARY
CIRCULATION SECTION
4500N ROOM 175
LIBRARY LOAN COPY
DO NOT TRANSFER TO ANOTHER PERSON
If you wish someone else to see this report, send in name with report and the library will arrange a loan.
UCN-7969 (3 9-77)

OPERATED BY
MARTIN MARIETTA ENERGY SYSTEMS, INC.
FOR THE UNITED STATES
DEPARTMENT OF ENERGY

This report has been reproduced directly from the best available copy.

Available to DOE and DOE contractors from the Office of Scientific and Technical Information, P.O. Box 62, Oak Ridge, TN 37831; prices available from (615) 576-8401, FTS 626-8401.

Available to the public from the National Technical Information Service, U.S. Department of Commerce, 5285 Port Royal Rd., Springfield, VA 22161.

This report was prepared as an account of work sponsored by an agency of the United States Government. Neither the United States Government nor any agency thereof, nor any of their employees, makes any warranty, express or implied, or assumes any legal liability or responsibility for the accuracy, completeness, or usefulness of any information, apparatus, product, or process disclosed, or represents that its use would not infringe privately owned rights. Reference herein to any specific commercial product, process, or service by trade name, trademark, manufacturer, or otherwise, does not necessarily constitute or imply its endorsement, recommendation, or favoring by the United States Government or any agency thereof. The views and opinions of authors expressed herein do not necessarily state or reflect those of the United States Government or any agency thereof.

ORNL/CSD/TM 272

BENCHMARK SHIELDING CALCULATIONS FOR THE NEACRP WORKING GROUP ON SHIELDING ASSESSMENT OF TRANSPORTATION PACKAGES

B L Broadhead, M C Brady, and C V Parks
Computing and Telecommunications Division
at Oak Ridge National Laboratory
P O Box 2008
Oak Ridge, TN 37831 6370

DATE PUBLISHED — November 1990

NOTICE	This document contains information of a preliminary nature It is subject to revision or correction and therefore does not represent a final report

Prepared for the
U S Department of Energy
Transportation Management Division
Washington, DC 20585

MARTIN MARIETTA ENERGY SYSTEMS, INC
managing the
Oak Ridge National Laboratory Oak Ridge Y 12 Plant
Oak Ridge Gaseous Diffusion Plant Paducah Gaseous Diffusion Plant
for the
U S DEPARTMENT OF ENERGY
under contract DE AC05 84OR21400

3 4456 0324845 7

CONTENTS

LIST OF FIGURES v
LIST OF TABLES vii
ACKNOWLEDGMENTS ix
ABSTRACT xi
1 INTRODUCTION 1
2 PROBLEM SET DESCRIPTION 1
2 1 PROBLEM SETS 1–4 1
2 2 PROBLEM SETS 5 AND 6 2
3 CROSS SECTION LIBRARY INTERCOMPARISON/SELECTION 2
3 1 COMPUTATIONAL TOOLS 3
3 2 CROSS SECTION LIBRARIES 3
3 3 RESULTS AND DISCUSSION 5
3 3 1 Neutron Results 5
3 3 2 Gamma Doses 8
3 3 3 Library Selection 10
4 PROBLEMS 1–4 ANALYSIS 10
4 1 SOLUTION METHODOLOGY AND ASSUMPTIONS 10
4 2 RESULTS AND DISCUSSIONS 17
4 2 1 Problem Set 1 Results 17
4 2 2 Problem Set 2 Results 22
4 2 3 Problem Set 3 Results 22
4 2 4 Problem Set 4 Results 26
5 PROBLEMS 5 AND 6 ANALYSIS 26
5 1 SOLUTION TECHNIQUES 26
5 1 1 SAS2H/ORIGEN S 31
5 1 2 ORIGEN2 31
5 2 RESULTS 33
5 2 1 Neutron Sources 33
5 2 2 Photon Sources 41
5 2 3 Dose Calculations (Problem 5) 41
5 3 DISCUSSION 50
6 SUMMARY AND CONCLUSIONS 53
7 REFERENCES 56
APPENDIX 61

LIST OF FIGURES

Fig		Page
1	Neutron dose energy distribution using library 1b	7
2	Primary gamma dose energy distribution using library 1b	7
3	Geometry of problem 1 cast iron cask specified by OECD Working Group	13
4	DORT R Θ geometry model	15
5	Problem 3b approximate DORT model	16
6	Azimuthal neutron dose distribution for problem 2a	24
7	Azimuthal secondary gamma dose distribution for problem 2a	24
8	Azimuthal FP gamma dose distribution for problem 2a	24
9	Neutron equivalent dose rate axial distribution on the cask outer surface (problem 3b)	27
10	Neutron induced gamma equivalent dose rate axial distribution on the cask outer surface (problem 3b)	28
11	Fission product gamma equivalent dose rate distribution on the cask outer surface (problem 3b)	29
12	Basic flow invoked by SAS2H	32
13	Problem 5 Axially distributed neutron source as a percentage of total	37
14	Problem 6 (MOX) Axially distributed neutron source as a percentage of total	40
15	Problem 5 Axially distributed photon source as a percentage of total	46
16	Problem 6 (MOX) Axially distributed photon source as a percentage of total	49
A 1	Characteristics of additional neutron shield Case a polyethylene within the cask wall	72
A 2	Characteristics of additional neutron shield Case b epoxi cast resin at outer surface, set within the outer diameter of 156 cm	74
A 3	Characteristics of cooling fins Case a neutron shield within the cask wall, the midplane of the first fin is located on the level of the cask cavity top	76
A 4	Characteristics of cooling fins Case b neutron shield in between the fins, set within the outer diameter of 156 cm	78
A 5	Cross section view of assembly and single rod arrangement of fuel rods and guide tubes	80
A 6	Construction of basket	81
A 7	Cross section view of prototypic cask	94

LIST OF TABLES

Table		Page
1	Multigroup cross section libraries used for shielding analysis	4
2	Radial surface doses (μSv/h) from a cast iron cask model using a 1 D discrete ordinates code and various multigroup cross section libraries	6
3	Total neutron cross sections for several materials in the 27n 18g library selected for use	11
4	Total photon cross sections for several materials in the 27n 18g library selected for use	12
5	Neutron and gamma ray groupwise sources	15
6	Summary results of model problem 1	18
7	Summary results of model problem 2	23
8	Summary results of model problem 3b	25
9	Summary results of model problem 4	30
10	Problem 5 (UO_2) Results for five fuel assemblies, comparison of neutron source strength at average burnup	34
11	Problem 5 (UO_2) Contribution to neutron source strength from important nuclides for five fuel assemblies (SAS2H)	34
12	Problem 5 (UO_2) Contribution to neutron source strength from important nuclides for five fuel assemblies (ORIGEN2)	35
13	Problem 5 (UO_2) Results for five fuel assemblies (SAS2H)	35
14	Problem 5 (UO_2) Neutron source spectra for five fuel assemblies (SAS2H)	36
15	Problem 6 Comparison of neutron source strength at average burnup to axially dependent burnup	36
16	Problem 6 (MOX) Contribution to neutron source strength from important nuclides for five fuel assemblies	38
17	Problem 6 (MOX) Results for five fuel assemblies	38
18	Problem 6 (MOX) Neutron source spectra for five fuel assemblies	39
19	Problem 5 (UO_2) Results for five fuel assemblies, comparison of photon source strength at average burnup	42
20	Problem 5 (UO_2) Contribution to gamma source strength from important nuclides for five fuel assemblies (SAS2H)	42
21	Problem 5 (UO_2) Contribution to gamma source strength from important nuclides for five fuel assemblies (ORIGEN2 cases)	43
22	Problem 5 (UO_2) Results for five fuel assemblies (SAS2H)	43
23	Problem 5 (UO_2) Photon source spectra for five fuel assemblies (SAS2H)	44
24	Problem 5 (UO_2) Photon source spectra for five fuel assemblies (ORIGEN2 cases)	45
25	Problem 6 (MOX) Comparison of photon source strength at average burnup	47

26 Problem 6 (MOX) Contribution to gamma source strength from important nuclides for five fuel assemblies 47
27 Problem 6 (MOX) Results for five fuel assemblies 48
28 Problem 6 (MOX) Photon source spectra for five fuel assemblies 48
29 Problem 5 (UO_2) Axial midplane dose rate results using cask model 1a 51
30 Comparisons with and without bremsstrahlung, (photons/s/eV) at 5 year cooling time 51
31 Photon dose rates illustrating effect of bremsstrahlung radiation (μSv/h) 52
32 Problem 5 (UO_2) Comparison of photon source strength for one assembly 52
33 Problem 6 (MOX) Comparison of photon source strength for one assembly 52
A 1 Nomenclature 64
A 2 Basic quantities to be used for the calculation 65
A 3 Characteristics of model problem 1, case a 68
A 4 Characteristics of model problem 1, case b 69
A 5 Characteristics of model problem 1, case c 70
A 6 Characteristics of model problem 2, case a 71
A 7 Characteristics of model problem 2, case b 73
A 8 Characteristics of model problem 3, case a 75
A 9 Characteristics of model problem 3, case b 77
A 10 Characteristics of model problem 4, case a 82
A 11 Characteristics of model problem 4, case b 83
A 12 Characteristics of model problem 5 84
A 13 Characteristics of model problem 6 85
A 14 Dimensions of cask body 89
A 15 Characteristics of basket 89
A 16 Characteristics of model fuel assembly 90
A 17 Composition of fresh fuel of model assembly 91
A 18 Composition of materials used 92
A 19 Energy spectrum of neutron and gamma radiation source 93

ACKNOWLEDGMENTS

The authors wish to acknowledge R E Glass of Sandia National Laboratories for his assistance in obtaining the funding for this work Appreciation is expressed to J S Tang, S N Cramer, and B L Kirk for their calculations in support of this work The review of this document by J S Tang and D T Ingersoll is also acknowledged

Participation in the international working group has been supported by the Transportation Management Division of the U S Department of Energy (DOE) Some of the support calculations were performed as part of an assessment evaluation task funded by the DOE Office of Civilian Radioactive Waste Management and a code validation task funded by the DOE Cask Certification Branch

ABSTRACT

In 1985, the Nuclear Energy Agency–Committee on Reactor Physics (NEACRP) es tablished a working group on shielding assessment of transportation packages Following the initial distribution of a set of six problems, discussions were held at the Organization for Economic Cooperation and Development (OECD) Headquarters in Paris, France, in June/July 1986, May 1987, May 1988, and February/March 1990 The U S contribution to the working group is documented in this report

The results from this effort permit the evaluation of a number of approximations and effects that must be considered in a typical shielding analysis of a transportation cask Among the effects reported here are the performance of multiple cross section sets, the com parison of several source generation codes, and multidimensional versus one dimensional (1 D) analyses

1 INTRODUCTION

Under the auspices of the Nuclear Energy Agency—Committee on Reactor Physics (NEACRP), a working group on shielding assessment of transportation packages was formed in 1985 Initially a set of six problems was drawn up and distributed to the work ing group participants Following preliminary computations by the various participating countries, the initial working group meeting was held in June/July 1986 at the Headquar ters for the Organization for Economic Cooperation and Development (OECD) located in Paris, France Subsequent meetings were held in May 1987 and May 1988 to distribute and discuss solutions to the initial set of six problems At the 1988 meeting, an experi mental benchmark was approved for analysis by each of the participants The next phase of the international effort will be the inclusion of direct calculational and experimental intercomparisons

The U S contributions to the working group prior to 1990 were provided by the au thors of this report and are documented herein Section 2 of this report briefly describes the set of six problems that comprised the initial work effort The sensitivity of selected problem solutions to various input cross section sets and the subsequent cross section li brary selection are discussed in Sect 3 Details of the methods used and a discussion of the results for problems 1–4 and 5–6 are given in Sects 4 and 5, respectively Section 6 summarizes the findings of this study

2 PROBLEM SET DESCRIPTION

Specifications for the original six problem set were described in the document NEACRP L 290 issued to the program participants Several amendments have been issued since the original release This section briefly describes the six problems For completeness, a condensed version of NEACRP L 290 is included as the Appendix

2 1 PROBLEM SETS 1–4

The concept behind the definition of problems 1–4 is to begin with a simple cask geometry and add additional details for each subsequent problem Problem 1 consists of three subcases case 1a is a 38 cm thick cylindrical shaped cast iron cask body with a dry homogeneous fuel region of 40 cm radius, case 1b adds a 6 cm thick polyethylene neutron shield recessed within the outer radius of the cast iron shield body, and case 1c is identical to case 1a except the cavity is water filled

Problem 2 consists of two subcases case 2a adds to the case 1a shield a total of 60 polyethylene cylindrical rods placed as shown in Fig A 1 in the Appendix, and case 2b places 35 5 cm thick by 8 cm high epoxy cast resin rings axially within the outer radius of the shield body (see Fig A 2) In both problem 2 subcases the cavity region is dry

Problem 3 is identical to problem 2 with the addition of 35 radial cooling fins placed axially along the outer cask body (see Fig A 3) Case 3a was not analyzed because the difficulty in modeling both cylindrical rods within the shield and radial cooling fins external to the shield was beyond the scope of this project The placement of the cooling fins/neutron absorber rings for case 3b is shown in Fig A 4 in the Appendix

Problems 1–3 have a common approximation that the fuel, structural materials, and water/void are homogeneously mixed and smeared over the entire cavity region Problem 4 examines the effect of cavity heterogeneity by including the basket and explicit assembly model in the calculations The two subcases for problem 4 consist of a dry (4a) and a wet

(4b) cask cavity The shield for both subcases is the same as case 1a (this is a change from the original specification and was issued as an addendum to NEACRP L 290 and is not included in the Appendix to this document)

Radial dose results at a point along the cask axial midplane at the cask surface and 1, 2, and 10 m away were requested Doses averaged over the cavity height at the same locations radially were also desired for comparison In the axial direction, point and surface averaged doses were required along the cavity centerline at the cask surface and 1, 2, and 10 m away for both the top and bottom ends of the cask

In all problems described above, the neutron and fission product gamma sources were specified in the problem definition The total neutron source rate was $1\ 0 \times 10^9$ n/s, the total fission product gamma source rate was $5\ 0 \times 10^{16}$ g/s The formula to compute the individual spectra is given in Table A 19 in the Appendix (see Sect 4 1 for a discussion of the spectra)

2 2 PROBLEM SETS 5 AND 6

The basic specifications for problems 5 and 6 are identical with the exception that the fuel in problem 5 was UO_2 and a mixed oxide (MOX) fuel was used for problem 6 In NEACRP L 290 the problem was described as a cylindrical iron cask with additional neutron shield and no predefined source The Appendix provides information concerning operating histories and fuel composition (Table A 17) and characteristics of the model fuel assembly (Table A 16) to permit the calculation of the radiation (neutron and photon) sources in the spent fuel at a cooling time of 2 years An axial burnup distribution was also given in Table A 17 of NEACRP L 290 to be used in determining the effect of axially dependent burnup versus an average burnup (40 GWd/MTU) for the fuel assembly After the 1987 meeting, it was decided that the earlier problems (1–4) had provided adequate information concerning the shielding calculations and that problems 5 and 6 should em phasize the calculation of sources from the spent fuel assembly At that time the simplified cask model of problem 1 was chosen for those who wished to perform dose calculations using their predicted sources The first results for problems 5 and 6 were presented at the May 1988 meeting Fairly good agreement was observed for the neutron sources, however, differences as large as factors of 2 7 were noted for the photon sources These large differ ences and the propensity of data for problems 1–4 led the working group to concentrate primarily on the calculation of radiation sources

3 CROSS-SECTION LIBRARY INTERCOMPARISON/SELECTION

Due to the benchmark nature of the problems to be solved and the wide range of cross section libraries available for use, a detailed investigation[1] was performed to compare the various multigroup libraries and then select the one most appropriate The original thrust of the study was to provide a relative comparison of the dose results obtained using several different broad group cross section libraries The libraries were selected and/or generated to investigate the importance of the available resonance self shielding, the energy collapsing spectrum, and the parent fine group data (e g , ENDF/B IV versus ENDF/B V data) However, in an effort to better understand the initial results, analyses using the parent fine group libraries were also performed along with calculations using point cross section data

The selection criteria for the broad group cross section library to be used in the remainder of the analysis focused on the library that gave both good agreement with the point data and good agreement with the parent fine group results

3 1 COMPUTATIONAL TOOLS

All of the analyses in the intercomparison study were performed using the SCALE modular code system [2] BONAMI S (Bondarenko method for cross section libraries with f factors) and NITAWL S (Nordheim treatment for cross section libraries with resonance parameters) were used for the problem dependent resonance processing while XSDRNPM S was used for a 1 D radial analysis of the radiation transport via discrete ordinates techniques The XSDOSE module of SCALE was used to provide the cask surface dose based on the XSDRNPM S angular flux and the flux to dose conversion factors of ANSI/ANS 6 1 1 1977 The code parameter data were identical for all the comparative analyses performed with the multigroup libraries The broad group calculations were $S_{16}P_3$, and the fine group calculations were S_8P_3

The analyses using XSDRNPM S were performed to provide a consistent comparison of the multigroup cross section libraries The model chosen for analysis was problem 1a as given in the Appendix In an effort to provide a comparison with point cross section data, the problem was also analyzed using the MCNP Version 3b code[3] as obtained from the Radiation Shielding Information Center (RSIC) at Oak Ridge National Laboratory (ORNL)

3 2 CROSS-SECTION LIBRARIES

Table 1 provides a brief description of the 17 multigroup libraries used for the 1 D cylindrical shielding analysis Four broad group libraries distributed by RSIC and routinely used for spent fuel shielding analyses served as the basis for this study the 47n 20g BUGLE 80 library,[4] the 22n 21g FCXSEC library,[5] the 27n 18g library from the SCALE system,[2] and the 22n 18g CASK library [6] These four libraries are, respectively, 1a, 2a, 3a, and 4 of Table 1 Variations of these broad group libraries (1b 1e, 2b 2c, 3b 3d of Table 1) were also created from parent fine group libraries to better determine the effect of the data origin (ENDF/B IV or ENDF/B V), the available resonance shielding, and the collapsing spectrum on the final dose

The library descriptions provided in Table 1 should be carefully studied to distinguish the subtle differences between libraries Identical collapses using the 171n 36g VITAMIN C library[7] (ENDF/B IV data), the 174n 38g VITAMIN E library[8] (ENDF/B V Mod 3 data), and the 227n 44g CSRL V[9] fine group libraries (ENDF/B V Mod 1 data) were performed to study the effect of the data origin on the broad group library results All the broad group libraries except 1a, 2a, and 4 contain Bondarenko factors (libraries created from VITAMIN C or VITAMIN E) or resonance parameters (libraries created from CSRL IV[10] or CSRL V) for all materials such that the resonance self shielding can be handled in a problem dependent fashion by the BONAMI or NITAWL codes prior to input to XSDRNPM Comparisons with library 1a, which has no resonance self shielding for the shield materials used in this analysis, provide a means to determine the importance of the resonance self shielding The effect of different collapsing spectra was studied by using (1) the generic spectra (typically fission 1/E Maxwellian for neutrons and flat for photons) provided with the fine group library, (2) the concrete spectra reported in ref 4, and (3) iron spectra obtained from fine group 1 D analyses of the cask

Table 1 Multigroup cross section libraries used for shielding analysis

Cross section library	Description
1a	47n 20g group collapsed from 171n 36g VITAMIN C library with concrete spectrum–ENDF/B IV data Concrete materials only have been processed by BONAMI This is the BUGLE-80 library
1b	47n 20g group collapsed from 171n 36g VITAMIN C library with concrete spectrum–ENDF/B IV data All resonance materials have Bondarenko factors
1c	47n 20g group collapsed from 174n 38g VITAMIN E library with concrete spectrum–ENDF/B V (Fe Mod 3) data All resonance materials have Bondarenko factors
1d	47n 20g group collapsed from 174n 38g VITAMIN E library with iron cask spectrum–ENDF/B V (Fe Mod 3) data All resonance materials have Bondarenko factors
1e	47n 20g group collapsed from 174n 38g VITAMIN E library with iron cask spectrum–ENDF/B V (Fe updated Mod 3) data All resonance materials have Bondarenko data
2a	22n 21g group collapsed from 171n 36g VITAMIN C library with fusion/fission 1/E-Maxwellian weighting for neutrons flat weighting for photons–ENDF/B IV data (converted from RSIC ANISN Library) All materials have been resonance processed via BONAMI and σ_o values of 0 1 1000 and 10^8 are provided This is the FCXSEC library
2b	22n 21g group collapsed from 171n 36g VITAMIN C library with concrete spectrum–ENDF/B IV data All resonance materials have Bondarenko factors
2c	22n 21g group collapsed from 171n 36g VITAMIN C library with fusion fission 1/E-Maxwellian weighting for neutrons and flat weighting for photons All resonance materials have Bondarenko factors
3a	27n 18g group collapsed from 218n ENDF/B IV library Gamma data created in 18 group format Fission 1/E-Maxwellian weighting for neutrons and flat weighting for photons
3b	27n 18g group collapsed from 227n 44g CSRL-V libraries with fission 1/E-Maxwellian weight function for neutron groups flat weight for photons–ENDF/B V (Fe Mod 1) data All resonance materials contain resonance parameters
3c	27n 18g group collapsed from 227n 44g CSRL V libraries with iron cask spectrum–ENDF/B V (Fe Mod 1) data All resonance materials contain resonance parameters
3d	34n 18g group collapsed from 227n 44g CSRL V libraries with iron cask spectrum–ENDF/B V (Fe Mod 1) data All resonance materials contain resonance parameters
4	22n 18g group CASK library assorted data sources Neutron cross sections collapsed from 104 group structure using weighting spectrum for uranium/water mixture
5	227n 44g CSRL V libraries processed through AMPX II from ENDF/B V data Bondarenko factors provided for unresolved resonance region
6	174n 38g VITAMIN E library processed through MINX (neutron) and AMPX (gammas) from ENDF/B V data
7	218n CSRL IV library processed with AMPX from ENDF/B IV data with a fission 1/E-Maxwellian weighting function
8	218n CSRL IV library processed same as Library 7 but Fe cross sections have 1/E Σ_T stainless steel weight

In addition, shielding analyses with the VITAMIN E, CSRL V, and 218n CSRL IV libraries (5–8 of Table 1) were performed to provide a comparison with their broad group counterparts These comparisons indicate the adequacy of the collapsing procedure used Resonance self shielding was performed in a problem dependent fashion for each of the analyses unless otherwise noted

3 3 RESULTS AND DISCUSSION

Table 2 provides the dose rates obtained from 1 D analyses of the case 1a cask model using the multigroup cross section libraries of Table 1 The energy distributions of the neutron and gamma dose rates are shown in Figs 1–2, respectively The plots were obtained from the analytic results with library 1b and show that the bulk of the neutron dose occurs between 0 1 and 1 MeV while the primary gamma dose is concentrated in the 0 2 to 3 MeV range (due primarily to the 2 1 MeV line source) The neutron and gamma ray results are discussed in the following subsections

3 3 1 Neutron Results

The first five libraries of Tables 1 and 2 all have the 47n 20g energy group structure of the BUGLE 80 library The 50% increase between the neutron doses obtained without and with resonance shielding for iron (libraries 1a and 1b, respectively) indicates the importance of adequate resonance shielding for this problem Intercomparison of the neutron doses obtained with libraries 1b, 1c, and 1d show that the ENDF/B IV results are about 8% higher than the ENDF/B V (Fe, Mod 3) results (1b versus 1c) while use of an iron weighting spectrum (library 1d) versus a concrete weighting spectrum (library 1c) has little effect on the surface doses The dose results with libraries 1c–1d agree to 8% or better with those obtained using the parent fine group library (library 6)

The second set of broad group libraries (libraries 2a–2c) in Table 2 have the 22n 21g energy group structure of the FCXSEC library Library 2a is the FCXSEC library and differs from library 2c only in the resonance treatment Library 2c was processed using resonance shielding appropriate to this specific problem, while library 2a was processed by picking background cross section values that were closest to the actual values The concrete weighting function used in the collapse for library 2b is the only thing that distinguishes library 2b from library 2c Libraries 2a and 2c were collapsed using a fusion fission 1/E Maxwellian spectrum The dose values from libraries 2a and 2c are very high relative to the other results in Table 2, but are in general agreement with each other In contrast, the results from library 2b are in much better agreement with the other results in Table 2 This library shows the dramatic errors that can result from using a broad group structure combined with an inappropriate collapsing spectrum

The third set of broad group libraries (libraries 3a–3d) in Table 2 is based on the 27n 18g group structure with library 3d having seven high energy neutron groups in place of the one (6–20 MeV) found in the others The libraries 3b–3d are all in very good agreement with each other as well as the neutron dose value obtained with the parent 227 44g CSRL V library (library 5) The broad group CSRL V libraries (libraries 3b–3d) agree to within 3% with the fine group results The cross sections for library 3a are based on ENDF/B IV and were collapsed to the 27n 18g group structure by a fission 1/E Maxwellian spectrum The agreement between neutron doses obtained with the corresponding ENDF/B V libraries (libraries 3b–3d) is only fair with the 3a results about 20% higher than the results based on ENDF/B V Comparing the neutron dose results from library 3a with those obtained with the parent fine group library (library 7) shows the broad group results to be nearly 70% higher! This difference indicates an inadequacy (for this problem) of the collapsing

Table 2 Radial surface doses (μSv/h) from a cast iron cask model using a 1 D discrete ordinates code and various multigroup cross section libraries

Cross-section library[a]	Case 1a [b] Fixed source results		
	Neutron	Primary gamma	Secondary gamma
1a (47n 20g BUGLE-80)	368	522	4 7
1b (47n 20g)	543	522	4 5
1c (47n 20g)	505	514	4 4
1d (47n 20g)	513	341	4 3
1e (47n 20g)	519	341	4 3
2a (22n 21g FCXSEC)	1401		
2b (22n 21g)	578	418	4 3
2c (22n 21g)	1501	449	3 8
3a (27n 18g SCALE)	620	417	4 1
3b (27n 18g)	504	411	4 1
3c (27n 18g)	518	267	4 1
3d (34n 18g)	518	267	4 1
4 (22n 18g CASK)	596	416	4 2
5 (227n 44g CSRL V)	502	280	–
6 (174n 38g VITAMIN E)	548	398	–
7 (218n CSRL-IV) 1/E collapse for Fe	368	–	–
8 (218n CSRL IV) 1/E Σ_T collapse for Fe	491	–	–

[a]See Table 1 for library description

[b]Dry cask model with 38 cm of iron shielding

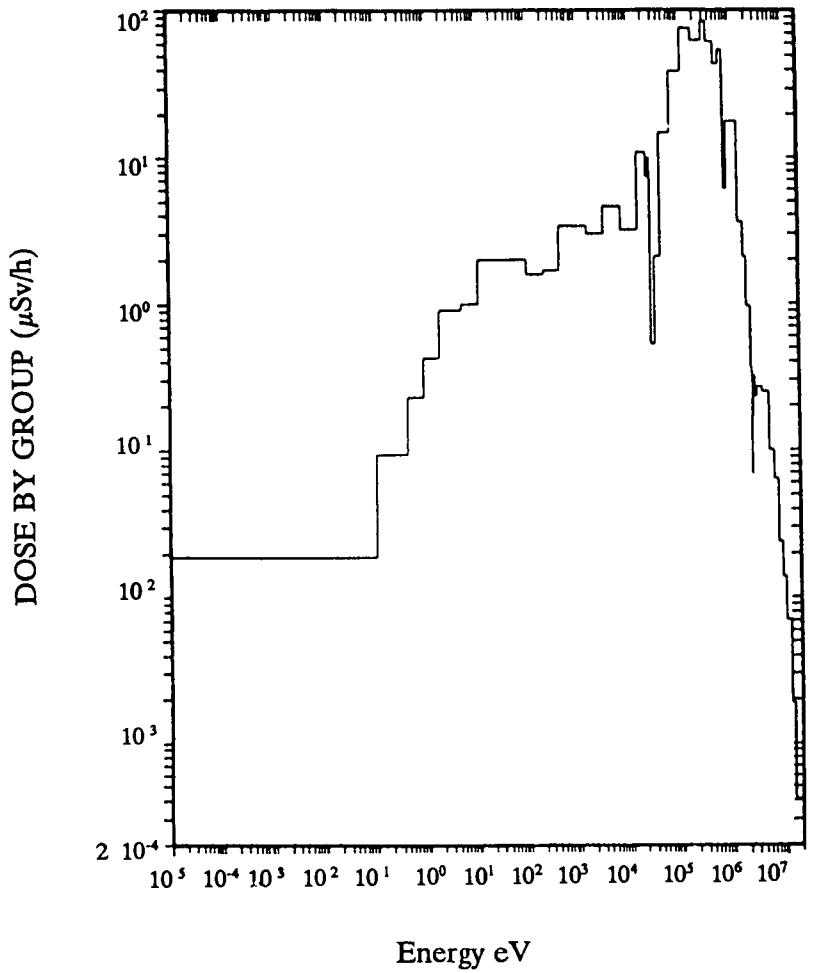

Fig 1 Neutron dose energy distribution using Library 1b

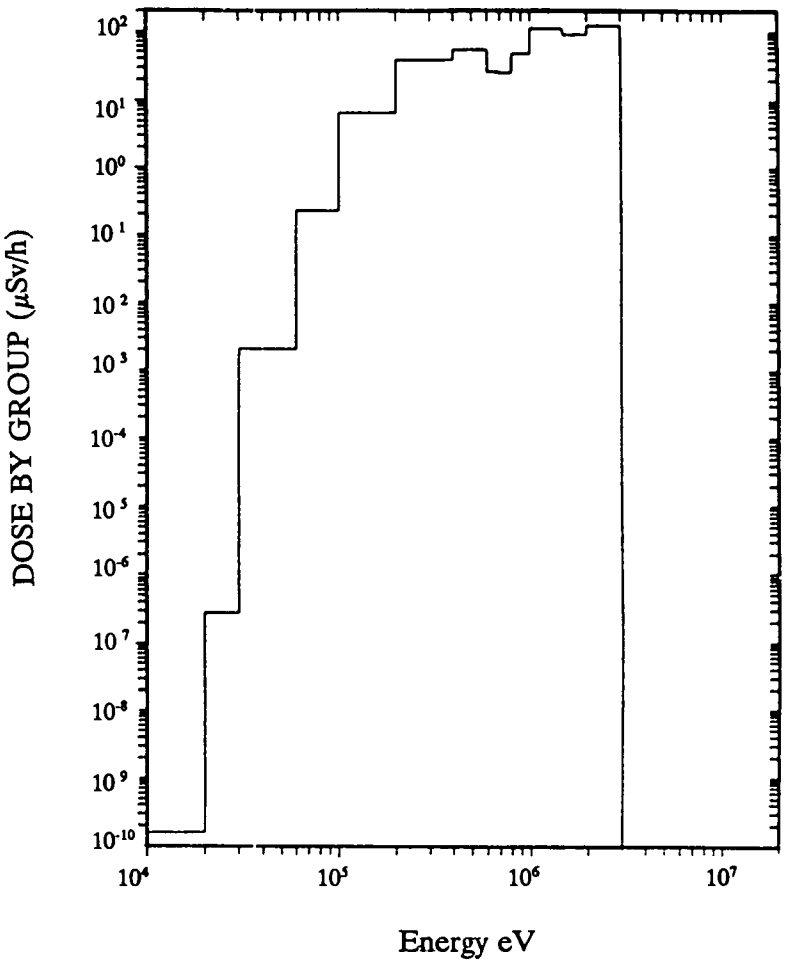

Fig 2 Primary gamma dose energy distribution using Library 1b

spectrum used to generate the library 3a cross sections This inadequacy is the same problem seen in libraries 2a and 2c, however, the extent is lessened due to energy group bounds (see Ref 1 for a complete discussion)

The ENDF/B IV 218n fine group results shown in Table 2 (libraries 7 and 8) differ appreciably and provide insight into some of the other differences between the various libraries The neutron dose results for library 7 are almost identical to those for library 1a, which contains no resonance processing However, library 7 does contain resonance processing One problem is that ENDF/B IV files represent iron cross sections with res onance parameters up to only 60 keV, well below the energy for which resolved data are now available ENDF/B V extends this range up to 400 keV, which does cover most of the resonances Since the CSRL libraries were processed from ENDF/B data to include resonance parameters for self shielding in the resolved resonance region only, the low (60 keV) cutoff of the iron resonance region in ENDF/B IV (libraries 7 and 8) caused no iron self shielding to be taken into account for the energy levels important to this problem The effect is clearly seen in the result for library 7, which shows no effect from resonance processing Library 8 provides dose results for the identical data and group structure, however, the iron cross sections were generated with a $1/E\ \Sigma_T$ weighting corresponding to stainless steel This is pseudo-resonance processing, and hence, the results from library 8 correspond much closer to the CSRL V (ENDF/B V) results

The VITAMIN C and VITAMIN E libraries are not particularly affected by the change in the iron resonance region The processing method used for these fine group libraries first uses the resonance parameters to construct the point cross section profile in the given resonance energy range Then, using the point profile over the entire energy spectrum, f factors are developed for use in resonance shielding via the Bondarenko technique [7 8] The inclusion of resonance self shielding above the 400 keV ENDF/B V cutoff is felt to be the cause for the results from VITAMIN E (library 6) being slightly higher than those from CSRL V (library 5)

The neutron dose results using library 4 are somewhat higher than most of the others It should be noted that the cross sections were collapsed using 104 fine group ENDF/B II data and a weighting spectrum for a uranium/water mixture Little more about the details of this library has been documented and therefore an explanation of the causes of this difference will not be attempted

Neutron dose results obtained by the MCNP code and both ENDF/B IV and ENDF/B V point cross section libraries were also included in the cross section study The use of a three dimensional (3 D) method and point cross sections allows a standard to mea sure the performance of the remaining cross section libraries The surface averaged doses were 641 μSv/h using the ENDF/B IV point data and 589 μSv/h using the ENDF/B V data Both of these results are higher than any of the fine group results The best fine group to point data agreement is for library 6 with a 7% difference seen (approximately a 7% factor should also be added to account for the peak versus surface averaged effect

3 3 2 Gamma Doses

Surface dose results for primary gamma rays are given in column 2 of Table 2 for most of the libraries included in the neutron results The mechanisms involved in the gamma transport are not as complex as those of the neutrons and, thus, the gamma dose differences seen in Table 2 are almost entirely due to differences in weighting spectra and broad group boundary selection For example, a 50% decrease in the dose rates from libraries 1a–1c is seen when using libraries 1d and 1e, which utilized a collapsing spectrum corresponding

to the fine group cask calculation (i e , cask spectrum in the iron cask body) The results using libraries 1a–1c are in good agreement with each other and were produced with broad group libraries collapsed from the fine group libraries with a calculated concrete spectrum In comparison with the parent fine group results of library 6, the iron weighted broad group libraries (libraries 1d and 1e) provide results that agree to within 15% while the results from the concrete weighted libraries 1a–1c are nearly 30% high

The gamma dose results obtained with libraries 2b and 2c are in good agreement, indicating that the concrete and flat weighting spectra produce cross sections that are very nearly the same The parent fine group library result is not given in the table, however, these results agree quite well with VITAMIN E results (library 6), which is the ENDF/B V version of the parent library

The gamma cross sections of libraries 3c and 3d are identical, and, thus, the gamma dose results shown in Table 2 are identical The agreement with their fine group counter part, library 5, is also very good Both of these libraries were collapsed from the CSRL V 227n 44g library using the calculated spectrum from the fine group iron cask analysis The results obtained with libraries 3a–3b are in agreement with each other (both were collapsed with a flat weighting), but are about 50% higher than the results obtained with libraries 3c–3d and the parent fine group library (library 5) Again this difference is due to the differing weights assumed in the collapse It can also be seen that the gamma results using library 4 (22n 18g) are in good agreement with those using libraries 3a–3b

Somewhat surprising is the degree of discrepancy shown in Table 2 between the gamma doses from the fine group libraries (i e , libraries 5 and 6) Better agreement between fine group calculations was expected and, hence further investigation was warranted The conclusion derived from this investigation was that the VITAMIN E gamma library does not represent an adequate "fine group" library for the source defined in this problem It was noted earlier that the 2 1 MeV line source is the major contributor to the dose for this problem (confirmed by calculations with QAD CGGP and MCNP using individual line source data) A review of the group structure indicates that in the energy range from 2–2 5 MeV, the CSRL V library has four groups while the VITAMIN E library has only two groups The QAD CGGP and MCNP results using individual line sources gave gamma dose results of 294 μSv/h and 279 6 $\pm$ 6% μSv/h, respectively [For direct comparison to the peak doses shown in Table 2, a factor of about 1 03 (see Sect 4 2) should be included in the surface averaged values from MCNP] These compare well with the dose results from the CSRL V library but are about 30% lower than the result obtained with the VITAMIN E library

The discussion above illustrates that in this problem the energy group containing the 2 1 MeV gamma line is very important Comparison of the VITAMIN E derived (47n 20g BUGLE) and CSRL V derived (27n 18g SCALE) libraries shows differences of 30% between libraries with similar flux weighting The consistently lower gamma dose results from the 27n 18g library are due to the fact that the SCALE library structure has a group width (2–2 25 MeV) that is able to define the line source at 2 1 MeV better than that in the BUGLE structure (2–2 5 MeV group width) This variation in gamma results due to the energy bounds about 2 1 MeV was confirmed by additional QAD CGGP runs using the BUGLE gamma group structure (502 μSv/h) and the SCALE gamma group structure (358 μSv/h) However, it was suspected that the dominance of the 2 1 MeV gamma line was not entirely representative of realistic spent fuel sources For this reason, the problems using libraries 3a and 3c were rerun using the spent fuel radiation source generated for problem 5 (see Sect 5 2 2) The approximately 58% difference seen between the libraries 3a and 3c results was reduced to 26% with the more realistic source This suggests that

the differences seen in Table 2 for the gamma results would be smaller if a more realistic spent fuel source had been used in the problem definition

3 3 3 Library Selection

With the conclusion of the investigation of the various multigroup cross section libraries, it was evident that none of the publicly available broad group libraries (1a, 2a, 3a, and 4) were appropriate to use for the ensuing benchmark work The most expedient option was to generate an appropriate broad group library from the available fine group libraries In comparison to the MCNP dose results obtained with ENDF/B V point cross section data, the VITAMIN E library provides the best neutron doses while the CSRL V library provides the best gamma doses Without funding to produce a library with the best features of both existing libraries, the library labeled 3c in Table 2 was selected to be used for the remaining multigroup calculations This library has the advantage in that both neutron and gamma results agree reasonably well with both the MCNP results and the fine group results The resulting library has 27n and 18g groups (see Tables 3–4) and is based on ENDF/B V data The broad group library was processed by collapsing the CSRL V 227n and 44g group library using an iron cask spectrum The total microscopic cross sections for selected materials from this library are given in Tables 3–4 along with the dose conversion factors for the 27n 18g groups

4 PROBLEMS 1–4 ANALYSIS

The goal of the analysis of problems 1–4 is to examine in successively increasing detail the accurate modeling of existing shipping cask designs The initial problem consists of three subcases that examine the effects of wet and dry cavities and the presence of a simple neutron shield The second problem set requires the modeling of two different geometrically complex neutron shields The third problem set is identical with the second but adds outer cooling fins to the shield body The fourth problem set utilizes the simple shield of problem 1 with a detailed modeling of the cavity (i e , explicit basket with assemblies)

4 1 SOLUTION METHODOLOGY AND ASSUMPTIONS

Analyses were performed with several different computer programs and cross section libraries In particular, the tools utilized were QAD CGGP[11] (primary gamma only), DORT,[12] MCNP Version 3,[3] and two shielding analytic sequences developed for the SCALE system[2]–SAS1 and SAS4 QAD CGGP is a point kernel code with built in attenuation and buildup factor data The code DORT is an updated version of the multigroup discrete ordinates transport code DOT The MCNP code utilizes the Monte Carlo method along with point cross section data The SAS1 and SAS4 sequences are new additions to the SCALE system and have only recently (February 1990) become available via the release of SCALE 4 Basically, SAS1 is a convenient module for problem dependent cross section preparation and subsequent 1 D discrete ordinates shielding analysis via the XSDRNPM S code For detector points exterior to the cask, SAS1 employs the XSDOSE module to integrate the outgoing angular flux over the finite cask height and obtain the scalar flux at a detector point The SAS4 sequence prepares the cross sections and uses 1 D adjoint results from XSDRNPM S to automatically prepare biasing parameters for a subsequent Monte Carlo cask analysis with MORSE SGC/S

As noted above, the analyses were performed with a variety of different cross section libraries The DORT, SAS1, and SAS4 analyses were performed with the 27n 18g group library selected in Sect 3 and based on ENDF/B V cross sections The iron neutron cross

Table 3 Total neutron cross sections for several materials in the 27n 18g library selected for use

Group	Upper energy (eV)	Hydrogen σ_T	Carbon σ_T	Iron σ_T	^{238}U σ_T	Dose factors (Sv/h/unit flux)
1	2 0+7[a]	1 19	1 21	3 47	6 50	1 49 6
2	6 43+6	1 92	1 91	3 56	7 82	1 45 6
3	3 0+6	2 68	1 80	3 24	7 52	1 27 6
4	1 85+6	3 30	1 94	2 97	7 06	1 28 6
5	1 4+6	4 02	2 45	2 59	7 02	1 30 6
6	9 0+5	5 58	3 23	3 13	8 02	1 03 6
7	4 0+5	9 60	4 08	2 36	1 06+1	5 12 7
8	1 0+5	1 57+1	4 59	3 91	1 28+1	1 23 7
9	1 7+4	1 93+1	4 73	5 29	1 44+1	3 84 8
10	3 0+3	2 02+1	4 73	8 49	1 40+1	3 72 8
11	5 5+2	2 04+1	4 74	1 10+1	1 53+1	4 02 8
12	1 0+2	2 05+1	4 74	1 14+1	1 57+1	4 29 8
13	3 0+1	2 05+1	4 74	1 15+1	1 44+1	4 47 8
14	1 0+1	2 05+1	4 74	1 16+1	1 59+1	4 57 8
15	3 05	2 05+1	4 74	1 17+1	9 54	4 56 8
16	1 77	2 07+1	4 74	1 17+1	9 51	4 52 8
17	1 30	2 09+1	4 74	1 18+1	9 06	4 49 8
18	1 13	2 11+1	4 75	1 18+1	8 92	4 47 8
19	1 00	2 13+1	4 75	1 18+1	9 23	4 43 8
20	8 0 1	2 23+1	4 75	1 19+1	9 74	4 33 8
21	4 0 1	2 46+1	4 76	1 21+1	9 47	4 20 8
22	3 25 1	2 61+1	4 76	1 22+1	9 64	4 10 8
23	2 25 1	2 94+1	4 77	1 24+1	1 00+1	3 84 8
24	1 0 1	3 64+1	4 82	1 29+1	1 01+1	3 67 8
25	5 0 2	4 57+1	4 86	1 35+1	1 08+1	3 67 8
26	3 0 2	5 69+1	5 00	1 44+1	1 09+1	3 67 8
27	1 0 2	7 90+1	5 80	1 75+1	1 36+1	3 67 8

[a]Read as $2\ 0 \times 10^7$

Table 4 Total photon cross sections for several materials in the 27n 18g library selected for use

Group	Upper energy (eV)	Hydrogen σ_T	Carbon σ_T	Iron σ_T	^{238}U σ_T	Dose factors (Sv/h/unit flux)
1	1 0+7[a]	5 81 2	4 07 1	2 76	1 99+1	8 77 8
2	8 0+6	6 50 2	4 37 1	2 77	1 89+1	7 48 8
3	6 5+6	7 74 2	4 97 1	2 84	1 79+1	6 37 8
4	5 0+6	9 19 2	5 74 1	2 98	1 73+1	5 41 8
5	4 0+6	1 07 1	6 61 1	3 20	1 72+1	4 62 8
6	3 0+6	1 22 1	7 44 1	3 45	1 75+1	3 96 8
7	2 5+6	1 43 1	8 66 1	3 87	1 87+1	3 47 8
8	2 0+6	1 55 1	9 31 1	4 11	1 95+1	3 02 8
9	1 66+6	1 72 1	1 03	4 52	2 14+1	2 63 8
10	1 33+6	1 96 1	1 18	5 12	2 59+1	2 21 8
11	1 00+6	2 22 1	1 33	5 82	3 37+1	1 83 8
12	8 0+5	2 50 1	1 50	6 60	4 58+1	1 52 8
13	6 0+5	2 89 1	1 74	7 73	7 48+1	1 17 8
14	4 0+5	3 34 1	2 00	9 13	1 44+2	8 76 9
15	3 0+5	3 78 1	2 27	1 11+1	3 05+2	6 31 9
16	2 0+5	4 30 1	2 66	1 78+1	7 49+2	3 83 9
17	1 0+5	5 09 1	3 10	4 58+1	1 02+3	2 67 9
18	5 0+4	5 57 1	3 53	1 58+2	3 79+3	9 35 9

[a]Read as $1\ 0 \times 10^7$

ORNL DWG 90M 10357

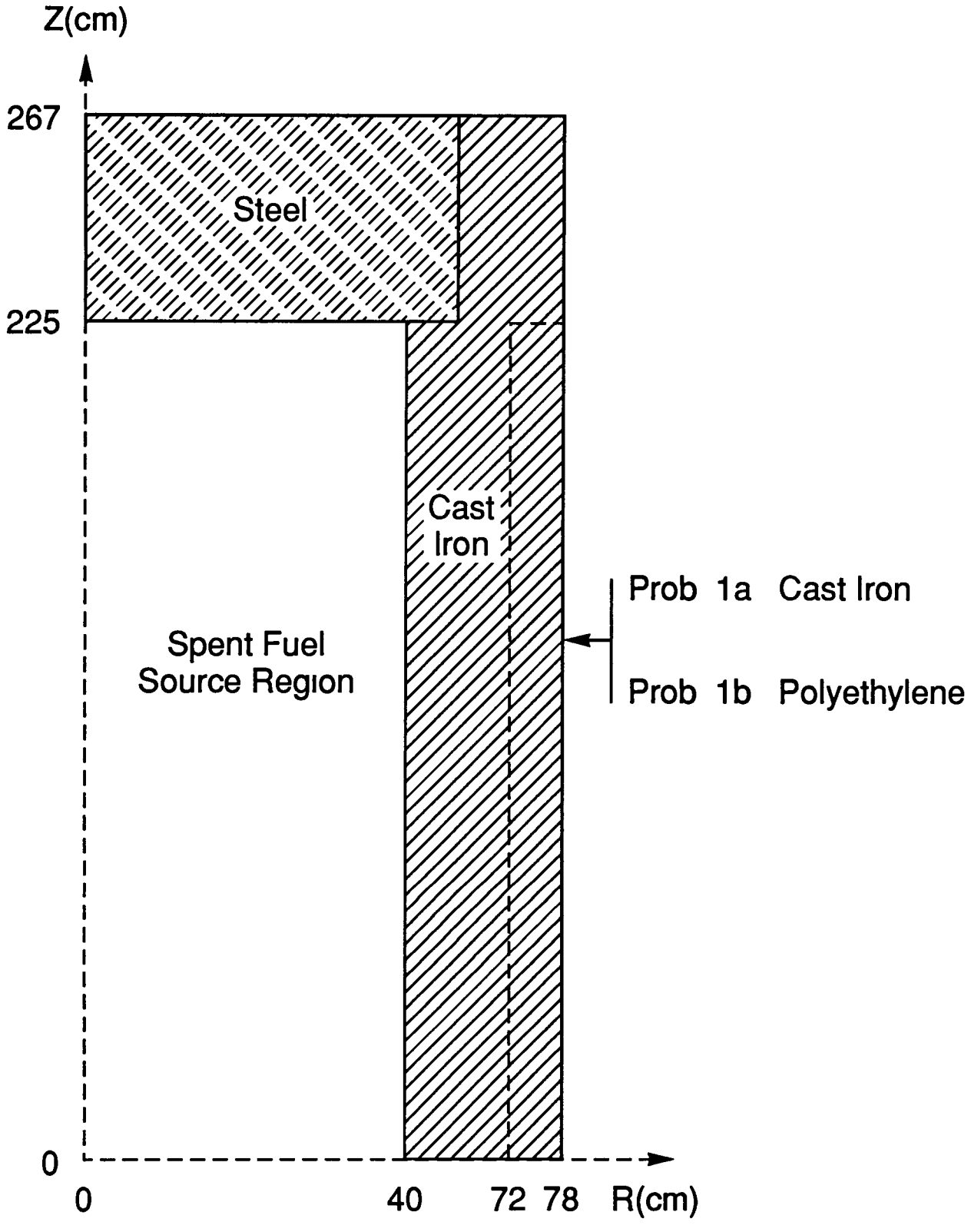

Fig 3 Geometry of problem 1 cast iron cask specified by OECD Working Group

sections that were utilized were collapsed from the 227 fine group using cast iron spectrum weighting The MCNP calculations were done with the point (continuous energy) cross section library provided with MCNP Version 3b and based on ENDF/B V The QAD CGGP analyses were done using the available built in attenuation coefficients and log log interpolation methods

As a point Monte Carlo code, it was possible to input the neutron source spectrum for MCNP using the specified analytic function and input the photon sources at their discrete energy levels (the QAD CGGP calculations also used this technique) However, for the multigroup codes, the analytic function for the neutron source spectrum was integrated to provide groupwise values while the discrete gamma ray line data were binned into energy groups by conserving the total photon energy (see next paragraph for discussion of why this approach was taken) For example, the intensity I_g of photon particles at energy E_g was altered to a new intensity I_{avg} at group average energy E_{avg} by the formula $I_{avg} = I_g E_g / E_{avg}$ Discrete line sources located on group boundaries were split between the higher and lower energy groups The multigroup neutron and gamma ray sources are included in Table 5

The primary gamma dose rates are, in most cases, sensitive to whether the multigroup analyst attempts to conserve the number of photon particles or the photon energy For the BUGLE library and the SCALE 27n 18g library discussed in Sect 3, dose differences of 15% and 9% were seen between the particle conserved and the energy conserved source results The particle conserved source results were higher for this problem, however, lower results are possible depending on the relation between the dominant line source s energy with respect to the mean energy of the group The general tendency should be to exacer bate the dose overprediction or underprediction (relative to a calculation with line sources or fine multigroups) due to the broad groups as seen in Sect 3

The geometry model for problem set 1 is shown in Fig 3 A P_3S_8 quadrature set was utilized in the DORT analysis while a P_3S_{16} was used in the SAS1 cases For the SAS1 analyses, a 1 cm mesh size was used in the cavity while a 0 5 cm mesh size was used in the cask body The radial and axial meshes used for DORT neutron analyses were about 4 cm in the cavity and about 1 cm in the cask body with finer mesh spacing used near boundaries The radial mesh spacing for fission product gamma ray calculations was 4 cm in the cavity and 1 0 cm in the cask body (select calculations were performed for 0 5 cm mesh to insure agreement with 1 D cases) An auxiliary code called FALSTF[13] was used with DORT to evaluate doses exterior to the cask using a sum of last flight contributions from collision sights in the shield Use of FALSTF eliminates the problem with ray effects in the void region outside the cask model

Both cases 2a and 2b require a fairly complex geometrical description that can only be precisely modeled in two or three dimensions Case 2a is essentially 3 D, while case 2b can be modeled quite well in two dimensions Both cases were analyzed using the combinatorial geometry in SAS4 (3 D) Case 2a was analyzed in two dimensions using DORT R θ geometry This effectively gives only midplane values and these will be reported as such Figure 4 gives the geometry model in which 15 θ intervals were used along with appropriately chosen r intervals to describe the off centered polyethylene cylindrical rods It is only necessary to model two half rods while specifying reflected boundary conditions on the first and last θ intervals to model the entire azimuthal area The r intervals in the cavity were 1 cm apart with a 0 5 cm mesh used in the shield except as needed to model the polyethylene rods The DORT code was then utilized in R Z geometry to analyze case 2b The r mesh was identical to earlier R Z runs except a 0 5 cm mesh was used in the epoxy material The axial intervals were changed to give either a 2 5 cm or 3 0 cm mesh

Table 5 Neutron and gamma ray groupwise sources

Group no	Neutron source	Group no	Gamma source
1	$1\,768 \times 10^{-2}$	1	–
2	$1\,912 \times 10^{-1}$	2	–
3	$2\,223 \times 10^{-1}$	3	–
4	$1\,273 \times 10^{-1}$	4	–
5	$1\,666 \times 10^{-1}$	5	–
6	$1\,758 \times 10^{-1}$	6	$1\,34 \times 10^{12}$
7	$8\,472 \times 10^{-2}$	7	$2\,55 \times 10^{14}$
8	$1\,285 \times 10^{-2}$	8	$5\,71 \times 10^{12}$
9	$2\,830 \times 10^{-4}$	9	–
10	$6\,900 \times 10^{-5}$	19	$9\,12 \times 10^{14}$
11	–	11	$3\,86 \times 10^{14}$
12	–	12	$3\,40 \times 10^{16}$
13	–	13	$1\,52 \times 10^{16}$
14	–	14	–
15	–	15	–
16	–	16	–
17	–	17	–
18	–	18	–
19	–		
20	–		
21	–		
22	–		
23	–		
24	–		
25	–		
26	–		
27	–		

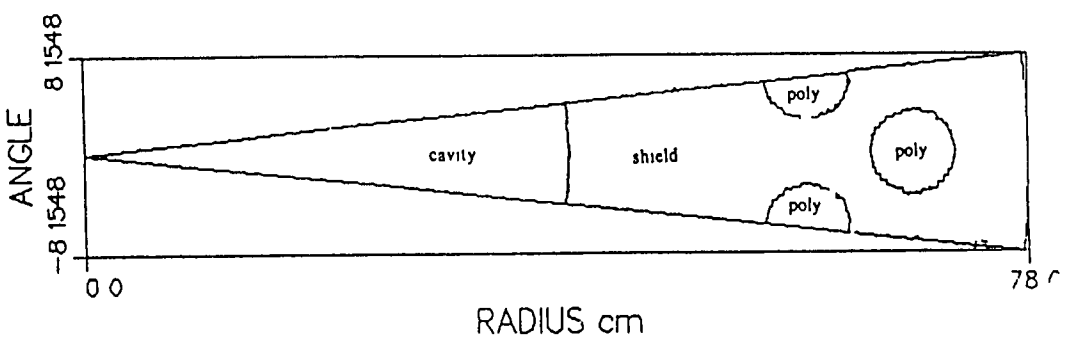

Fig 4 DORT R θ geometry model

to correspond to the axial epoxy strip boundaries SAS1 was also used to analyze case 2a in an approximate manner The approach taken was to form two concentric polyethylene rings centered at radii of 60 cm and 68 5 cm The width of each ring was chosen to conserve the polyethylene volume

An analysis was not attempted for case 3a, however, case 3b was analyzed using a method similar to that used in case 2a A DORT R Z model was constructed that consisted of half of one fin and half of the accompanying 8 cm high epoxy resin section with top and bottom reflected boundary conditions (see Fig 5) The results should therefore be applicable to the cask section near the axial midplane Surface averaged solutions were not attempted for this problem

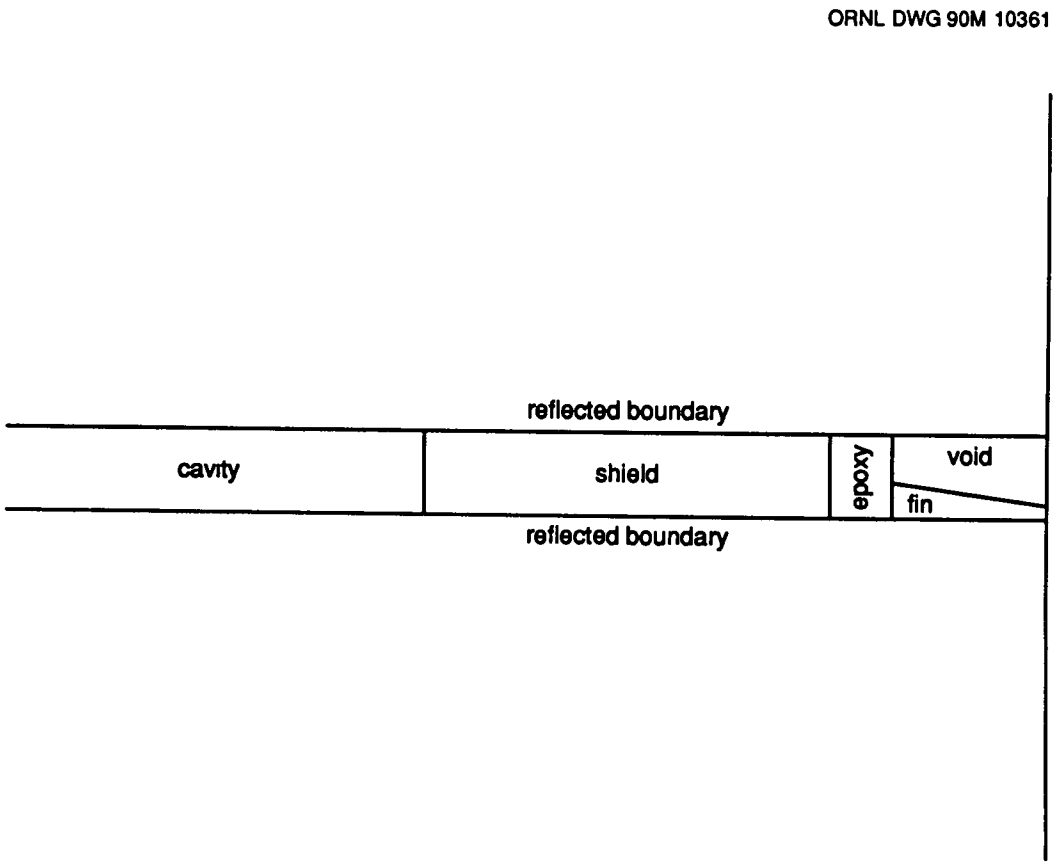

Fig 5 Problem 3b approximate DORT model

For cases 4a and 4b, both a simplified 1 D model using SAS1 and a more complex model using SAS4 were analyzed The 1 D model consisted of an inner ring of dry (wet for case 4b) source material with the volume corresponding to one assembly, followed by a 1 cm thick ring of basket material, the remaining four assemblies (and water for case 4b) were then smeared to occupy all the remaining cavity area except for a 1 cm thick ring of basket material on the inner shield wall The SAS4 geometry modeled the basket explicitly

while homogenizing the fuel assemblies in the basket Case 4a was also modeled in SAS4 with an explicit pin by pin assembly model

4 2 RESULTS AND DISCUSSIONS

Each problem set will be discussed separately with emphasis placed on the internal consistency, or lack thereof, between the various solutions to each problem The comparison of these results with those of other countries will not be attempted in this document since the primary aim is to disseminate the U S results for analysis and comparison among the working group participants

4 2 1 Problem Set 1 Results

A 1 D cylindrical model should provide a good representation of a long slender cask for calculation of sidewall doses Thus, the 1 D model for this problem (H/D = 3) is expected to compare well with the multidimensional model that represents the finite height of the cask The sidewall surface doses given in Table 6 show excellent agreement between the 1 D SAS1 values and the 2 D DORT values An interesting effect can be observed by comparing these 1 D values (using a 0 5 cm mesh in the shield) with the 2 D values (using a 1 0 cm mesh in the shield) The two neutron cases with a homogeneous shield (1a and 1c) give essentially identical results, while the two material shield (1b) results are about 15% different A similar effect is also seen for the fission product gamma results When the DORT mesh is refined to 0 5 cm, each of these cases then agrees well with the fine mesh 1 D results Thus, for fission product gammas transported through heterogeneous shields the mesh needs to be finer for a given degree of accuracy

The QAD CGGP results shown in Table 6 indicate that for this problem the point kernel technique performs quite well The QAD CGGP results are, in general, 15–20% high compared to the discrete ordinates values In this instance, the QAD CGGP result that compares best with the discrete ordinates results is that for the multiregion shield This result is most likely fortuitous since the approximations within QAD CGGP are less accurate for multiregion shields

The DORT, SAS4, and MCNP results for the sidewall surface averaged doses allow for several different comparisons to be made First, the results labeled DORT avg give the 2 D discrete ordinates solution averaged over the cavity height The SAS4 avg results utilize the same multigroup cross sections as the DORT avg case but employ the Monte Carlo method Both methods give results that agree to 10% or better The MCNP fission product (FP) gamma results similarly agree to within 10% For the neutrons, the agreement is only about 20%, with the point cross sections giving higher results than the multigroup cross sections The most likely cause is the better representation of the iron neutron cross section minima with the point cross section data Lack of an appropriate multigroup cross section library for this problem (see Sect 3 3) thus appears to induce a 20% error in the neutron dose with the multigroup codes

The results for the cask lid and bottom surface doses follow somewhat similar trends as those of the surface sidewall The FP gamma results are all very consistent as was seen before The agreement between the multigroup discrete ordinates and Monte Carlo results continues to be good The MCNP neutron results are somewhat confusing in that the 20% trend seen at the sidewall surface is not maintained In fact, the agreement at the bottom is much better (2% between the DORT and MCNP) and much worse at the top (60% difference between DORT and MCNP) A simple explanation would be the reversals of the

Table 6 Summary results of model problem 1[a]

Surface doses (μSv/h)

	Neutron			FP gamma			Capture gamma		
	a	b	c	a	b	c	a	b	c
Sidewall									
QAD	–	–	–	296	1336	203	–	–	–
SAS1	517	53 7	47 1	268	1300	185	4 1	40 6	0 30
DORT	518	45 8[d]	47 2	240[d]	1168[d]	166[d]	4 1	49 9	0 30
DORT avg[b]	485	40 1	45 8	233	1134	162	3 81	45 8	0 29
SAS4-avg	476(4)[c]	51 3(2)	48 0(4)	260(3)	1244(5)	193(3)	3 53(4)	38 5(3)	0 30(5)
MCNP avg	589(2)	–	–	279(6)	–	–	–	–	–
Lid									
QAD	–	–	–	35 6	35 6	22 8	–	–	–
DORT	413	412	47 0	36 7	36 7	25 8	2 8	2 8	0 26
DORT avg	313	312	36 1	31 4	23 1	16 4	2 19	2 18	0 20
SAS4-avg	304(6)	284(5)	37 0(10)	26 6(7)	24 5(8)	17 7(7)	2 31(16)	2 45(11)	0 19(13)
MCNP avg	524(6)	–	–	29 0(8)	–	–	–	–	–
Bottom									
QAD	–	–	–	382	382	245	–	–	–
DORT	541	541	61 5	403	403	287	3 9	3 9	0 38
DORT avg	410	410	47 4	291	267	190	3 11	3 08	0 30
SAS4 avg	352(7)	385(10)	41 3(8)	325(10)	252(7)	183(9)	2 78(8)	2 74(13)	0 28(16)
MCNP avg	422(7)	–	–	316(10)	–	–	–	–	–

Doses at 1 m (μSv/h)

	Neutron			FP gamma			Capture gamma		
	a	b	c	a	b	c	a	b	c
Sidewall									
QAD	–	–	–	128	577	87 6	–	–	–
SAS1	161	17 8	14 7	102	493	70 5	1 32	11 5	0 10
DORT	156	14 2	14 4	93 9	453	65 0	1 28	11 8	0 10
SAS4	155(6)	18 0(3)	15 1(5)	113 6(11)	437(11)	68 6(9)	1 30(12)	10 8(4)	0 09(12)
SAS4-avg	106(4)	15 3(3)	10 7(4)	69 4(3)	332(5)	52 1(3)	0 83(3)	7 45(2)	0 07(5)
MCNP	198(2)	–	–	111(8)	–	–	–	–	–
Lid									
QAD	–	–	–	14 1	14 1	9 23	–	–	–
DORT	47 3	47 1	5 50	7 02	7 02	4 97	0 37	0 37	0 035
SAS4	49 1(5)	44 8(5)	6 43(13)	9 19(6)	7 75(5)	6 45(7)	0 38(13)	0 33(7)	0 034(17)
SAS4-avg	24 2(5)	21 8(5)	3 19(15)	2 95(8)	3 03(10)	1 99(7)	0 21(14)	0 17(9)	0 020(18)
MCNP	81(4)	–	–	9 27(7)	–	–	–	–	–
Bottom									
QAD	–	–	–	140	140	91 4	–	–	–
DORT	61 8	61 5	7 16	77 6	77 6	55 1	0 53	0 52	0 052
SAS4	56 1(7)	57 0(8)	6 75(8)	94 0(7)	78 9(7)	56 1(7)	0 51(11)	0 44(12)	0 045(12)
SAS4 avg	28 7(8)	27 5(8)	3 20(8)	26 0(8)	21 8(6)	15 2(7)	0 26(15)	0 23(12)	0 025(16)
MCNP	73(4)	–	–	98 4(8)	–	–	–	–	–

Table 6 (continued)

Dose attenuation at 1 m

	Neutron			FP gamma			Capture gamma		
	a	b	c	a	b	c	a	b	c
Sidewall									
QAD	–	–	–	0 432	0 432	0 432	–	–	–
SAS1	0 311	0 331	0 312	0 381	0 379	0 381	0 322	0 283	0 333
DORT	0 301	0 310	0 305	0 391	0 388	0 392	0 312	0 236	0 333
SAS4	0 305	0 307	0 305	0 424	0 341	0 347	0 341	0 257	0 290
SAS4-avg	0 223	0 298	0 223	0 267	0 267	0 270	0 235	0 194	0 233
MCNP	0 315	–	–	0 386	–	–	–	–	–
Lid									
QAD	–	–	–	0 396	0 396	0 405	–	–	–
DORT	0 115	0 114	0 117	0 191	0 191	0 193	0 132	0 132	0 135
SAS4	0 122	0 119	0 133	0 296	0 199	0 232	0 129	0 106	0 138
SAS4 avg	0 0796	0 0768	0 0862	0 111	0 124	0 112	0 0909	0 0694	0 105
MCNP	0 117	–	–	0 273	–	–	–	–	–
Bottom									
QAD	–	–	–	0 366	0 366	0 373	–	–	–
DORT	0 114	0 114	0 116	0 193	0 193	0 192	0 136	0 133	0 137
SAS4	0 121	0 112	0 126	0 209	0 207	0 203	0 146	0 128	0 127
SAS4 avg	0 0815	0 0714	0 0775	0 0800	0 0865	0 0831	0 0935	0 0839	0 0893
MCNP	0 131	–	–	0 225	–	–	–	–	–

Doses at 2 m (μSv/h)

	Neutron			FP gamma			Capture gamma		
	a	b	c	a	b	c	a	b	c
Sidewall									
QAD	–	–	–	81 4	366	55 8	–	–	–
SAS1	89 6	10 2	8 18	61 8	298	42 8	0 75	5 97	0 05
DORT	81 5	8 35	7 61	55 6	266	38 5	0 68	5 67	0 05
SAS4	82 2(5)	10 5(3)	8 09(4)	57 5(8)	292(10)	41 6(8)	0 62(9)	5 62(7)	0 05(12)
SAS4 avg	59 0(5)	8 45(3)	6 00(4)	41 9(3)	201(5)	31 2(3)	0 47(3)	3 98(3)	0 04(6)
MCNP	104(1)	–	–	67 0(6)	–	–	–	–	–
Lid									
QAD	–	–	–	6 06	6 06	3 94	–	–	–
DORT	14 7	14 6	1 71	2 50	2 50	1 77	0 12	0 12	0 011
SAS4	15 4(5)	14 0(5)	2 04(14)	3 39(6)	3 03(4)	2 42(6)	0 11(6)	0 10(8)	0 011(19)
SAS4 avg	11 2(6)	10 6(6)	1 48(14)	1 86(9)	2 06(13)	1 34(8)	0 10(18)	0 08(14)	0 008(19)
MCNP	26(4)	–	–	3 37(6)	–	–	–	–	–
Bottom									
QAD	–	–	–	58 2	58 2	37 8	–	–	–
DORT	19 2	19 1	2 23	27 3	27 3	19 3	0 17	0 17	0 017
SAS4	17 6(7)	17 6(8)	2 10(8)	35 9(8)	29 0(6)	20 8(8)	0 16(10)	0 15(13)	0 013(12)
SAS4 avg	12 4(7)	13 1(8)	1 49(8)	17 3(11)	14 6(7)	10 4(9)	0 13(27)	0 11(16)	0 015(23)
MCNP	24(4)	–	–	35 5(7)	–	–	–	–	–

Table 6 (continued)

Dose attenuation at 2 m

	Neutron			FP gamma			Capture gamma		
	a	b	c	a	b	c	a	b	c
Sidewall									
QAD	–	–	–	0 275	0 274	0 275	–	–	–
SAS1	0 173	0 190	0 174	0 231	0 229	0 231	0 183	0 147	0 167
DORT	0 157	0 182	0 161	0 232	0 228	0 232	0 166	0 114	0 167
SAS4	0 162	0 179	0 164	0 215	0 228	0 210	0 163	0 134	0 161
SAS4-avg	0 124	0 165	0 125	0 161	0 162	0 162	0 133	0 103	0 133
MCNP	0 165	–	–	0 233	–	–	–	–	–
Lid									
QAD	–	–	–	0 170	0 170	0 173	–	–	–
DORT	0 0356	0 0354	0 0364	0 0681	0 0681	0 0686	0 0429	0 0429	0 0423
SAS4	0 0384	0 0373	0 0423	0 1090	0 0778	0 0869	0 0374	0 0321	0 0445
SAS4 avg	0 0368	0 0373	0 0400	0 0699	0 0841	0 0757	0 0433	0 0327	0 0421
MCNP	0 0376	–	–	0 0994	–	–	–	–	–
Bottom									
QAD	–	–	–	0 152	0 152	0 154	–	–	–
DORT	0 0355	0 0353	0 0363	0 0677	0 0677	0 0672	0 0436	0 0436	0 0447
SAS4	0 0379	0 0346	0 0392	0 0798	0 0762	0 0752	0 0457	0 0435	0 0367
SAS4-avg	0 0352	0 0340	0 0361	0 0532	0 0579	0 0568	0 0468	0 0401	0 0536
MCNP	0 0431	–	–	0 0811	–	–	–	–	–

Doses at 10 m (μSv/h)

	Neutron			FP gamma			Capture gamma		
	a	b	c	a	b	c	a	b	c
Sidewall									
QAD	–	–	–	11 7	50 7	8 06	–	–	–
SAS1	8 00	0 99	0 73	7 44	35 1	5 15	0 067	0 47	0 005
DORT	6 67	0 85	0 64	6 01	28 0	4 17	0 055	0 41	0 004
SAS4	6 68(5)	1 02(3)	0 67(4)	6 88(7)	23 5(6)	4 86(6)	0 049(7)	0 38(4)	0 004(8)
MCNP	8 5(1)	–	–	7 5(5)	–	–	–	–	–
Lid									
QAD	–	–	–	0 39	0 39	0 25	–	–	–
DORT	0 66	0 66	0 077	0 13	0 13	0 09	0 005	0 005	0 001
SAS4	0 70(5)	0 63(5)	0 094(15)	0 19(5)	0 18(4)	0 13(5)	0 005(9)	0 005(7)	0 001(21)
MCNP	1 2(4)	–	–	0 26(6)	–	–	–	–	–
Bottom									
QAD	–	–	–	3 59	3 59	2 30	–	–	–
DORT	0 87	0 86	0 10	1 41	1 41	0 99	0 008	0 008	0 001
SAS4	0 80(7)	0 80(7)	0 10(8)	1 91(7)	1 59(6)	1 09(7)	0 007(12)	0 006(14)	0 001(15)
MCNP	1 1(4)	–	–	1 88(6)	–	–	–	–	–

Table 6 (continued)

Dose attenuation at 10 m

	Neutron			FP gamma			Capture gamma		
	a	b	c	a	b	c	a	b	c
Sidewall									
QAD	–	–	–	0 0395	0 0379	0 0397	–	–	–
SAS1	0 0155	0 0184	0 0155	0 0278	0 0270	0 0278	0 0163	0 0116	0 0167
DORT	0 0129	0 0186	0 0136	0 0250	0 0240	0 0251	0 0134	0 00822	0 0133
SAS4	0 0131	0 0174	0 0135	0 0257	0 0183	0 0246	0 0129	0 00906	0 0129
MCNP	0 0135	–	–	0 0261	–	–	–	–	–
Lid									
QAD	–	–	–	0 0110	0 0110	0 0110	–	–	–
DORT	0 00160	0 00160	0 00164	0 00354	0 00354	0 00349	0 00179	0 00179	0 00385
SAS4	0 00175	0 00168	0 00195	0 00611	0 00462	0 00467	0 00170	0 00160	0 00405
MCNP	0 00174	–	–	0 00767	–	–	–	–	–
Bottom									
QAD	–	–	–	0 00940	0 00940	0 00939	–	–	–
DORT	0 00161	0 00159	0 00163	0 00350	0 00350	0 00345	0 00205	0 00205	0 00263
SAS4	0 00172	0 00157	0 00187	0 00424	0 00418	0 00394	0 00200	0 00174	0 00282
MCNP	0 00198	–	–	0 00430	–	–	–	–	–

[a]Case a = dry fuel 38 cm solid cast iron shield
Case b = dry fuel 32 cm cast iron with 6 cm polyethylene
Case c = wet fuel 38 cm solid cast iron shield
Calculations with SAS1 DORT and SAS4 performed using 27n 18g group cross sections (ENDF/B V)
QAD used built in attenuation data and log log interpolation

[b] avg indicates dose is averaged over cavity height for the sidewall doses and over cavity diameter for axial doses Otherwise point detectors are used and located at the axial midplane for the sidewall doses and at the radial center for the axial doses

[c]Number in parentheses indicates percentage standard deviation

[d]Upon rerunning with a finer spatial mesh agreement with the SAS1 results is obtained

top and bottom MCNP results, however, upon close examination of the calculations, no reversal in the geometry model or the dose results was seen

For dose calculations off the cask surface, 1 m, 2 m, and 10 m, the comparisons among the various codes remain very nearly the same There are some exceptions and/or points that need to be discussed, however

1 The QAD CGGP and SAS1 results, while very accurate on the surface, should tend to become more and more conservative[14] at larger distances This trend is seen with the QAD CGGP values being, in general, more con servative than the SAS1 values

2 The MCNP and the nonaveraged SAS4 dose attenuation values are the ra tios of a point dose at locations off the surface to a pseudo point dose at the surface The procedure to produce these pseudo point doses is to scale the surface averaged Monte Carlo doses by a ratio of the DORT point to DORT average doses This scaling is necessary since point detectors were not included at the surface in the Monte Carlo calculations

3 The SAS4 averaged doses and attenuations at locations off the surface tend to be low compared to other sets of results This anomaly is due to the larger surface averaging area employed by SAS4 The larger area (1 m is added to both top and bottom distances) increases the number of particles (improving statistics) contributing to the dose, but yields a lower attenuation factor This effect can be quantified by comparing the dose attenuation factors for average and point values, and appears to be about 30% for neutrons and nearly 50% for gammas

4 2 2 Problem Set 2 Results

The results for problem set 2 are given in Table 7 Calculations performed for this problem included 1 and 2 D discrete ordinates and 3 D Monte Carlo each with multigroup cross sections The 1 D model for case 2a was performed to estimate the magnitude of the approximation, since the problem is clearly 3 D in nature The 2 D approximation for case 2a is shown in Fig 4, followed by plots of the azimuthal variation of the dose in Figs 6–8 Direct comparisons for the results presented in Table 7 are limited since QAD CGGP and MCNP calculations were not performed for this problem It is clear from the results that the 1 D model underestimates the average azimuthal dose by some 40% for both neutrons and FP gammas The results labeled DORT avg are obtained by averaging over the azimuthal direction and are not directly averaged over the axial direction The DORT avg values compare very well with the SAS4 avg values although they are not directly comparable since the SAS4 avg values are averaged over both the azimuthal and axial directions Some spurious results are seen where the SAS4 peak gamma ray doses are lower than the average, however, this can be attributed to the large gamma ray standard deviations at some of the point detector locations

4 2 3 Problem Set 3 Results

Only a select set of calculations was performed for problem set 3 Case 3a was not analyzed and case 3b was analyzed only with the 2 D DORT code The model utilized in these calculations is shown in Fig 5 The infinite height approximation was used, which gives essentially peak or near midplane results Also, only surface doses were calculated

Table 7 Summary results of model problem 2

Doses at specified location (μSv/h)

Dose location	Code	Neutron a	Neutron b	FP gamma a	FP gamma b	Capture gamma a	Capture gamma b
Surface sidewall							
	SAS1	34 3	–	385	–	3 9	–
	DORT	46 2	167	999	652	3 9	22 1
	DORT avg[a]	50 1	186	533	584	3 4	19 6
	SAS4 avg	47 0(3)[b]	188(2)	532(2)	601(2)	–	–
1 m							
	SAS1	10 8	–	147	–	1 4	–
	DORT	–	63 3	–	230	–	5 58
	SAS4	14 9(7)	68 4(6)	127(23)	216(15)	–	–
	SAS4 avg	12 3(4)	46 1(2)	141(2)	162(2)	–	–
2 m							
	SAS1	6 0	–	88 9	–	0 84	–
	DORT	–	34 8	–	139	–	2 78
	SAS4	8 0(5)	37 1(4)	80 2(17)	138(12)	–	–
	SAS4 avg	6 7(4)	26 0(2)	84 6(2)	97 7(2)	–	–
10 m							
	SAS1	0 56	–	10 7	–	0 08	–
	DORT	–	3 14	–	15 4	–	0 22
	SAS4	0 72(4)	3 21(4)	8 77(17)	15 8(11)	–	–

Dose attenuation at specified location

Dose location	Code	Neutron a	Neutron b	FP gamma a	FP gamma b	Capture gamma a	Capture gamma b
1 m							
	SAS1	0 315	–	0 382	–	0 359	–
	DORT	–	0 379	–	0 353	–	0 252
	SAS4	0 323	0 410	0 127	0 331	–	–
	SAS4 avg	0 262	0 245	0 265	0 270	–	–
2 m							
	SAS1	0 175	–	0 231	–	0 215	–
	DORT	–	0 208	–	0 213	–	0 126
	SAS4	0 173	0 222	0 0803	0 212	–	–
	SAS4 avg	0 143	0 138	0 159	0 163	–	–
10 m							
	SAS1	0 0163	–	0 0278	–	0 0205	–
	DORT	–	0 0188	–	0 0236	–	0 0100
	SAS4	0 0156	0 0192	0 00878	0 0242	–	–

[a] Averaged over θ not over Z for case a

[b] Number in parentheses indicates percentage standard deviation

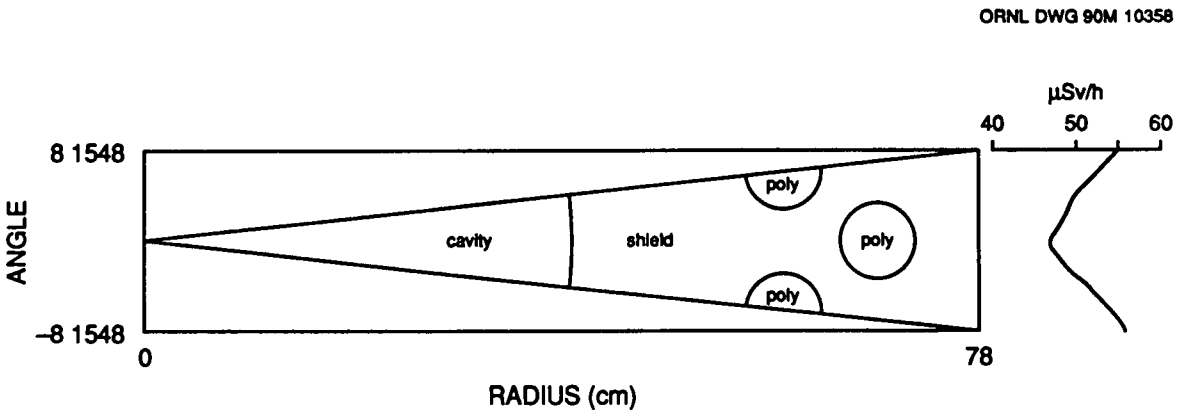

Fig 6 Azimuthal neutron dose distribution for problem 2a

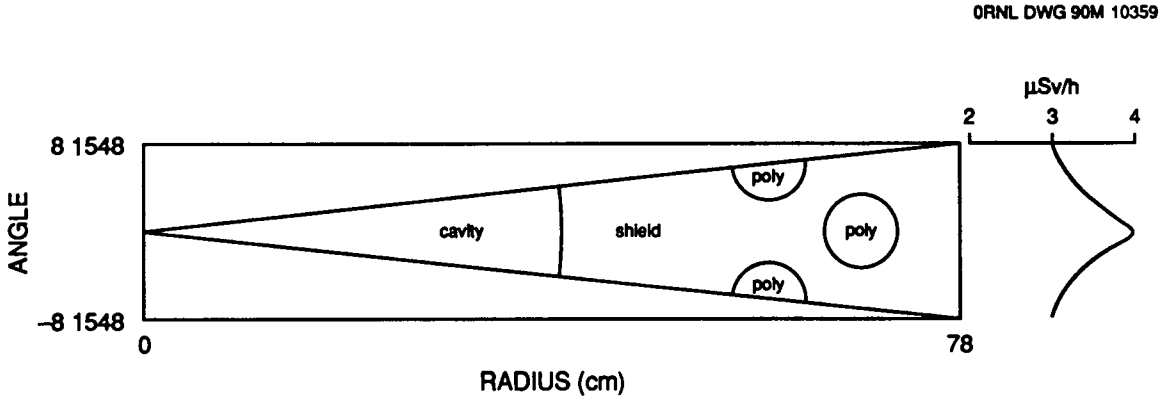

Fig 7 Azimuthal secondary gamma dose distribution for problem 2a

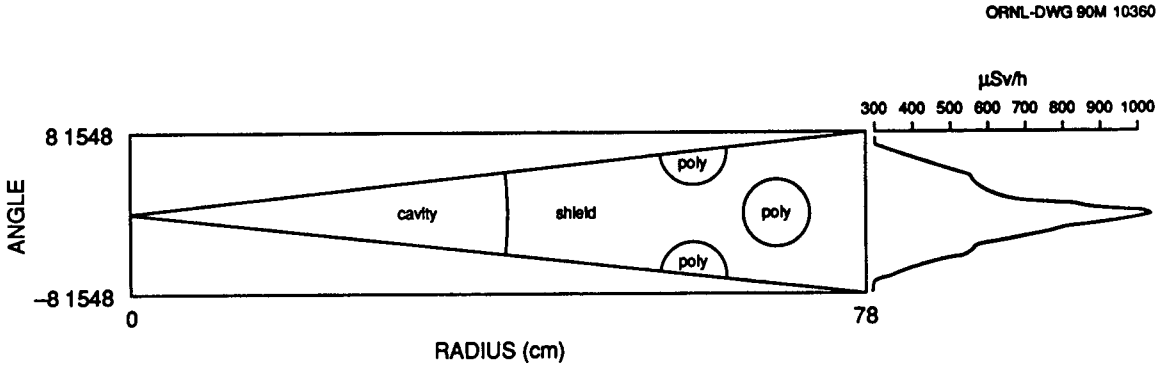

Fig 8 Azimuthal FP gamma dose distribution for problem 2a

Table 8 Summary results of model problem 3b

Dose location	Code	Doses at specified locations (μSv/h) Neutron	FP gamma	Capture gamma
Surface sidewall				
	DORT[a]	156	481	13 1
	DORT avg[b]	133	325	12 3

[a]Peak doses at or near axial midplane

[b]Doses averaged over Z near axial midplane only, does not account for axial leakage

since the results thus far have shown the relationship between surface doses and attenuation at dose locations away from the surface Table 8 gives both the peak doses on the cask surface and the dose averaged over a typical fin axial region (both the fin and epoxy regions) Plots of the axial variation of the dose over one of these fin regions is given in Figs 9–11 The location of peak doses seen in Figs 9–10 is quite interesting and appears to be due to "streaming" between the neutron absorber and the tapered cooling fin While not completely ruled out, the peak location is not believed to be caused by numerical instabilities

4 2 4 Problem Set 4 Results

The final problem set of this series deals primarily with the amount of modeling detail required for the cask basket and assemblies to assure accurate dose results Both cases 4a (dry basket) and 4b (wet basket) were analyzed using a 1 D approximate model Selected calculations were performed for a cast iron shield body (SAS4 only) and a steel cask body (SAS4 and SAS1) since the original specifications were for a steel cask body, but were later modified to specify a cast iron body The 3 D results shown in Table 9 include models with pin by pin and homogenized assemblies within the basket model Only case 4a was analyzed for both pin by pin and homogeneous assembly descriptions The pin by pin neutron results are about 15% higher than the homogeneous assembly results The pin by pin gamma results are some 44% higher than those for a homogeneous assembly However, the pin by pin calculations were performed with the standard SCALE 27n 18g library (library 3a in Table 1), while the homogeneous assembly calculations were performed with the modified 27n 18g library (library 3c in Table 1) From Table 2 it can be seen that library 3a yields neutron/gamma doses 20 and 56% higher than those from library 3c Applying these corrections results in pin by pin values for neutron/gammas of 5 and 8% lower than the homogeneous results These trends are in agreement with a previous study[1] where neutron/gamma differences of 5 and 15% were seen

The only difference in problems 4a/b and problems 1a/c is the explicit modeling of the basket in problem 4 This allows a direct comparison of the effect of basket smearing For the dry cases, 1a and 4a, the neutron dose results appear to be higher for the explicit basket than for a smeared basket The difference is only about 5%, which is still somewhat surprising since it is generally assumed that basket smearing will overpredict the dose This dose overprediction by basket smearing is seen for the neutron wet case (1c versus 4b) as well as both the wet and dry gamma cases

5 PROBLEMS 5 AND 6 ANALYSIS

Model problems 5 and 6 are unique in that they require the user to calculate the neutron and photon source strengths and spectra The sources in the previous problems are specified in Table A 19 of NEACRP L 290 (attached as the Appendix) This phase of the shielding benchmark problem introduces an additional level of complexity and should serve to identify problem areas concerning the calculation of sources

5 1 SOLUTION TECHNIQUES

The basic computational tool used for these problems was the Shielding Analysis Sequence 2H (SAS2H) of the SCALE code system [2] This sequence uses the point de pletion code ORIGEN S[2] to calculate burnup and decay and to produce the radiation source strengths and spectra Another popular depletion code, ORIGEN2,[15] was used

ORNL-DWG 90M 10363

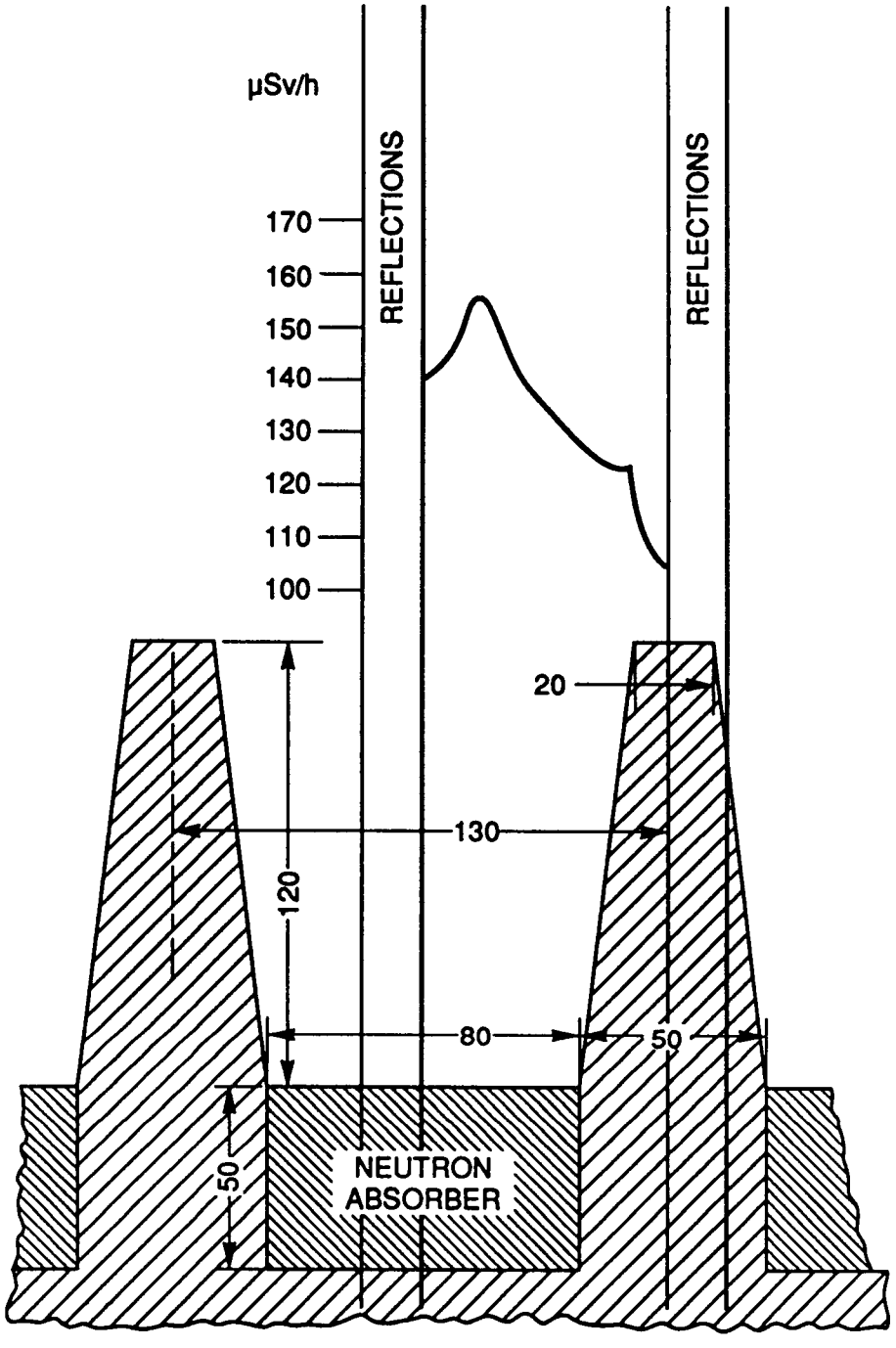

Fig 9 Neutron equivalent dose rate axial distribution on the cask outer surface (problem 3b) All dimensions in mm

ORNL DWG 90M 10362

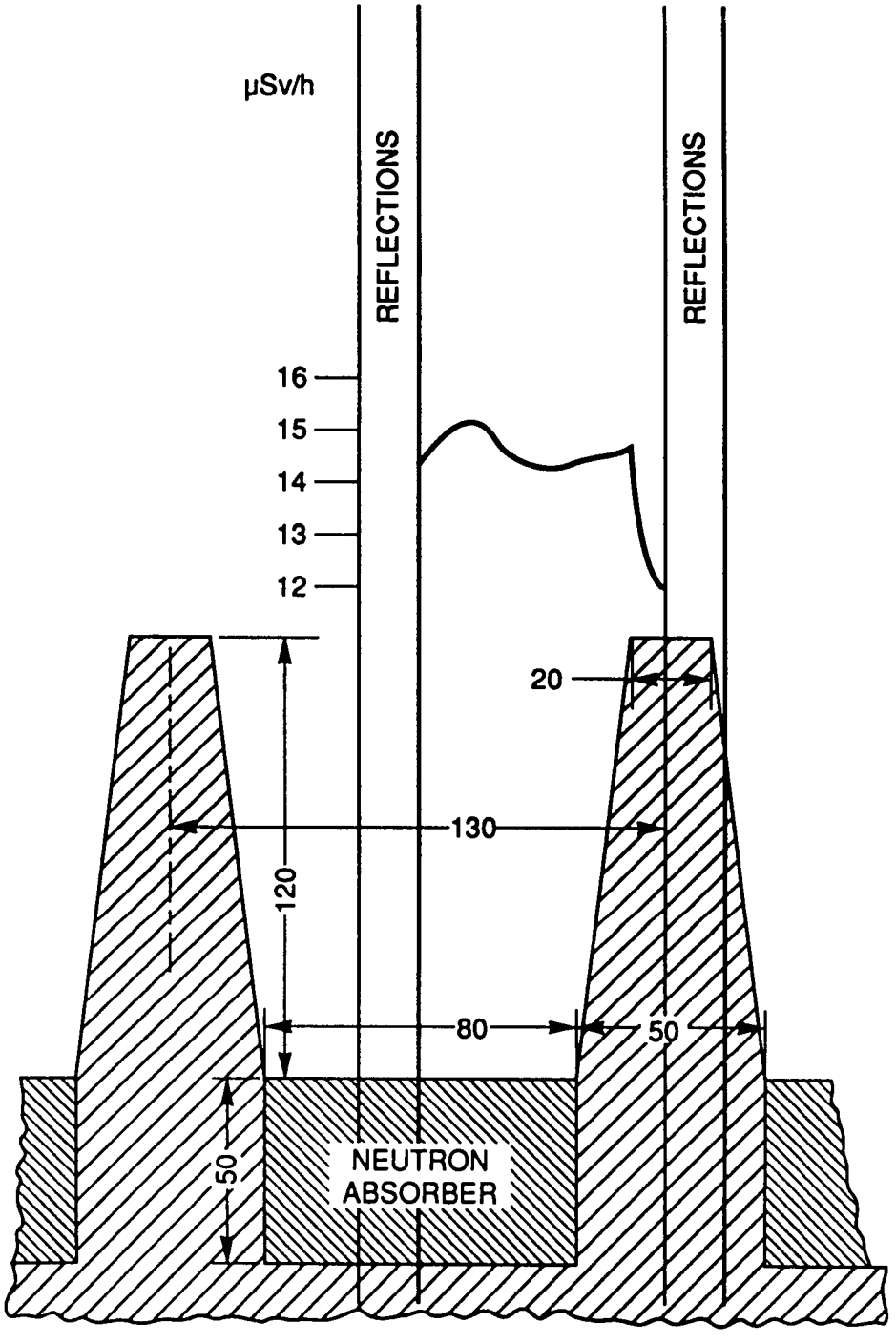

Fig 10 Neutron induced gamma equivalent dose rate axial distribution on the cask outer surface (problem 3b) All dimensions in mm

ORNL DWG 90M 10364

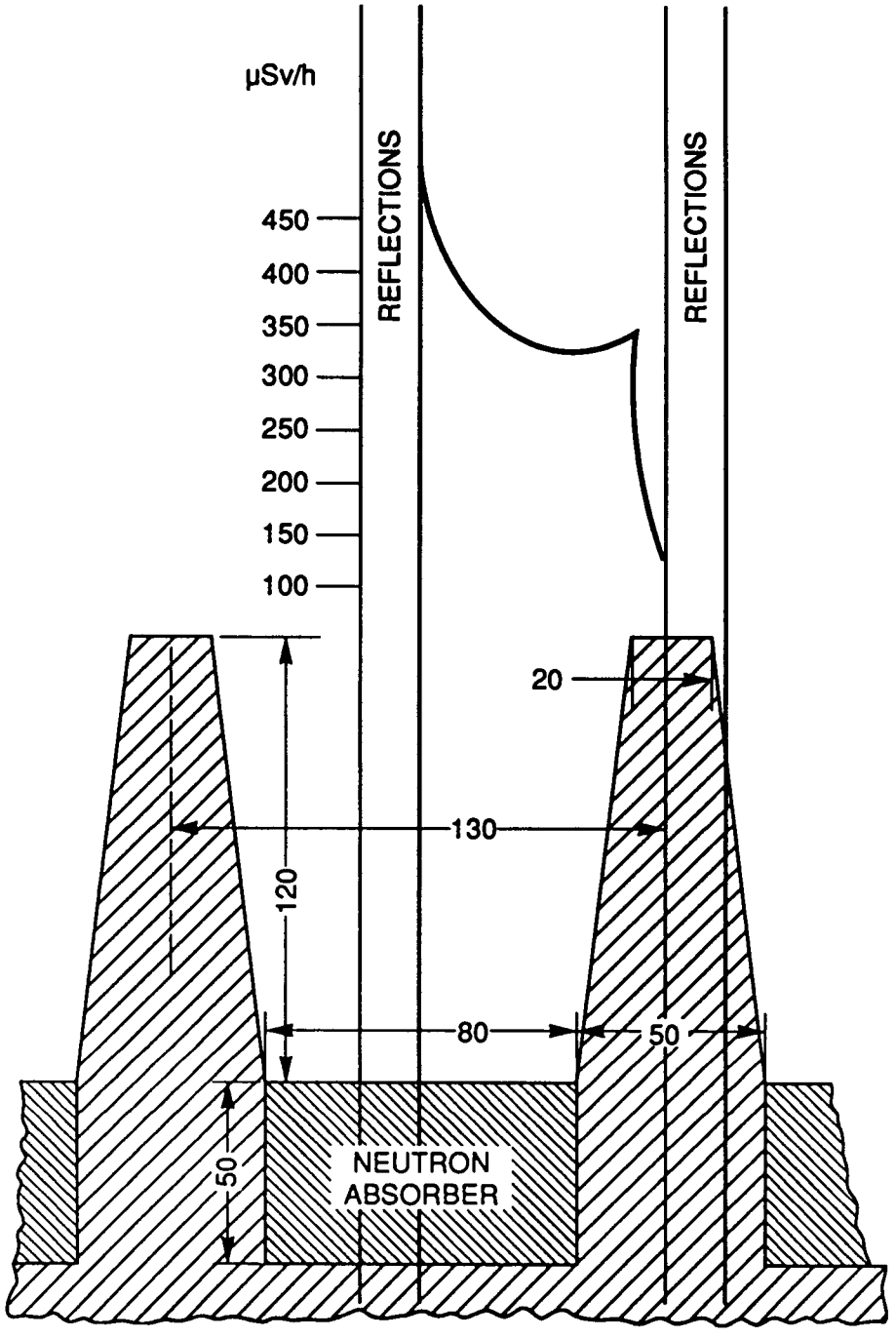

Fig 11 Fission product gamma equivalent dose rate distribution on the cask outer surface (problem 3b) All dimensions in mm

Table 9 Summary results of model problem 4

Doses at specified location (μSv/h)

Dose location	Code	Neutron a	Neutron b	FP gamma a	FP gamma b	Capture gamma a	Capture gamma b
Surface sidewall							
	SAS1[a]	1183	61 7	136	79 6	10 8	0 44
	SAS4 avg[b]	507(2)[c]	35 8(3)	205(5)	118(4)	–	–
	SAS4-avg[a]	–	–	64 5(6)	–	–	–
	SAS4-avg[d]	484(3)	–	189(10)	–	–	–
1m							
	SAS1[a]	368	19 2	51 5	30 2	3 53	0 14
	SAS4	162(4)	12 5(8)	73 6(12)	57 0(10)	–	–
	SAS4-avg	109(1)	7 17(3)	52 2(5)	29 3(4)	–	–
	SAS4[a]	–	–	21 2(13)	–	–	–
	SAS4-avg[a]	–	–	16 2(5)	–	–	–
	SAS4[d]	175(6)	–	80 6(9)	–	–	–
	SAS4-avg[d]	104(3)	–	48 2(10)	–	–	–
2m							
	SAS1[a]	204	10 7	31 3	18 3	1 99	0 08
	SAS4	79 9(3)	5 76(8)	41 6(10)	32 1(9)	–	–
	SAS4-avg	59 1(1)	3 91(3)	31 1(5)	17 5(4)	–	–
	SAS4[a]	–	–	14 3(11)	–	–	–
	SAS4-avg[a]	–	–	9 70(6)	–	–	–
	SAS4[d]	87 6(4)	–	54 0(8)	–	–	–
	SAS4 avg[d]	56 6(3)	–	28 7(11)	–	–	–
10m							
	SAS1[a]	18 3	0 95	3 83	2 24	0 18	0 007
	SAS4	5 89(3)	0 40(6)	4 07(8)	2 82(8)	–	–
	SAS4[a]	–	–	1 51(12)	–	–	–
	SAS4[d]	5 44(4)	–	3 44(8)	–	–	–

Dose attenuation at specified location

Dose location	Code	Neutron a	Neutron b	FP gamma a	FP gamma b	Capture gamma a	Capture gamma b
1m							
	SAS1	0 311	0 311	0 379	0 379	0 327	0 318
	SAS4 avg	0 215	0 200	0 255	0 248	–	–
	SAS4 avg[a]	–	–	0 251	–	–	–
	SAS4 avg[d]	0 216	–	0 255	–	–	–
2m							
	SAS1	0 172	0 173	0 230	0 230	0 184	0 182
	SAS4 avg	0 117	0 109	0 152	0 148	–	–
	SAS4 avg[a]	–	–	0 150	–	–	–
	SAS4-avg[d]	0 117	–	0 152	–	–	–
10m							
	SAS1	0 0155	0 0154	0 0282	0 0281	0 0167	0 0159

[a]Cask material is 1 4541 material instead of cast iron for all others the cask material is cast iron

[b] Avg indicates case is averaged over cavity height

[c]Number in parentheses indicates percentage standard deviation

[d]Indicates pin by pin assembly model all others use a homogeneous assembly model Includes a factor to account for use of different cross-section library (see Sect 4 2 4)

to calculate the average burnup case for problem 5 for comparison This section briefly describes the methodologies and data used by each of these codes

5 1 1 SAS2H/ORIGEN-S

Figure 12 illustrates the basic calculational procedure used by SAS2H to produce cross section data, calculate spent fuel sources, and subsequently use this data in a shipping cask shielding analysis The sequence SAS2H starts with data describing a particular fuel assembly including compositions, temperatures, geometry, and time dependent specific power A standard cross section library is specified, in this case the SCALE 27n 18g shielding library[2] was used This is the standard SCALE 27n 18g library, not the special purpose library used in analysis of problems 1–4 BONAMI S and NITAWL S are then used to perform resonance self shielding treatments for nuclides with the appropriate data Cell weighted cross sections are computed for a fuel pin cell (PART A) using XSDRNPM S A second unit cell (PART B) is defined as to be representative of the fuel assembly The PART B model has an assembly guide tube or other non fuel type rod at its center and is surrounded by a region of the cell weighted fuel Cross sections are computed for this larger unit cell and the sequence invokes COUPLE to update the ORIGEN S working library with these cell weighted data ORIGEN S uses these cross section data to compute the number densities of the various nuclides in the fuel as a function of time and the process is repeated for each step in the specified power history (specific power and exposure times) In the final pass, after COUPLE has updated the ORIGEN S working library, an ORIGEN S depletion case using these burnup dependent, time dependent cross sections is used to calculate the discharge composition of the fuel assembly and a decay only subcase is used to predict the composition for the cooling time at which the fuel is to be loaded and shipped This final composition is used in the determination of neutron and gamma sources to be applied in the final shipping cask analysis

In the shielding analysis, cell weighted cross sections for the fuel zone in the shipping cask are calculated using the BONAMI S, NITAWL S, XSDRNPM S sequence These fuel zone cross sections are used in the shipping cask model and the XSDRNPM S calculated fluxes are then used in XSDOSE to obtain dose rates

5 1 2 ORIGEN2

The ORIGEN2 and ORIGEN S (used in SAS2H) codes use the same basic matrix exponential expansion method and numerical scheme as the original ORIGEN[16] code released in 1973 The primary differences between ORIGEN S and ORIGEN2 are the cross section and fission product yield data used by the two codes Both codes use essentially identical decay data (half lives, branching ratios, etc) and photon data (energies and intensities of gamma and x ray spectra

ORIGEN2 uses specific burnup dependent cross section and fission product yield libraries developed by performing multigroup reactor physics and depletion calculations for specific reactor models These libraries include a uranium fueled PWR using a once through fuel cycle at a typical burnup (33 GWd/MTU) nd at an extended burnup (50 GWD/MTU) [17] The average burnup for problems 5 nd 6 was given as 40 GWd/MTU The library recommended for problem 5 is the PWR library with extended burnup as there is no provision for reactor problems where the burnup exceeds the library maximum The 33 GWd/MTU library has also been used to illustrate the differences that can be expected as a result of improper cross section data

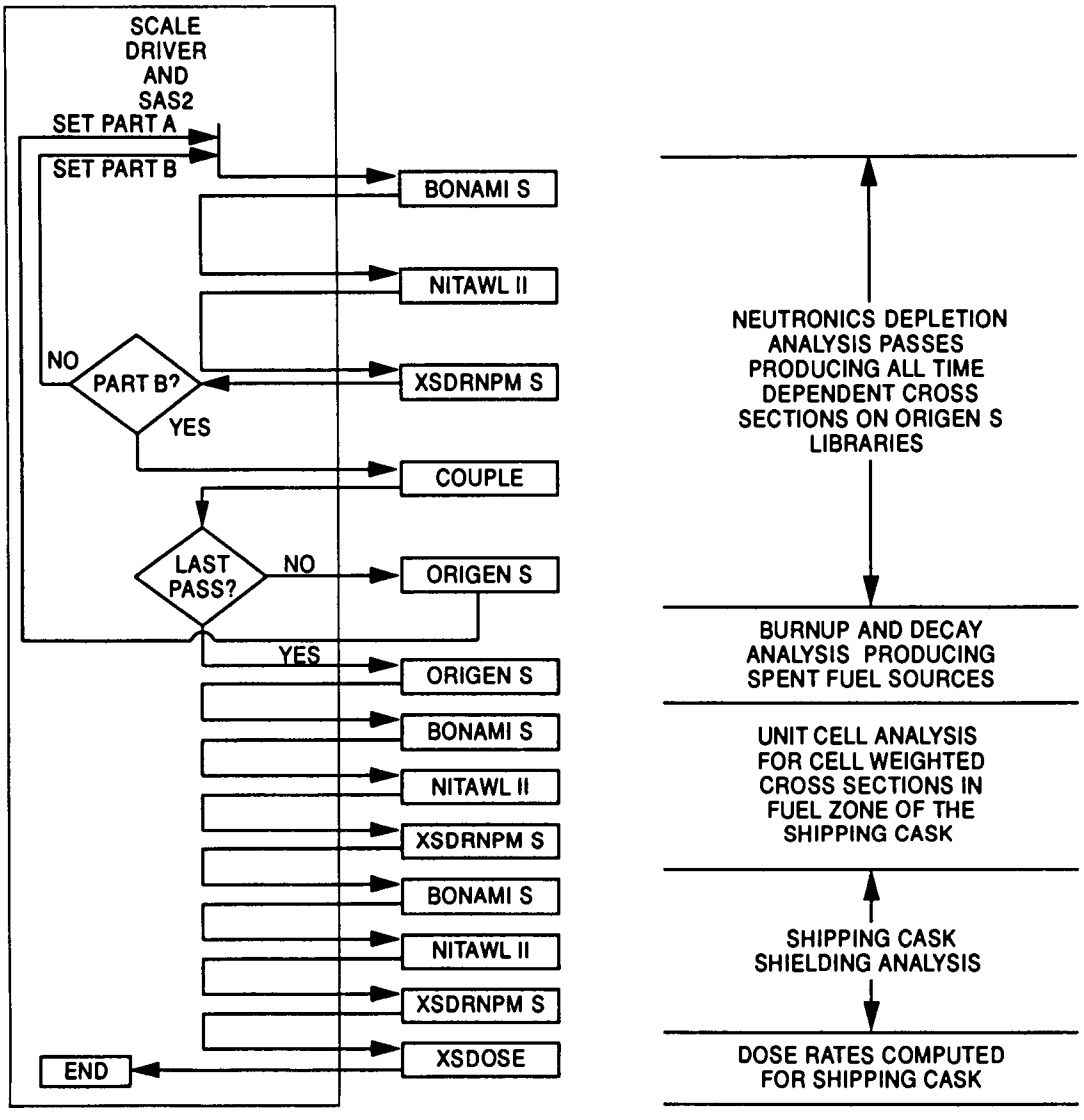

Fig 12 Basic flow invoked by SAS2H

The ORIGEN2 calculations were performed only for problem 5 and include neutron and photon source strengths and photon spectra Neutron spectra are not calculated by ORIGEN2

5 2 RESULTS

This section summarizes the results for the UO_2 fuel (problem 5) using both the SAS2H/ORIGEN S sequence and the ORIGEN2 code Two different cross section libraries were used for the ORIGEN2 calculations and those results are compared The results for the mixed oxide fuel (problem 6) using the SAS2H/ORIGEN S sequence are also given All results are for a two year cooling time

5 2 1 Neutron Sources

The results of the neutron source analysis for problem 5 are summarized in Tables 10–14 and Fig 13 A comparison of neutron source strengths for an average burnup of 40 GWd/MTU is given in Table 10 The neutron production rates from spontaneous fission, (α,n) reactions, and the total source for five fuel assemblies are given in units of n/s Both ORIGEN2 results predict higher neutron source strengths than the SAS2H/ORIGEN S result, with ORIGEN2/ORIGEN S ratios of 1 04 and 1 14 for the 33 and 50 GWd/MTU cases Tables 11–12 show the contribution to the total neutron source from several important nuclides Table 11 contains the SAS2H/ORIGEN S results, and the ORIGEN2 results using the 33 GWd/MTU and the 50 GWd/MTU libraries are given in Table 12 The contribution of each nuclide is given as n/s for five fuel assemblies, and also as the percentage of total More than 99% of the total neutron source is produced by the nuclides specified in Tables 11 and 12

The problem specification included a study based on axial distributed burnup Neutron source strengths as a function of axial peaking factor are given in Table 13 for the SAS2H/ORIGEN S sequence (the ORIGEN2 calculations were performed for the average burnup case only) Figure 13 shows how the various axial peaking factors (in brackets) are distributed along the length of the fuel rod The percentage of the total neutron source produced in each section of the fuel rod is also given The sources given in Table 13 are weighted by the appropriate fractional rod height and summed to yield a burnup dependent source strength of $2\ 099 \times 10^9$ n/s This value is significantly (>55%) higher than the neutron source strength reported in Table 10 for an average burnup (i e , axial peaking factor equal to 1 0)

SAS2H/ORIGENS also calculates the energy spectrum of the neutron source, which is given in Table 14 The group structure given in this table corresponds to the first seven groups of the 27 neutron groups in the SCALE 27n 18g shielding library used for these calculations Groups 8 through 27 contain no source neutrons

The neutron results for the MOX used in problem 6 are given in Tables 15–18 and Fig 14 Neutron source strengths at the average burnup (40 GWd/MTU) are given in Table 15 (Only the SAS2H/ORIGEN S sequence was used to calculate problem 6) The contributions from both spontaneous fission and (α,n) production are given Essentially all source neutrons are produced by the nuclides listed in Table 16 where the contribution by each nuclide is given as both n/s and percentage of total neutron source Table 17 gives the MOX neutron source strengths as a function of axial peaking factors The distribution along the rod height of the neutron source as a percentage of total is illustrated in Fig 14 The total neutron source strength calculated using axially dependent burnup

Table 10 Problem 5 (UO_2) Results for five fuel assemblies, comparison of neutron source strength at average burnup

	Spontaneous fission (n/s)	α,n (n/s)	Total (n/s)
SAS2H	1 3185E9[a]	3 0675E7	1 3490E9
ORIGEN2[b]	1 5040E9	3 6540E7	1 5400E9
ORIGEN2[c]	1 371E9	3 364E7	1 405E9

[a]Read as $1\ 3185 \times 10^9$
[b]Using 50 GWd/MTU library
[c]Using 33 GWd/MTU library

Table 11 Problem 5 (UO_2) Contribution to neutron source strength from important nuclides for five fuel assemblies (SAS2H)

Nuclide	Nuclide source strength n/s	%
^{238}Pu	1 155E7[a]	0 856
^{239}Pu	5 303E5	0 039
^{240}Pu	5 805E6	0 430
^{242}Pu	2 688E6	0 199
^{241}Am	1 245E6	0 092
^{243}Am	5 829E4	0 004
^{242}Cm	5 285E7	3 918
^{243}Cm	2 238E4	0 002
^{244}Cm	1 265E9	93 773
^{246}Cm	7 450E6	0 552
^{248}Cm	6 400E4	0 005
^{250}Cf	4 130E4	0 003
^{252}Cf	2 490E6	0 1846

[a]Read as $1\ 155 \times 10^7$

Table 12 Problem 5 (UO_2) Contribution to neutron source strength from important nuclides for five fuel assemblies (ORIGEN2)

Nuclide	50 GWd/MTU (n/s)	33 GWd/MTU (n/s)
^{238}Pu	1 300E7[a]	1 2573E7
^{239}Pu	5 928E5	5 233E5
^{240}Pu	6 088E6	6 378E6
^{242}Pu	2 794E6	2 550E6
^{241}Am	1 551E6	1 277E6
^{243}Am	6 606E4	6 039E4
^{242}Cm	5 922E7	5 249E7
^{243}Cm	1 205E5	1 019E5
^{244}Cm	1 449E9	1 321E9
^{246}Cm	7 587E6	7 314E6
^{248}Cm	2 636E4	
^{250}Cf	1 461E4	
^{252}Cf	5 337E5	

[a]Read as $1\ 300 \times 10^7$

Table 13 Problem 5 (UO_2) Results for five fuel assemblies (SAS2H)

Axial peaking	Neutron source strength (n/sec)		
	Spon fission	(α,n)	Total
0 18	1 4550E6[a]	8 1050E5	2 2655E6
0 4	2 2825E7	3 8245E6	2 6650E7
0 6	1 3570E8	9 2550E6	1 4495E8
0 8	4 9580E8	1 7915E7	5 135E8
1 0	1 3185E9	3 0675E7	1 3490E9
1 2	2 8295E9	4 8375E7	2 8780E9
1 32	4 1590E9	6 1600E7	4 2205E9

[a]Read as $1\ 4550 \times 10^6$

Table 14 Problem 5 (UO_2) Neutron source spectra for five fuel assemblies (SAS2H)

Group	Group energy limits (MeV)	(n/sec)
1	20 00 – 6 43	2 48E7[a]
2	6 43 – 3 0	2 85E8
3	3 00 – 1 85	3 15E8
4	1 85 – 1 4	1 76E8
5	1 40 – 0 9	2 38E8
6	0 90 – 0 4	2 60E8
7	0 40 – 0 1	5 09E7
Total		1 35E9

[a]Read as $2\ 48 \times 10^7$

Table 15 Comparison of neutron source strength at average burnup

	Spontaneous fission (n/s)	α,n (n/s)	Total (n/s)
Average burnup	4 858E9[a]	9 625E7	4 954E9
Axially dependent burnup	–	–	6 035E9

[a]Read as $4\ 858 \times 10^9$

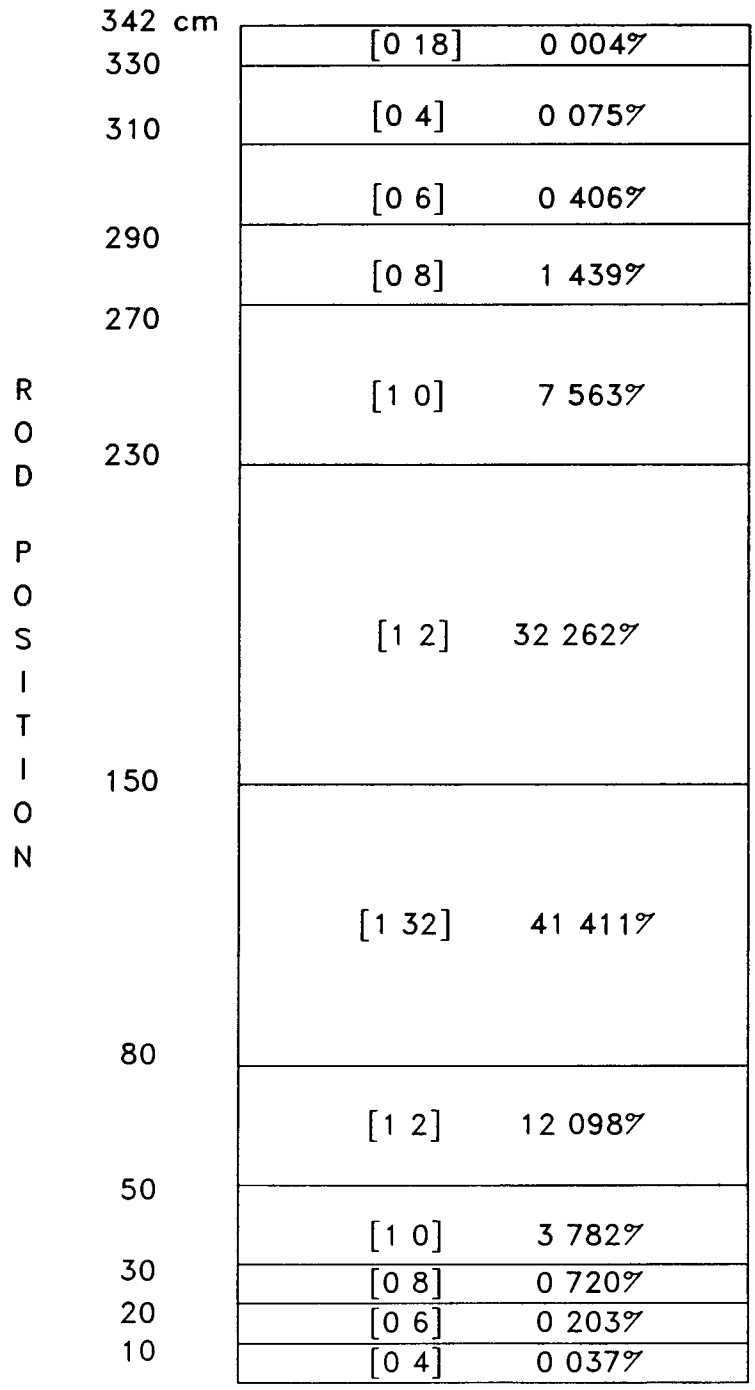

Fig 13 Problem 5 Axially distributed neutron source as a percentage of total (Values in brackets are axial peaking factors)

Table 16 Problem 6 (MOX) Contribution to neutron source strength from important nuclides for five fuel assemblies

Nuclide	Nuclide source strength	
	n/s	%
^{238}Pu	1 674E7[a]	0 338
^{239}Pu	1 151E6	0 023
^{240}Pu	2 077E7	0 419
^{242}Pu	6 859E6	0 138
^{241}Am	4 997E6	0 101
^{243}Am	1 754E5	0 004
^{242}Cm	2 314E8	4 671
^{243}Cm	5 612E4	0 001
^{244}Cm	4 625E9	93 359
^{246}Cm	3 225E7	0 651
^{248}Cm	4 400E5	0 009
^{250}Cf	2 850E5	0 006
^{252}Cf	1 665E7	0 336

[a]Read as 1 674 $\times$ 10^7

Table 17 Problem 6 (MOX) Results for five fuel assemblies

Axial peaking	Neutron source strength (n/s)		
	Spon fission	(α,n)	Total
0 18	1 2430E8[a]	1 855E7	1 4285E8
0 4	5 5300E8	3 240E7	5 8550E8
0 6	1 3625E9	4 941E7	1 4120E9
0 8	2 7405E9	7 065E7	2 8115E9
1 0	4 8580E9	9 625E7	4 9545E9
1 2	7 8900E9	1 264E8	8 0150E9
1 32	1 0240E10	1 467E8	1 0390E10

[a]Read as 1 2430 $\times$ 10^8

Table 18 Problem 6 (MOX) Neutron source spectra for five fuel assemblies

Group	Group energy limits (MeV)	(n/s)
1	20 00 – 6 43	9 15E7[a]
2	6 43 – 3 0	1 05E9
3	3 00 – 1 85	1 15E9
4	1 85 – 1 4	6 45E8
5	1 40 – 0 9	8 75E8
6	0 90 – 0 4	9 57E8
7	0 40 – 0 1	1 87E8
Total		4 95E9

[a]Read as 9 15 $\times$ 10^7

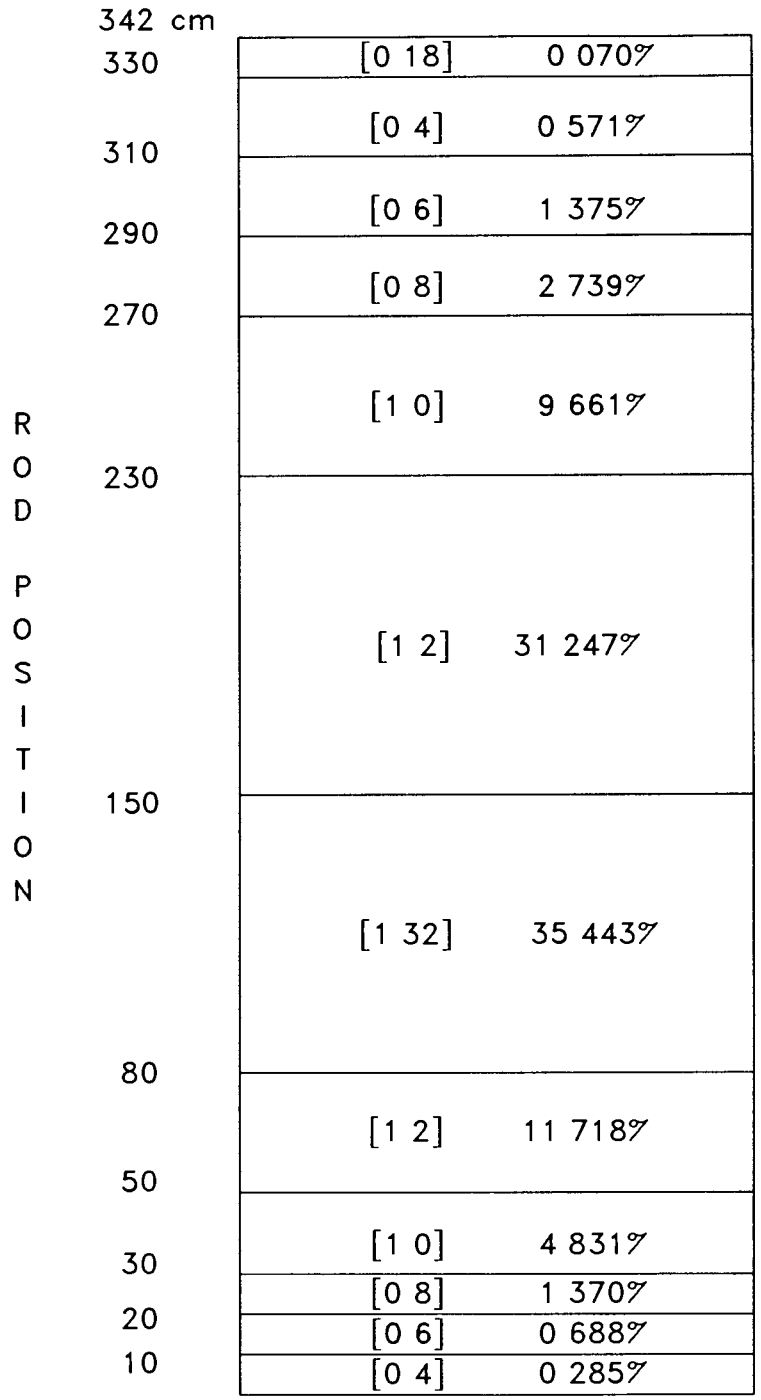

Fig 14 Problem 6 (MOX) Axially distributed neutron source as a percentage of total (Values in brackets are axial peaking factors)

is 6 035 × 10^9 n/s, ~22% higher than the value calculated at the average burnup Table 18 gives the total neutron source spectrum for five MOX fuel assemblies

5 2 2 Photon Sources

Results from the analysis of the photon sources in the UO_2 fuel of problem 5 are given in Tables 19–24 and Fig 15 A comparison of photon source strengths at average burnup for five fuel assemblies, including the results from the SAS2H/ORIGEN S sequence and the two ORIGEN2 cases, is given in Table 19 Contributions to the photon source strength (γ/s) from actinide and fission product nuclides are given, as well as the total photon production rates The ORIGEN2 calculations show very small (<2%) differences between the results using the 33 GWd/MTU library and those using the 50 GWd/MTU library Tables 20 and 21 give the contribution to gamma source strength from important nuclides for five assemblies at average burnup The SAS2H/ORIGEN S results are given in Table 20 in units of γ/s and as a percentage of the total photon source Greater than 96% of the total photon source predicted by ORIGEN S is produced by the nuclides listed in Table 20 Table 21 gives the results from the ORIGEN2 calculations using the 50 GWd/MTU library in units of γ/s, MeV/s, and grams The 33 GWd/MTU results are given only in units of grams for comparison In the ORIGEN2 cases, the nuclides in Table 21 account for >98% of the total photon source

Photon source strengths as a function of axial peaking factors (burnup) are given in Table 22 The axial variation in burnup was evaluated with only the SAS2H/ORIGEN S sequence The total photon source strength for problem 5 calculated using these axially dependent burnups is 1 069 × 10^{17} which is ~2 3% higher than the value at average burnup (see Table 19) Figure 15 shows the variation of axial peaking factors (in brackets) along the length of a fuel rod as well as the percentage of total photon source produced in each of the axial regions

Table 23 gives the photon source spectra in the 18 energy group structure of the SCALE 27n 18g shielding library as calculated by the SAS2H/ORIGEN S sequence The group structure used in the ORIGEN2 cases and given in Table 24 is fixed by ORIGEN2 itself and cannot be altered Therefore, a direct comparison of spectra by energy group is possible only between the two ORIGEN2 cases This comparison reveals that the two libraries perform similarly in predicting photon source spectra

The photon results for the MOX fuel of problem 6 are given in Tables 25–28 and Fig 16 Only the SAS2H/ORIGEN S sequence was used to predict photon sources in problem 6 Photon source strengths at average burnup are given in Table 25 for five MOX fuel assemblies Contributions from both actinide and fission product nuclides are noted Table 26 shows the contribution from individual nuclides, which account for >96% of the total gamma source The results based on axially dependent burnup are given in Table 27 and Fig 16 The total photon source calculated from these data for five fuel assemblies is 1 116 × 10^{17}, <2% higher than the source strength calculated at the average burnup Table 28 gives the photon source spectrum for five MOX fuel assemblies

5 2 3 Dose Calculations (Problem 5)

The neutron and photon source spectra calculated for problem 5 at average burnup and axial dependent burnup using the SAS2H/ORIGEN S sequence were used in conjunction with the cask model of problem 1a to predict dose rates on the cask midplane at the surface The dose calculations were performed using the 2 D discrete ordinates code, DORT, using a source corresponding to the one shown in Table 23, but in the SCALE 27n 18g group

Table 19 Problem 5 (UO_2) Results for five fuel assemblies, comparison of photon source strength at average burnup

	Actinides (γ/s)	Fission products (γ/s)	Total (γ/s)
USA			
SAS2H	2 160E14[a]	1 025E17	1 0450E17
ORIGEN2[b]	2 389E14	1 086E17	1 1026E17
ORIGEN2[c]	2 174E14	1 070E17	1 087E17

[a]Read as 2 160 × 10^{14}
[b]Using 50 GWd/MTU library
[c]Using 33 GWd/MTU library

Table 20 Problem 5 (UO_2) Contribution to gamma source strength from important nuclides for five fuel assemblies (SAS2H)

Nuclide	Nuclide source strength (γ/s)	%
^{90}Sr	1 124E15[a]	1 076
^{90}Y	7 109E15	6 803
^{95}Nb	1 275E14	0 122
^{106}Rh	2 658E16	25 435
^{110m}Ag	4 450E13	0 043
^{125}Sb	3 383E14	0 324
^{125m}Te	1 670E14	0 160
^{134}Cs	2 161E16	20 679
^{137}Cs	1 441E15	1 379
^{137m}Ba	9 365E15	8 962
^{144}Ce	5 580E15	5 340
^{144}Pr	2 444E16	23 388
^{154}Eu	2 052E15	1 964
^{155}Eu	4 195E14	0 401

[a]Read as 1 124 × 10^{15}

Table 21 Problem 5 (UO_2) Contribution to gamma source strength from important nuclides for five fuel assemblies (ORIGEN2 cases)

Nuclide	Nuclide source strength γ/s	MeV/s	50 GWd/MTU grams	33 GWd/MTU grams
^{90}Sr	1 202E15[a]	3 582E13	1 29E03	1 32E03
^{90}Y	7 377E15	4 891E14	3 24E 1	3 31E 1
^{95}Nb	1 010E14	8 345E13	7 53E 2	7 54E 2
^{106}Rh	3 033E16	5 116E15	1 10E 4	1 07E 4
^{110m}Ag	2 488E14	1 975E14	4 09E 1	3 95E 1
^{125}Sb	1 325E15	3 824E14	2 31E01	2 28E01
^{125m}Te	2 865E14	7 676E12	3 24E 1	3 18E 1
^{134}Cs	2 231E16	1 470E16	1 97E02	1 88E02
^{137}Cs	1 575E15	4 690E13	3 10E03	3 1E03
^{137m}Ba	1 037E16	5 606E16	4 74E 14	4 74E 4
^{144}Ce	5 175E15	3 565E14	1 39E02	1 39E02
^{144}Pr	2 487E16	2 391E15	5 86E 3	5 89E 3
^{154}Eu	2 311E15	1 326E15	1 07E02	1 05E02
^{155}Eu	5 182E14	3 755E13	3 58E01	3 30E01

[a]Read as 1 202 × 10^{15}

Table 22 Problem 5 (UO_2) Results for five fuel assemblies (SAS2H)

Axial peaking	Photon source strength (γ/s) Actinides	Fission products	Total
0 18	6 850E12[a]	1 360E16	1 389E16
0 4	3 425E13	3 345E16	3 413E16
0 6	7 600E13	5 400E16	5 509E16
0 8	1 355E14	7 750E16	7 903E16
1 0	2 160E14	1 025E17	1 045E17
1 2	3 215E14	1 290E17	1 315E17
1 32	3 990E14	1 460E17	1 489E17

[a]Read as 6 850 × 10^{12}

Table 23 Problem 5 (UO_2) Photon source spectra for five fuel assemblies (SAS2H)

Group	Group energy limits (MeV)	γ/s
1	0 00 – 0 02	3 00E16[a]
2	0 02 – 0 04	1 29E16
3	0 04 – 0 07	7 13E15
4	0 07 – 0 10	4 35E15
5	0 10 – 0 14	5 20E15
6	0 14 – 0 20	2 83E15
7	0 20 – 0 40	3 29E15
8	0 40 – 0 90	3 54E16
9	0 90 – 1 35	2 89E15
10	1 35 – 1 80	4 35E14
11	1 80 – 2 20	1 71E14
12	2 20 – 2 60	1 51E13
13	2 60 – 3 00	2 43E12
14	3 00 – 3 50	3 98E11
15	3 50 – 4 00	2 26E8
16	4 00 – 4 50	2 94E7
17	4 50 – 5 00	1 71E7
18	5 00 – 6 00	1 55E7
Total		1 045E17

[a]Read as $3\ 00 \times 10^{16}$

Table 24 Problem 5 (UO_2) Photon source spectra for five fuel assemblies (ORIGEN2 cases)

Group	Group energy limits (MeV)	50 GWd/MTU γ/s	33 GWd/MTU γ/s
1	0 00 – 0 02	3 19E16[a]	3 17E16
2	0 02 – 0 03	7 45E15	7 39E15
3	0 03 – 0 045	7 42E15	7 37E15
4	0 045 – 0 07	6 63E15	6 58E15
5	0 07 – 0 10	4 62E15	4 58E15
6	0 10 – 0 15	5 16E15	5 13E15
7	0 15 – 0 30	4 05E15	4 02E15
8	0 30 – 0 45	2 33E15	2 31E15
9	0 45 – 0 70	2 81E16	2 74E16
10	0 70 – 1 00	9 67E15	9 25E15
11	1 00 – 1 50	2 63E15	2 65E15
12	1 50 – 2 00	1 12E14	1 09E14
13	2 00 – 2 50	1 46E14	1 46E14
14	2 50 – 3 00	3 22E12	3 13E12
15	3 00 – 4 00	4 00E11	3 95E11
16	4 00 – 6 00	6 63E7	6 04E7
17	6 00 – 8 00	7 64E6	6 97E6
18	8 00 – 11 00	8 78E5	8 00E5
Total		1 102E17	1 087E17

[a]Read as $3\ 19 \times 10^{16}$

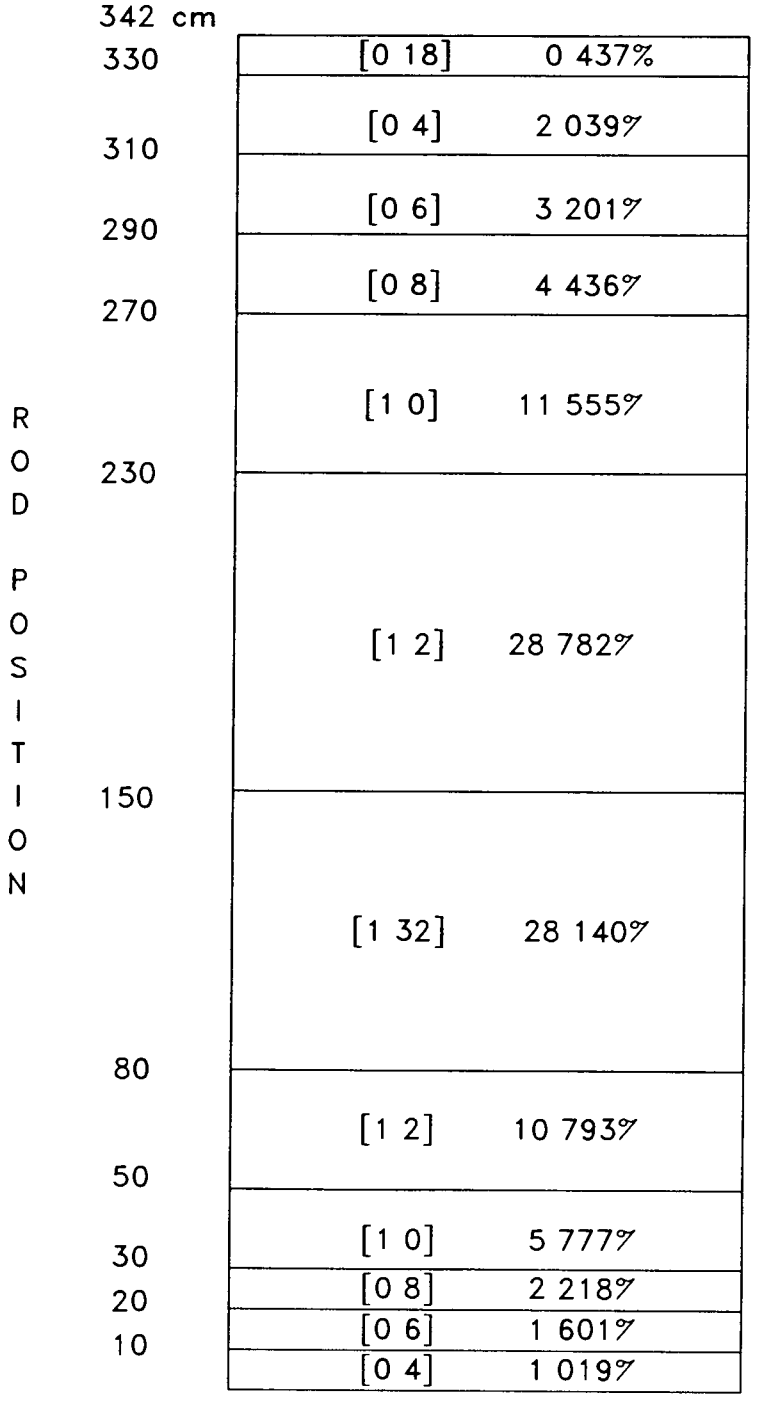

Fig 15 Problem 5 Axially distributed photon source as a percentage of total (Values in brackets are axial peaking factors)

Table 25 Problem 6 (MOX) Comparison of photon source strength at average burnup

	Actinides (γ/s)	Fission products (γ/s)	Total (γ/s)
Average burnup	6 800E14[a]	1 075E17	1 096E17
Axially dependent burnup	–	–	1 116E17

[a]Read as 6 800 × 10^{14}

Table 26 Problem 6 (MOX) Contribution to gamma source strength from important nuclides for five fuel assemblies

	Nuclide source strength	
Nuclide	n/s	%
^{90}Sr	4 350E14[a]	0 397
^{90}Y	4 212E15	3 843
^{95}Nb	1 180E14	0 108
^{106}Rh	3 936E16	35 912
^{110m}Ag	4 314E14	0 394
^{125}Sb	1 036E15	0 945
^{125m}Te	2 480E14	0 226
^{134}Cs	1 944E16	17 737
^{137}Cs	1 449E15	1 322
^{137m}Ba	9 475E15	8 645
^{144}Ce	4 865E15	4 439
^{144}Pr	2 126E16	19 398
^{154}Eu	2 531E15	2 309
^{155}Eu	6 075E14	0 554

[a]Read as 4 350 × 10^{14}

Table 27 Problem 6 (MOX) Results for five fuel assemblies

Axial peaking	Photon source strength (γ/s)		
	Actinides	Fission products	Total
0 18	1 9450E14[a]	1 615E16	1 658E16
0 4	3 0450E14	3 785E16	3 869E16
0 6	4 1605E14	5 950E16	6 075E16
0 8	5 4000E14	8 250E16	8 418E16
1 0	6 8000E14	1 075E17	1 096E17
1 2	8 4000E14	1 330E17	1 356E17
1 32	9 4500E14	1 495E17	1 525E17

[a]Read as 1 9450 $\times$ 10^{14}

Table 28 Problem 6 (MOX) Photon source spectra for five fuel assemblies

Group	Group energy limits (MeV)	(γ/s)
1	0 00 – 0 02	3 21E16[a]
2	0 02 – 0 04	1 35E16
3	0 04 – 0 07	7 74E15
4	0 07 – 0 10	4 68E15
5	0 10 – 0 14	5 36E15
6	0 14 – 0 20	3 11E15
7	0 20 – 0 40	3 65E15
8	0 40 – 0 90	3 58E16
9	0 90 – 1 35	2 90E15
10	1 35 – 1 80	4 67E14
11	1 80 – 2 20	1 64E14
12	2 20 – 2 60	2 16E13
13	2 60 – 3 00	3 53E12
14	3 00 – 3 50	5 90E11
15	3 50 – 4 00	4 47E8
16	4 00 – 4 50	1 09E8
17	4 50 – 5 00	6 30E7
18	5 00 – 6 00	5 70E7
Total		1 096E17

[a]Read as 3 21 $\times$ 10^{16}

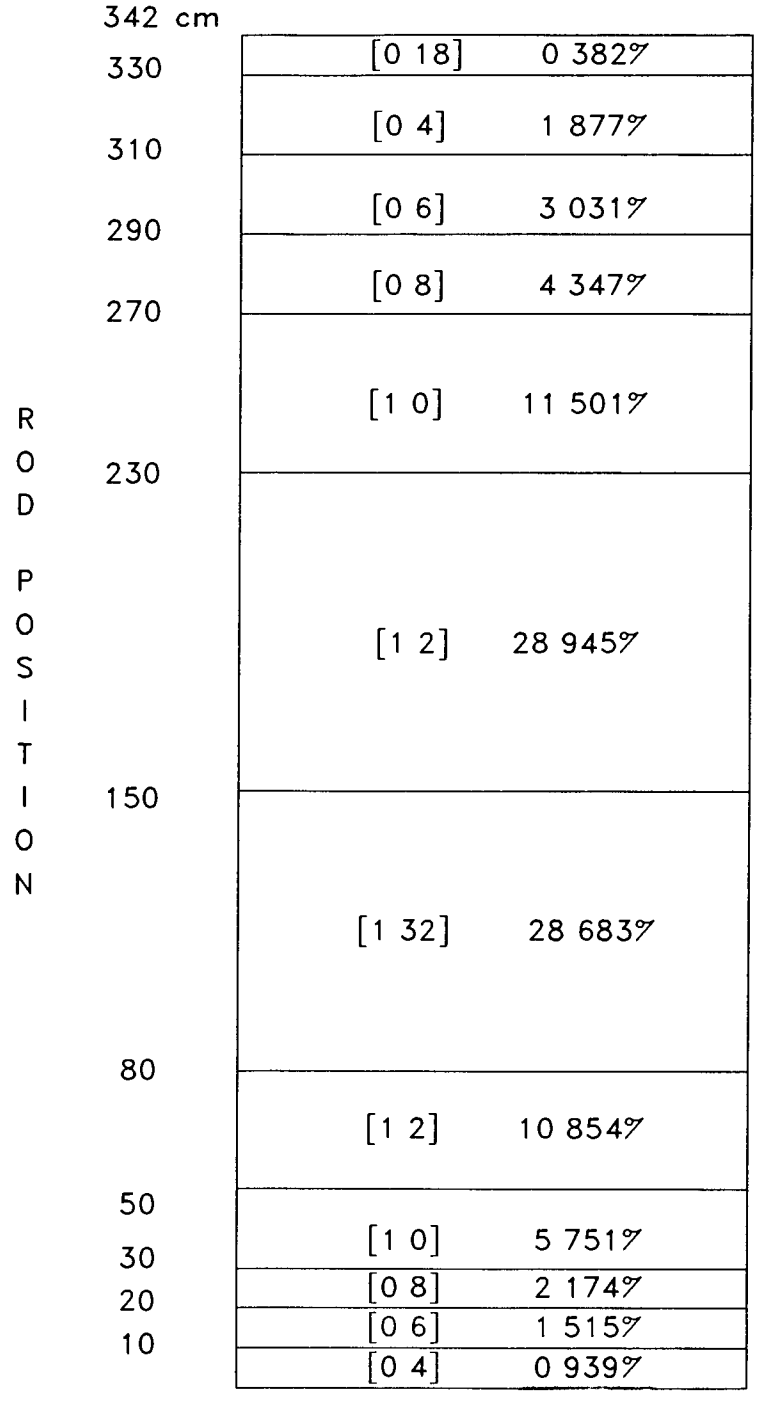

Fig 16 Problem 6 (MOX) Axially distributed photon source as a percentage of total (Values in brackets are axial peaking factors)

structure (the source in Table 23 is in a slightly different group structure) This source was smeared over the cavity region corresponding to the active fuel height The cross section set used in the calculations corresponded to library 3c described in Table 1 The dose results in Table 29 are axial midplane values at the radial sidewall surface and include both an average burnup and an axially variable burnup case The ratio of the photon dose rates for the axial dependent to the average case is 1 37 This corresponds very closely to the midplane peaking factor of 1 32 (see Fig 15) confirming the expected linear variation of the photon source with burnup The expected nonlinear behavior of the neutron source with burnup is also seen in Table 29 In practical situations, this nonlinear behavior of the neutron source may or may not be important The cask body for this problem contains no neutron shield, which is nontypical for many spent fuel casks Also, the doses reported are midplane surface doses, where the peak to average effects are expected to be maximum

5 3 DISCUSSION

In a previous study[18] comparing radiation spectra from selected point depletion codes, it was determined that the effect of bremsstrahlung radiation on photon dose rates can be significant Calculations were performed using ORIGEN S in which bremsstrahlung were included and then neglected The two data libraries used in the calculations were identical but for bremsstrahlung radiation The photon spectra with and without bremsstrahlung are repeated in Table 30 for a typical PWR, 33 GWd/MTU case with 5 years of cooling Large differences are seen below 0 45 MeV, however, these differences should not contribute to the dose The source energy range that dominates the dose is from 1 to 2 5 MeV (as seen in Sect 3 3) In this range, source differences of 7 to 27% are seen when bremsstrahlung is neglected Dose results from Ref 18 are repeated in Table 31 for a PWR with an exposure of 33 GWd/MTU at cooling times of 2, 5, and 50 years These results show that neglecting bremsstrahlung radiation consistently underpredicted the photon dose rates by 10 to 30%

Comparing radiation sources can be encumbered if different energy group structures are used in the different calculations This dependence on group structure may be seen from the SAS2H/ORIGEN S results alone The output includes separate tables for the photon spectrum as a function of time for (1) "light elements, cladding, and structural materials," (2) "fission products," and (3) "heavy metals and their daughters " The total source for each tables is given in units of γ/s and MeV/S These tables use the standard ORIGEN S Photon Yield Library energy group structure Additionally, at the end of the SAS2H/ORIGEN S output, a summary table for the "Gamma Source Spectrum for Gamma Lines (SAS2)" is given that includes the contributions from light elements, actinides, and fission products The group structure for this table is that of the cross section library used in the SAS2 calculation–in this case, that of the 27n 18g shielding library Tables 32 and 33 give the photon source strengths as a function of axial peaking factor for a single fuel assembly in both units of photons/s and MeV/s The column heading "DETAILED TABLES" indicates the result from summing the contributions from the separate tables for light elements, fission products, and actinides in the ORIGEN S photon yield library group structure The source from the summary table where the spectrum is given in the SCALE cross section library group structure is under the column heading "SUMMARY TABLE " The comparison in units of photons/s appears to be quite bad (>25%) for most cases whereas the comparison of MeV/s is in very good agreement It is, in fact, a single calculation that is compared, simply in different units and group structures for each axial peaking factors, and therefore the results must be in agreement A simple way of avoiding confusion is to compare the source strengths in terms of MeV/s rather than particles/s

Table 29 Problem 5 (UO_2) Axial midplane dose rate results using cask model 1a

Source type	Radial surface dose rate (μSv/h)	
	Neutron	Photon
Average	1515[a]	403
Axial dependent	4120[a]	553

[a]Neutron doses are scaled by 1/(1−k) to account for source neutron multiplication, k was estimated to be 0 35 by 1 D transport analysis

Table 30 Comparisons with and without bremsstrahlung, (photons/s/eV) at 5 year cooling time

Energy (MeV)	ORIGEN S no bremsstrahlung	ORIGEN S	ORSNB/ORS
0 000–0 020	4 0206E+09[a]	1 5735E+11	0 026
0 020–0 030	1 0681E+10	7 3393E+10	0 146
0 030–0 045	2 5993E+10	5 8679E+10	0 443
0 045–0 070	1 3083E+09	2 2380E+10	0 058
0 070–0 100	1 6962E+09	1 3751E+10	0 123
0 100–0 150	3 7858E+09	9 6919E+09	0 391
0 150–0 300	1 9951E+08	2 4028E+09	0 083
0 300–0 450	4 1070E+08	1 4069E+09	0 292
0 450–0 700	2 0098E+10	2 0400E+10	0 985
0 700–1 000	3 6347E+09	3 7333E+09	0 974
1 000–1 500	4 1018E+08	4 3800E+08	0 936
1 500–2 000	1 4682E+07	2 0000E+07	0 734
2 000–2 500	9 8024E+06	1 0820E+07	0 906
2 500–3 000	2 0164E+05	3 0850E+05	0 654
3 000–4 000	1 4533E+04	1 9223E+04	0 756
4 000–6 000	4 9670E+00	4 9650E+00	1 000
6 000–8 000	5 7195E 01	5 7000E 01	1 003
8 000–11 000	4 3860E 02	4 4000E 02	0 997

[a]Read as 4 0206 × 10^9

Table 31 Photon dose rates illustrating effect of bremsstrahlung radiation (μSv/h)

Cooling time (year)	ORIGEN S	ORIGEN S (no bremsstrahlung)	% diff
2	1172 64	1008 52	14 00
5	214 90	194 34	9 57
50	4 82	3 47	28 01

Table 32 Problem 5 Comparison of photon source strength for one assembly

Axial peaking	Photons/s		MeV/s	
	Detailed tables	Summary table	Detailed tables	Summary table
0 18	2 778+15	2 039+15	5 866+14	5 827+14
0 4	6 826+15	5 129+15	1 643+15	1 630+15
0 6	1 102+16	8 459+15	2 899+15	2 885+15
0 8	1 581+16	1 224+16	4 420+15	4 404+15
1 0	2 090+16	1 640+16	6 175+15	6 153+15
1 2	2 630+16	2 085+16	8 104+15	8 082+15
1 32	2 978+16	2 363+16	9 332+15	9 305+15

Table 33 Problem 6 Comparison of photon source strength for one assembly

Axial peaking	Photons/s		MeV/s	
	Detailed tables	Summary table	Detailed tables	Summary table
0 18	3 316+15	2 474+15	7 196+14	7 162+14
0 4	7 738+15	5 866+15	1 858+15	1 851+15
0 6	1 215+16	9 313+15	3 130+15	3 122+15
0 8	1 684+16	1 309+16	4 615+15	4 603+15
1 0	2 196+16	1 715+16	6 294+15	6 274+15
1 2	2 712+16	2 147+16	8 135+15	8 108+15
1 32	3 050+16	2 416+16	9 303+15	9 278+15

In summary, it is recommended that attention be given to the effect of bremsstrahlung radiation on predicted dose rates and that a comparison of sources in units of MeV/s will yield results unbiased by group structure

6 SUMMARY AND CONCLUSIONS

This work summarizes the U S contribution to problems 1–6 of the OECD Working Group on Shielding Assessment of Transportation Packages Problems 1–6 constitute the first phase of study by the working group with primary focus on a series of computational benchmarks emphasizing various geometrical complexities These benchmarks begin with simple smeared cavities and single material shields and add model complexities of neutron shields, wet cavities, cylindrical polyethylene rods in the shield, epoxy strips in the shield, cooling fins, explicit basket and pin models, and realistic versus theoretical sources For the majority of these cases, multiple codes were used to obtain both accurate results and approximate results, allowing intercomparison of U S methods as well as comparison with other countries' methods

The initial U S effort was aimed at an understanding of the various cross section libraries available for use An intercomparison was performed with some 17 different sets of cross sections to analyze their strengths and weaknesses for these problems (problem 1a was chosen as the model for the intercomparison) In all cases, the response of interest was the cask sidewall surface dose, with all calculations performed by the SAS1/XSDRNPM 1 D transport package A summary of findings includes

1 ENDF/B V results were some 8% lower than ENDF/B IV results for neu trons and about the same for gammas

2 ENDF/B IV based libraries that were resonance processed with the NITAWL code (particularly libraries 3a and 7 in Table 2) contain essentially no iron resonance processing in important energy regions due to the ENDF/B IV resonance region specification

3 An underprediction of the neutron dose of nearly 50% is seen if resonance processing is omitted

4 For broad group analysis of deep penetration through iron shields, the method of fine to broad group collapse (i e , the weighting function) is very important to both neutron and gamma dose results Differences of factors of 2–3 are possible with inappropriate choices of broad group bounds and/or weighting functions

5 For the gamma dose results of problems 1–4, the gamma line source at 2 1 MeV is dominant causing high sensitivity to the broad group structure around 2 MeV Appropriate weighting functions or a fine energy gamma group structure can eliminate this sensitivity

6 The extreme dominance of the 2 1 MeV gamma line source (specified for problems 1–4) is somewhat nontypical The sources for problems 5–6 (cal culated to be appropriate for a specified spent fuel burnup) exhibit reduced sensitivity to weighting functions and broad group energy structures

7 Energy versus particle conservation in converting gamma line sources to group sources was found to produce dose differences of 9–15% with the en ergy conservation technique the most accurate in comparison to point energy calculations (both QAD and MCNP)

8 A general trend of a 10–20% underprediction in the neutron doses via multi group versus point calculations was seen This is felt to be due to inaccurate representation of the iron cross section minima in the rapidly varying reso nance region

In addition to a description of the energy group structure, discrete ordinates transport codes (DORT, XSDRNPM) require a spatial mesh to describe the problem geometry For the cases analyzed, both the neutron and gamma doses appear to be sensitive to the mesh size, with differences of 10–20% seen when the mesh size is doubled Specifically, a mesh size of 1 cm in the shield (4 cm appears to be sufficient in a smeared cavity) was adequate for neutron doses in an iron only shield For cases where a neutron shield material (epoxy or polyethylene) was present, a 0 5 cm mesh was necessary for accurate results For gamma doses, a 0 5 cm mesh in the shield was necessary regardless of the shield configuration

The appropriateness of 1 D approximations for multidimensional geometries is another consideration in a shielding analysis As stated earlier, the use of multiple models of varying complexity allowed a number of conclusions to be made regarding the validity of various simplifying geometry assumptions The first geometrical complexity addressed concerns the location of doses to be calculated One dimensional transport results for both neutron and gamma doses at the sidewall surface are generally of benchmark quality when the H/D for the cask is greater than 1 The H/D for these problems was about 3 with excellent 1 D to multidimensional agreement at the sidewall surface For dose locations at the cask axial midplane but away from the surface, the expected slightly conservative results (conservative with respect to multidimensional calculations, no experimental results are available) are seen with about a 20% overprediction at 10 m from the cask surface The QAD point kernel (gamma only) results similarly agree quite well with multidimensional calculations on the cask sidewall surface, but are up to a factor of 2 conservative at dose locations 10 m from the cask surface The point kernel methods also perform quite well on the cask top and bottom with very similar results as seen for the cask sidewall Transport calculations in one dimension were not performed for the cask top and bottom since previous experience has shown that benchmark quality calculations were not straightforward where a buckling correction was required

Additionally, 1 D approximations for the fuel/basket region and cylindrical polyethy lene rods in the shield were evaluated with respect to multidimensional dose results For gamma doses, the smeared basket cases for both wet and dry cavities produced higher (con servative) values than the explicit basket cases The neutron dose results for a smeared basket were conservative only in the wet cavity case For a dry cavity, the smeared neu tron dose results were about 5% lower than the explicit results An apparent conclusion is that for a basket with appreciable shielding (i e , water for neutrons, high z material for gammas) a smeared basket model should result in conservative doses A common approximation made when analyzing discrete assemblies in a shipping cask (using multi dimensional codes) is to homogenize the discrete pins into a smeared assembly This is generally assumed to be valid when a shielding only calculation is being performed (i e , this assumption is not generally valid for criticality calculations) The results presented herein again confirm this approximation For cylindrical polyethylene rods in the shield, smearing into rings while conserving polyethylene volume appears to underestimate both

neutron and gamma doses The neutron doses in problem 2 were underestimated by ~35%, the gamma doses were nearly a factor of 3 too low

Multidimensional calculations were performed using a 2 D discrete ordinates method (DORT) and two 3 D Monte Carlo codes (SAS4/MORSE and MCNP) The cross sections in SAS4/MORSE are groupwise as are those of DORT, while MCNP utilizes point cross sections Since both DORT and SAS4 used groupwise cross sections, agreement between the two independent methods generally indicates a quality solution, whereas further agreement with MCNP indicates adequate cross section processing as well In general, the SAS4 and DORT agreement is quite good, generally within the SAS4 standard deviations Comparing SAS4 and DORT versus MCNP also provides very good agreement for the gamma doses, but the groupwise neutron doses from SAS4 and DORT are about 20% lower than those based on point cross section values (MCNP)

A finding of importance for certain geometries that produce rapidly varying surface doses (e g , problem 2a with cylindrical polyethylene rods in the shield) is that the discrete ordinates method has the capability to model this variation quite readily in most cases, whereas the Monte Carlo method is quite cumbersome in duplicating such results For example, the dose profiles (or even peak dose rate) in Figs 8 and 9 would be extremely difficult to predict with Monte Carlo since results are normally averaged over a surface roughly comparable to the entire axis plotted

The axial variation of the neutron and gamma sources should be accounted for in the accurate determination of shipping cask dose rates Results shown herein confirm the linear dependence of the photon source with burnup, hence the average burnup photon dose rate values can be scaled with the peak axial burnup ratios to produce peak dose rates This procedure should yield accurate results at the cask surface and conservative results away from the surface The neutron generation rate is nonlinear with burnup as shown in Table 29 However, the dominance of the neutron doses as seen there is somewhat nontypical since the cask model analyzed had no neutron shield Also, no calculations were performed away from the surface where the peak to average effects should be smaller If peak neutron dose rates at the surface are important, the neutron source should be calculated carefully in light of the findings herein Further work is needed for specific recommendations at off surface locations

An additional finding with respect to the generation of spent fuel sources is that bremsstrahlung effects can be significant for shielding problems of this nature The primary U S depletion codes, ORIGEN S and ORIGEN2, both take into account bremsstrahlung, however, a number of popular codes in the United States and abroad do not Also, an important point to consider when intercomparing gamma source spectra is to compare based on MeV/s rather than solely on particles/s

As mentioned earlier, all comparisons made to date in the OECD working group's activities have been to other calculations The next phase of study will compare calculations with experimental results and should allow additional confirmation of the various calculational techniques studied thus far

7 REFERENCES

1 C V Parks et al , "Intercomparison of Cross Section Libraries Used for Spent Fuel Cask Shielding Analyses," *Proc of Theory and Practices in Radiation Protection and Shielding*, ISBN 0 89448 132 0, Vol 2, p 559, 1987

2 *SCALE A Modular Code System for Performing Standardized Computer Analyses for Licensing Evaluation, Vols 1–3*, NUREG/CR 0200, U S Nu clear Regulatory Commission (originally issued July 1980, reissued January 1982, Revision 1 issued July 1982, Revision 2 issued June 1983, Revision 3 is sued December 1984) SCALE 4 available from RSIC as CCC 545/SCALE 4

3 Los Alamos Monte Carlo Group, *MCNP – A General Monte Carlo Code for Neutron and Photon Transport*, LA 7396 M, Los Alamos Natl Lab , 1986 Version 3B available from RSIC as CCC 200/MCNP

4 *BUGLE 80 Coupled 47 Neutron, 20 Gamma Ray, P_3 Cross Section Library for LWR Shielding Calculations by the ANS 6 1 2 Working Group on Multi group Cross Sections*, available from RSIC as DLC 75/BUGLE 80

5 W E Ford, III et al , *FCXSEC Multigroup Cross Section Libraries for Nu clear Fuel Cycle Shielding Calculations*, ORNL/TM 7038, Union Carbide Corp , Nuclear Division, Oak Ridge Natl Lab , May 1980 Available from RSIC as DLC 85/FCXSEC

6 E A Straker, G W Morrison, and R H Odegaarden, "A Coupled Neutron and Gamma Ray Cross Section Library for Use in Shielding Calculations," *Trans Am Nucl Soc* **15**, 535, 1972 Available from RSIC as DLC 23/CASK

7 R W Roussin et al , *VITAMIN C The CTR Processed Multigroup Cross Section Library for Neutronics Studies*, ORNL/RSIC 37 (ENDF 296), Union Carbide Corp , Nuclear Division, Oak Ridge Natl Lab , 1978 Available from RSIC as DLC 41/VITAMIN C

8 C R Weisbin et al , *VITAMIN E An ENDF/B V Multigroup Cross Section Library for LMFBR Core and Shield, LWR Shield, Dosimetry and Fusion Blanket Technology*, ORNL 5505, Union Carbide Corp , Nuclear Division, Oak Ridge Natl Lab , 1979 Available from RSIC as DLC 113/VITAMIN E

9 W E Ford, III et al , *CSRL V Processed ENDF/B V 227 Neutron Group and Pointwise Cross Section Libraries for Criticality Safety, Reactor and Shielding Studies*, NUREG/CR 2306 (ORNL/CSD/TM 160), Union Carbide Corp , Nuclear Division, Oak Ridge Natl Lab , 1982

10 W E Ford, III et al , *A 218 Group Neutron Cross Section Library in the AMPX Master Interface Format for Criticality Safety Studies*,

ORNL/CSD/TM 4, Union Carbide Corp , Nuclear Division, Oak Ridge Natl Lab , 1976 Available from RSIC as DLC 43/CSRL

11 *QAD CGGP A Combinatorial Geometry Version of QAD P5A, A Point Kernel Code System for Neutron and Gamma Ray Shielding Calculations Using the GP Buildup Factor* Available from RSIC as CCC 493/QAD CGGP

12 W A Rhoades and R L Childs, "The DORT Two Dimensional Discrete Ordinates Code," *Nucl Sci Eng* **99**, 88–89, May 1988

13 V Baker and R L Childs, "FALSTF Calculator of Response of Detectors External to Shielding Configuration," Available as package CCC 351 of the RSIC Computer Code Collection, Oak Ridge Natl Lab , 1979

14 B L Broadhead and C V Parks, "Point Kernel Versus Radiation Transport for Iron Deep Penetration Problems," *Trans Am Nucl Soc* **55**, 295, June 1987

15 A G Croff, *ORIGEN2–A Revised and Updated Version of the Oak Ridge Isotope Generation and Depletion Code*, ORNL 5621, Union Carbide Corp , Nuclear Division, Oak Ridge Natl Lab , July 1980

16 M J Bell, *ORIGEN–The ORNL Isotope Generation and Depletion Code*, ORNL 4628, Union Carbide Corp , Nuclear Division, Oak Ridge Natl Lab , May 1973

17 A G Croff, M A Bjerke, G W Morrison, and L M Petrie, "Revised Uranium Plutonium Cycle PWR and BWR Models for the ORIGEN Com puter Code," ORNL/TM 6051, Union Carbide Corp Nuclear Div , Oak Ridge Natl Lab , 1978

18 M C Brady, O W Hermann, and W B Wilson, *Comparison of Radiation Spectra From Selected Source Term Computer Codes*, ORNL/CSD/TM 259, Martin Marietta Energy Systems, Inc , Oak Ridge Natl Lab , 1988

APPENDIX

APPENDIX *

An FRG Proposal for an International Intercomparison of
Codes for Radiation Protection Assessment
of Transportation Packages

INTRODUCTION

In June 1979, the Committee on the Safety of Nuclear Installations (CSNI) convened a meeting to investigate the possibility of setting up international projects on fuel cycle safety Most Nuclear Energy Agency (NEA) members expressed their interest in exchang ing information and experience on various aspects of spent reactor fuel transportation Special points of interest were criticality, heat transfer, and shielding code intercompar ison This proposal suggests a procedure for shielding code comparison and verification and includes a recommended set of problems This final version includes comments on the draft proposal made by the working group participants

Shielding analysis for radioactive material shipping casks requires the solution of some problems by more or less specialized calculational techniques developed for this purpose The computation of the neutron and gamma ray source term (absolute value and local distribution, respectively), the complex geometry (e g, of a fuel assembly consisting of a bundle of distinct rods that allow for streaming effects), presence of neutron absorbing materials in the cask wall, and different types of cooling fins at the cask surface are some examples for the problems mentioned above

As outlined in previous papers, "packages approved by national authorities for trans port of fissile materials, including spent fuel, may not be accepted for international ship ment unless the certification process in the originating country is examined and approved by the other countries in which the transport will occur " Therefore, an international in tercomparison of shielding calculational techniques used in licensing of spent fuel shipping casks should be beneficial to cask designers and licensing authorities in the international community Special care should be taken in the intercomparison to use the methods that are standard practice in the participating countries

This proposal suggests a procedure for accomplishing such an intercomparison exercise under the aegis of the Nuclear Energy Agency Committee on Reactor Physics (NEACRP) The proposal is based on the concept that it is necessary to validate calculational tech niques against actual experimental data as well as comparing results among several codes applied to the same basic problem For that purpose, it would be useful if the participants contribute experimental data with respect to their special knowledge In this manner, con sistent and accurate measurements should be obtained when the assessment procedures are completed

* This Appendix represents a condensed and edited version of NEACRP L 290, which was originally issued in 1986 A full copy of NEACRP L 290 can be obtained from the OECD/NEACRP Secretariat

This comparison and verification would be accomplished by the calculation by each participating country of a series of problems important to package certification procedure Code results would be made available to all the participants and reports of all the results issued

PROCEDURE

To carry out this exercise, it is proposed that a working group be established, comprised of specialists from the interested participating countries This group would be concerned with

1 Selection of standard problems, including

— use category (spent fuel storage, spent fuel transport, fresh fuel, plutonium, high active waste),

— parameters of transport package to be benchmarked (general constructional design, cask inventory, materials, construction details), and

— basic quantities (fission spectrum, flux to dose conversion fac tors to be used)

2 Compilation of available experimental data for related configurations due to special national contacts of the participants

3 Analysis of calculations and preparation of a report on the intercomparison results

SPECIFIC PROPOSAL FOR AN INTERNATIONAL STANDARD PROBLEM EXERCISE IN SHIELDING CODE BENCHMARKING

The most stringent regulatory requirement governing the shield design of a shipping cask are the dose rate limits for normal operation conditions of the International Atomic Energy Agency (IAEA) transport regulations In the case of a spent fuel storage facility, an additional restriction can arise when the national authorities set a limit for the envi ronmental radiation exposure The most important quantities to be checked for are the mean value of the dose rate at the cask body surface and in some given distances A point of some additional interest, especially for cask handling and maintaining, is the dose rate profile along the cask body For a given transportation package to be licensed, some points have to be considered that can affect the calculational result

— arrangement of radiation sources in the basket (e g , streaming effects in rod bundles, inhomogeneities in source density),

— basic parameters of the radioactive material (e g , for spent fuel, composition of fresh fuel, irradiation history, reactor type), and

— constructional details (wet or dry cask, material composition, basket and cask body construction, location of neutron absorbing materials, cooling fins, instrumentation holes)

In principle, most of these effects can be treated by exact three dimensional (3 D) modeling of the cask as a whole Because this is time consuming and expensive, the problem is simplified for treatment by less sophisticated methods But these simplifications have to be performed carefully to avoid misleading results

Having these margins in mind, we suggest dividing the standard problem exercise into two main parts

— First, deal with the influence of different geometrical models on the calculated dose rate

— Second, check the different methods for determining the neutron and gamma source strength as an essential input data quantity for the following shielding calculation This part is understood to be only a starting point, which can be followed by some other problems of interest

The main ideas in setting up the proposal were

— Because of different calculational models, start with a set of three rather simple problems to arrive at a basis of consensus

— Add just one complexity in a subsequent problem (leaving dimensions and materials unchanged in all model problems)

— Choose package conditions that require at least a minimum of neutron shield ing (preferably choosing a dry cask containing spent LWR fuel)

— Use input data that are as realistic as possible (not giving a detailed de scription of the fuel assembly top and bottom fittings because these data are usually unknown to the shield designer)

A general view is given showing the main features of the different model problems Each of them is discussed in detail in the following sections

The nomenclature and basic quantities used can be found in Tables A 1 and A 2, respectively

Table A 1 Nomenclature

Symbol	Explanation
<>	average value
n	neutron
γ	gamma ray
E	particle energy
$\phi(E)$	scalar flux density
DF(E)	flux to dose conversion factor
D	dose rate
$\Sigma(E)$	total macroscopic cross section
d	distance measured from the cask surface
z	axial coordinate
r	radial coordinate
ρ	density
T	temperature

Table A 2 Basic quantities to be used for the calculation

Avogadro's No $0\ 602252 \times 10^{24}$

Neutron Flux To Dose Rate Conversion Factors Polynomial Coefficients In Analytic Fit – $ln\ DF_a(E) = A + B\ X + C\ X^2 + D\ X^3$
$DF_n\ (E) = (rem/hr)/(n/cm^2\ s)$, E = neutron energy in MeV, and $X = ln\ E^*$

Neutron Energy (MeV)		A	B	C	D
2 5−08	to 1 0−07	−1 2514 +01			
1 0−07	to 1 0−02	−1 2210 +01	1 7165−01	2 6034−02	1 0273−03
0 01	to 0 1	−8 9302	7 8440−01		
0 1	to 0 5	−8 6632	9 0037−01		
0 5	to 1 0	−8 9359	5 0696−01		
1 0	to 2 5	−8 9359	−5 5979−02		
2 5	to 5 0	−9 2822	3 2193−01		
5 0	to 7 0	−8 4741	−1 8018−01		
7 0	to 10 0	−8 8247			
10 0	to 14 0	−1 1208+01	1 0352		
14 0	to 20 0	−9 1202	2 4395−01		

Gamma Ray Flux to Dose Rate Conversion Factors Polynomial Coefficients in Analytic Fit – $ln\ DF_g(E) = A + B\ X + C\ X^2 + D\ X^3$
$DF_g(E) = (rem/hr)/(photons/cm^2\ s)$, E = Photon energy in MeV, and $X = ln\ E^*$

Photon Energy (MeV)	A	B	C	D
0 01 to 0 03	−2 0477+01	−1 7454		
0 03 to 0 5	−1 3626+01	−5 7117−01	−1 0954	−2 4897−01
0 5 to 5 0	−1 3133+01	7 2008−01	−3 3603−02	
5 0 to 15 0	−1 2791+01	2 8309−01	1 0873−01	

*Taken from ANSI/ANS 6 1 1 1977

General View of Model Problems

PART 1 Geometric Modeling

	Model problem				
Attribute	1	2	3	4	5–6
Predefined source	Yes	Yes	Yes	Yes	No
Neutron shield	No/Yes	Yes	Yes	Yes	Yes
Cooling fins	No	No	Yes	Yes	No
Detailed basket	No	No	No	Yes	Yes
Wet/dry cask	Dry/Wet	Dry	Dry	Dry/Wet	Dry

PART II Source Term

	Model problem	
Attribute	5	6
Type of reactor	PWR	PWR
Type of fuel	UO_2	MOX
Axially varying source	Yes	Yes

GENERAL REMARKS ON OUTPUT NEEDS

In general, we suggest the reported results be kept to a minimum, that is,

— dose rate at the lateral cask surface and at a distance of 1, 2, and 10 m, measured from the surface and fin tips, respectively,

— dose rate at the lid surface and at a distance of 1, 2, and 10 m, and

— dose rate at the bottom surface and at a distance of 1, 2, and 10 m

The dose rates should be reported as surface averaged values as well as a function of position if these data are available from the calculation Furthermore, the dose rate

contributions of source neutrons, source gammas, and capture gammas should be reported separately All values should be given in SI units, preferably μSv/h

In addition, surface averaged scalar fluxes as a function of energy should be reported for the surface of the sidewall

On an additional sheet of paper, a short but complete description of the computational method used should be given It should show

— a short overall description of the method,

— codes,

— cross section libraries,

— energy, angular, and spatial mesh, if appropriate, and

— any additional assumptions made by the user

During the comparison of results, it may be necessary for participants to provide additional information to detect the causes of possible discrepancies

MODEL PROBLEM 1
CYLINDRICAL IRON CASK WITH HOMOGENEOUS SOURCE

Model problem 1 is a set of three simple basic problems, intended to ensure a basis of consensus Essentially, it consists of a cylindrical cask with a homogeneous source of given strength It is split into the following three subcases to obtain a basis check for as wide a range of applications as possible

Case a pure cast iron shield
no neutron absorbing or moderating materials
source region dry

Case b double layer shield containing 6 cm of polyethylene on the outer surface
source region dry

Case c pure cast iron shield as in case a
source region containing 30 wt % of water

A full description of the model characteristics is provided in Tables A 3 through A 5

Table A 3 Characteristics of model problem 1, case a[a]

Material Assignment	
Region	Material[b]
Source region	Homogeneous source (dry)
Sidewall	Cast iron
Cask bottom	Cast iron
Cask lid	1 4313
Cooling fins	None
Neutron shield	None
Source Description	
Source characteristic	Volume distributed fixed source
Source region	Identical with cask cavity
Total source strength	$1\ 0 \times 10^{9}$ n/s $5\ 0 \times 10^{16}$ g/s (Subcritical neutron multiplication not to be taken into account)
Energy distribution	See Table A 19
Spatial distribution	Constant in the whole source region, zero otherwise

[a]For dimensions, see Table A 14
[b]See Table A 18

Table A 4 Characteristics of model problem 1, case b[a]

Material Assignment	
Region	Material[b]
Source region	Homogeneous source (dry)
Sidewall	Cast iron plus 6 cm of polyethylene
Cask bottom	Cast iron
Cask lid	1 4313
Cooling fins	None
Neutron shield	Polyethylene, set within the outer diameter of 156 cm

Source Description	
Source characteristic	Volume distributed fixed source
Source region	Identical with cask cavity
Total source strength	$1\ 0 \times 10^{9}$ n/s $5\ 0 \times 10^{16}$ g/s (Subcritical neutron multiplication not to be taken into account)
Energy distribution	See Table A 19
Spatial distribution	Constant in the whole source region, zero otherwise

[a]For dimensions, see Table A 14
[b]See Table A 18

Table A 5 Characteristics of model problem 1, case c[a]

Material Assignment	
Region	Material[b]
Source region	Homogeneous source (wet)
Sidewall	Cast iron
Cask bottom	Cast iron
Cask lid	1 4313
Cooling fins	None
Neutron shield	None

Source Description	
Source region	Identical with cask cavity
Total source strength	$1\ 0 \times 10^{9}$ n/s $5\ 0 \times 10^{16}$ g/s (Subcritical neutron multiplication not to be taken into account)
Energy distribution	See Table A 19
Spatial distribution	Constant in the whole source region, zero otherwise

[a]For dimensions, see Table A 14
[b]See Table A 18

MODEL PROBLEM 2
AS MODEL PROBLEM 1A WITH REALISTIC NEUTRON MODERATOR DESIGNS ADDED

Model problem 2 consists of the same cask as used in model problem 1a with additional neutron moderator material Because at least two completely different philosophies exist on the best way to reduce the neutron dose rate, we suggest splitting model problem 2 as follows

Case a cylindrical polyethylene rods located in circular holes inside the cask wall serve as neutron moderator (see Fig A 1)

Case b stripes of epoxi cast resin are fixed on the outer surface of the sidewall, set within the outer diameter of 156 cm (see Fig A 2)

For the sake of simplicity, we assume the moderating material extends over the full height of the cask A description of the two subcases of model problem 2 is provided in Tables A 6 and A 7, respectively Because the addition of neutron moderating material should not affect the top and bottom dose rate to a great extent, these results can be omitted The description of the computational methods used should report only the changes made relative to model problem 1a

Table A 6 Characteristics of model problem 2, case a[a]

Material Assignment	
Region	Material[b]
Source region	Homogeneous source (dry)
Sidewall	1 4541
Cask bottom	1 4541
Cask lid	1 4313
Cooling fins	None
Neutron shield	Polyethylene Location as shown in Fig A 1

Source Description	
Source characteristic	Volume distributed fixed source
Source region	Same as cask cavity
Total source strength	$1\ 0 \times 10^9$ n/s $5\ 0 \times 10^{16}$ g/s (Subcritical neutron multiplication not to be taken into account)
Energy distribution	See Table A 19
Spatial distribution	Constant in the whole source region, zero otherwise

[a]For dimensions, see Table A 14
[b]See Table A 18

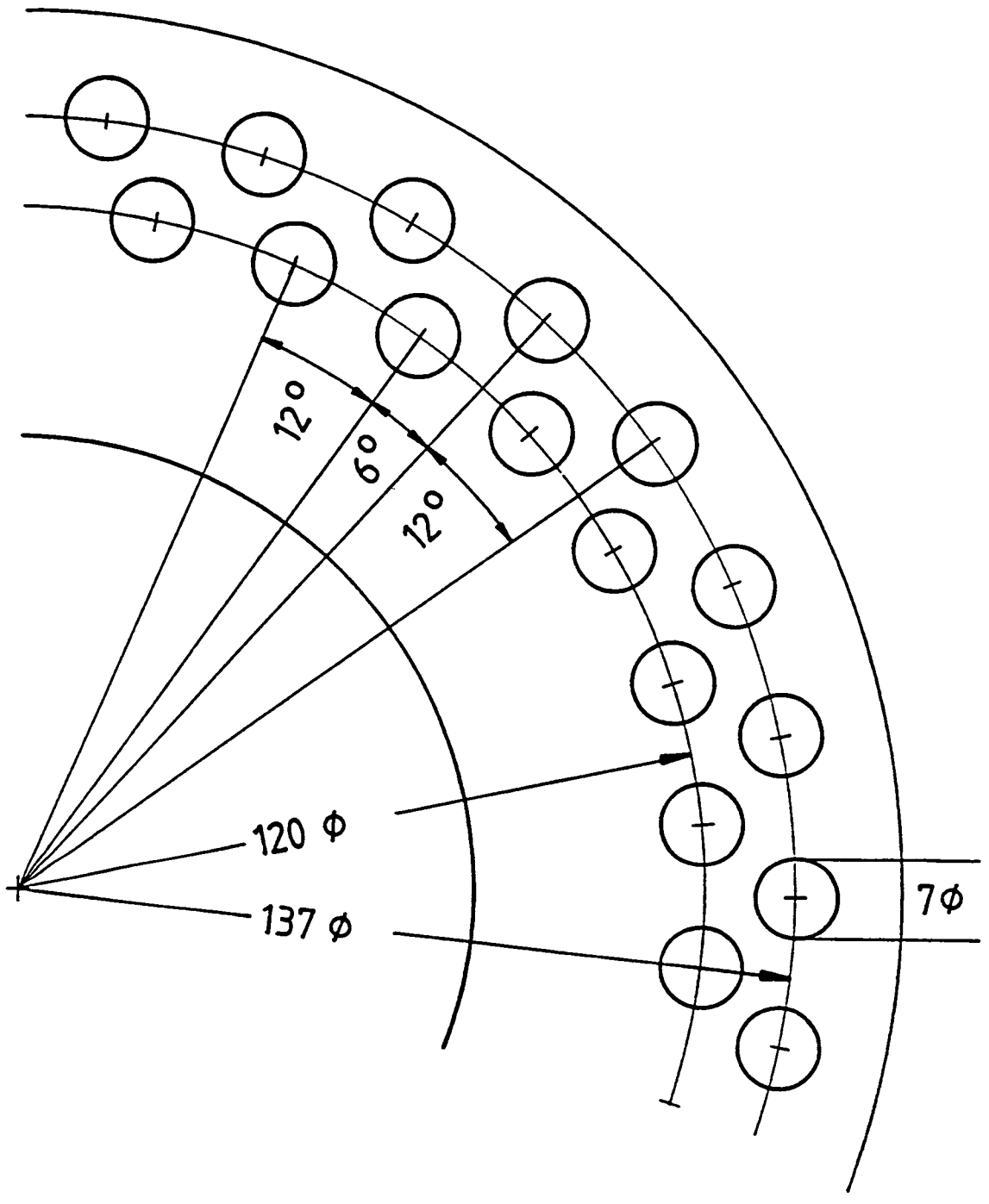

Fig A 1 Characteristics of additional neutron shield Case a polyethylene within the cask wall (dimensions given in cm)

Table A 7 Characteristics of model problem 2, case b[a]

Material Assignment	
Region	Material[b]
Source region	Homogeneous source (dry)
Sidewall	Cast iron
Cask bottom	Cast iron
Cask lid	1 4313
Cooling fins	None
Neutron shield	Epoxi cast resin, set within the outer diameter of 156 cm Location as shown in Fig A 2

Source Description	
Source description	Volume distributed fixed source
Source region	Identical with cask cavity
Total source strength	$1\ 0 \times 10^{9}$ n/s $5\ 0 \times 10^{16}$ g/s (Subcritical neutron multiplication not to be taken into account)
Energy distribution	See Table A 19
Spatial distribution	Constant in the whole source region, zero otherwise

[a]For dimensions, see Table A 14
[b]See Table A 18

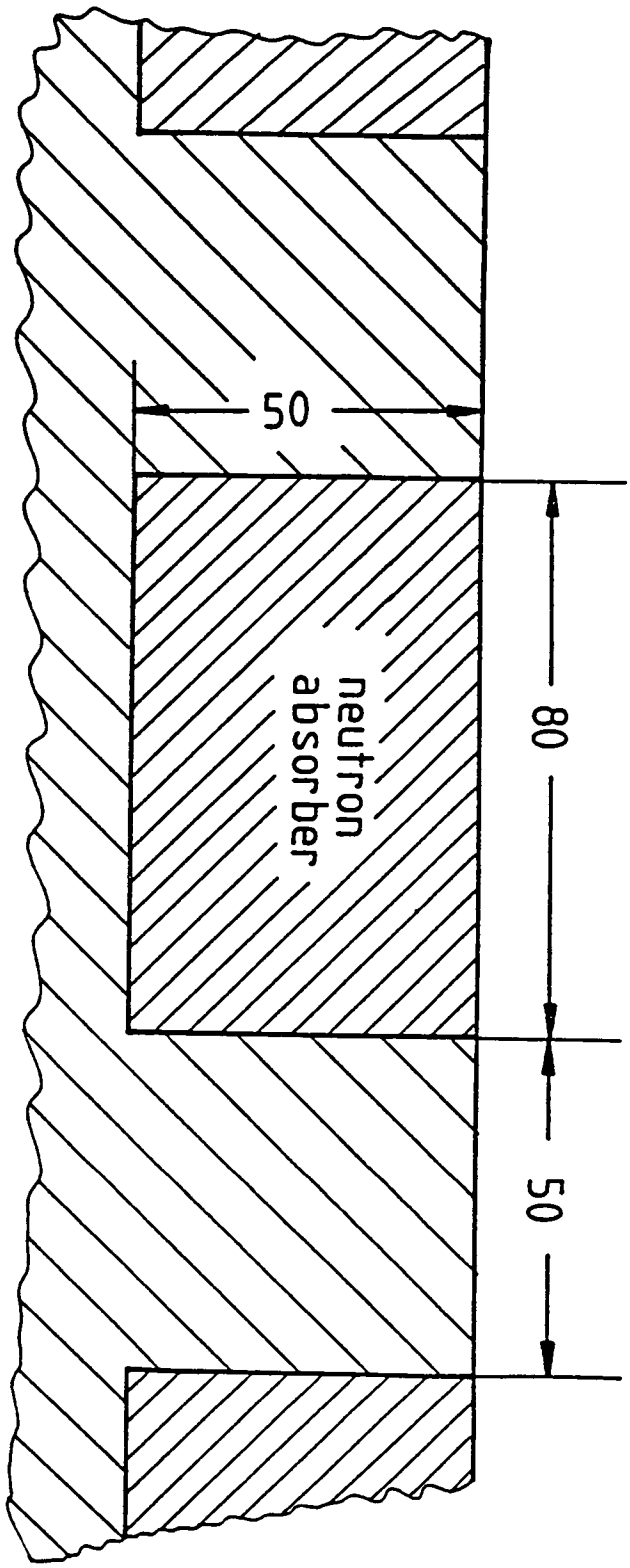

Fig A 2 Characteristics of additional neutron shield Case b epoxi cast resin at outer surface, set within the outer diameter of 156 cm (dimensions given in mm)

MODEL PROBLEM 3
AS MODEL PROBLEM 2 WITH COOLING FINS ADDED

Model problem 3 is identical to model problem 2, but cooling fins are added Because of the different constructions of the neutron moderator model, problem 3 should also be split into two subcases

Case 3a neutron moderating material inside the cask wall

Case 3b epoxi cast resin serving as neutron absorber located in between the fins at the outer surface of the sidewall

A full description of the model characteristics is provided in Tables A 8 and A 9, respectively The description of the computational methods should be reduced to a listing of the changes relative to model problem 2

Table A 8 Characteristics of model problem 3, case a[a]

Material Assignment	
Region	Material[b]
Source region	Homogeneous source (dry)
Sidewall	1 4541
Cask bottom	1 4541
Cask lid	1 4313
Cooling fins	See Fig A 3 Total number 35 Midplane of the first fin on the top level of cask cavity
Neutron shield	Polyethylene Same location as in problem 2a

Source Description	
Source characteristic	Volume distributed fixed source
Source region	Identical with cask cavity
Total source strength	$1\ 0 \times 10^{9}$ n/s $5\ 0 \times 10^{16}$ g/s (Subcritical neutron multiplication not to be taken into account)
Energy distribution	See Table A 19
Spatial distribution	Constant in the whole source region, zero otherwise

[a]For dimensions, see Table A 14
[b]See Table A 18

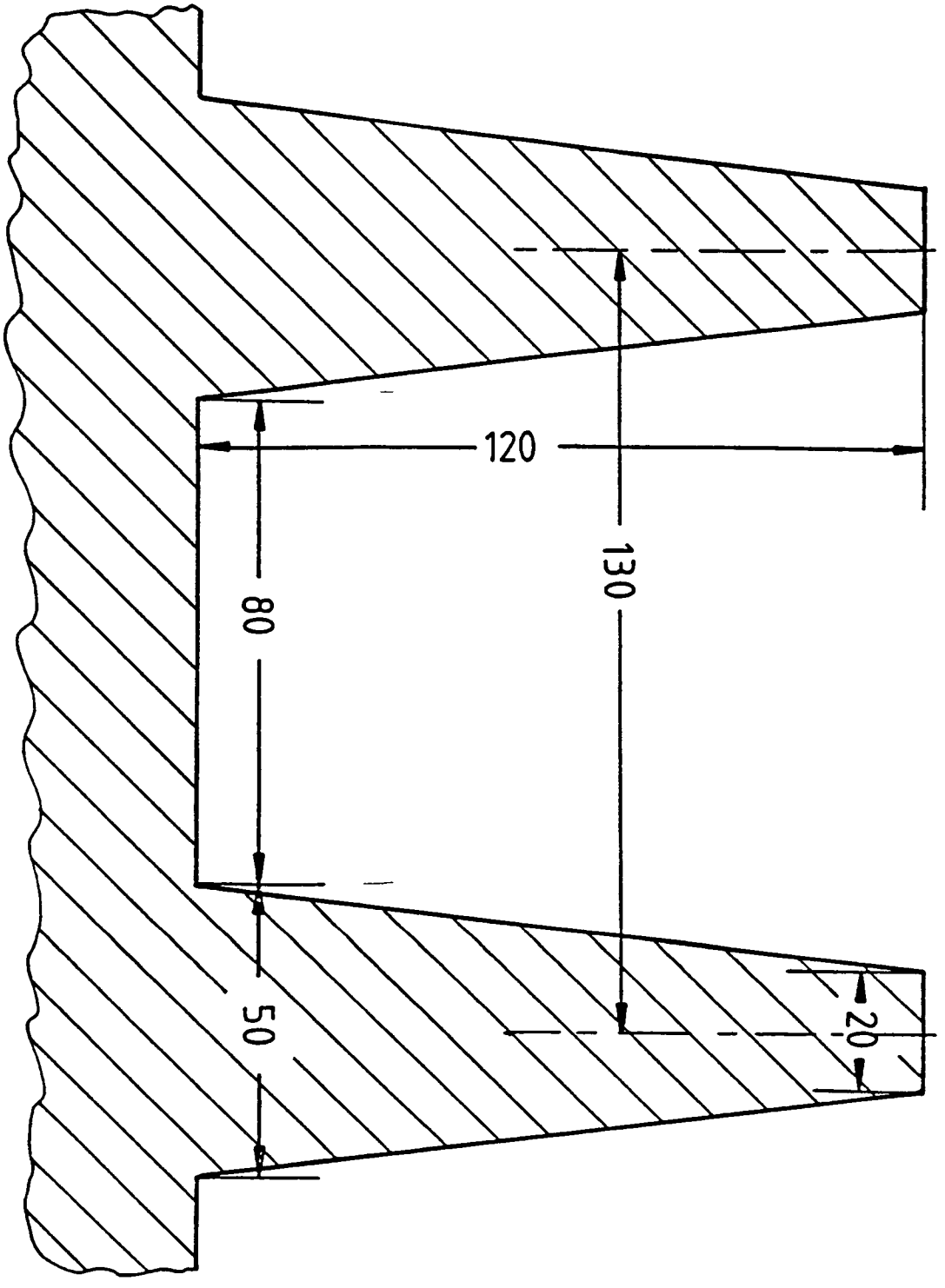

Fig A 3 Characteristics of cooling fins Case A neutron shield within the cask wall, the midplane of the first fin is located on the level of the cask cavity top (dimensions given in mm)

Table A 9 Characteristics of model problem 3, case b[a]

Material Assignment	
Region	Material[b]
Source region	Homogeneous source (dry)
Sidewall	Cast iron
Cask bottom	Cast iron
Cask lid	1 4313
Cooling fins	See Fig A 4 Total number 35 Midplane of the first fin on the top level of cask cavity
Neutron shield	Epoxi cast resin Same location as in problem 2b

Source Description	
Source characteristic	Volume distributed fixed source
Source region	Identical with cask cavity
Total source strength	$1\ 0 \times 10^{9}$ n/s $5\ 0 \times 10^{16}$ g/s (Subcritical neutron multiplication not to be taken into account)
Energy distribution	See Table A 19
Spatial distribution	Constant in the whole source region, zero otherwise

[a]For dimensions, see Table A 14
[b]See Table A 18

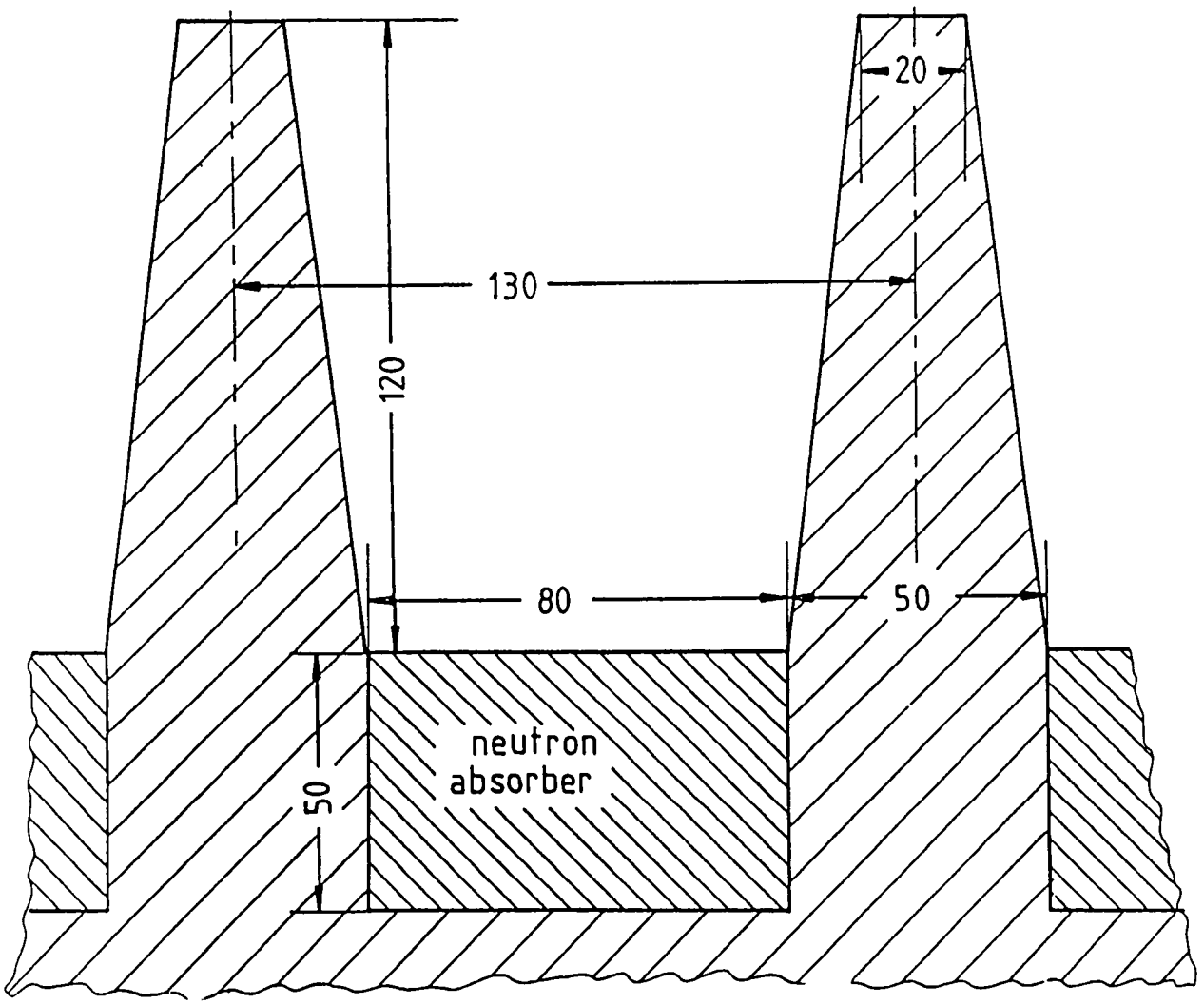

Fig A 4 Characteristics of cooling fins Case b neutron shield in between the fins, set within the outer diameter of 156 cm (dimensions given in mm)

MODEL PROBLEM 4
MODEL PROBLEM 3 WITH DETAILED MODELING OF BASKET AND FUEL ASSEMBLIES

Model problem 4 is identical to model problem 3, but the homogeneous volumetric source is replaced by a detailed stainless steel basket containing five fuel assemblies A drawing of the basket and the model assembly can be seen in Figs A 5 and A 6, respectively A list of the geometry data of basket and assembly is given in Tables A 15 and A 16, respectively To reduce the number of calculations, we do not distinguish two different neutron moderation techniques Because of the existence of dry and wet casks, model problem 4 consists of two subcases again

Case a dry basket

Case b wet basket

A full description of their characteristics is provided in Tables A 10 and A 11, respectively Because of the fact that exact descriptions of the top and bottom fittings for a particular fuel assembly usually are not available, we only give their total length and masses in Tables A 15 and A 16 To ensure the compatibility of the different results, we suggest modeling the fittings to be homogeneous over their length This yields a steel density of 1 01 g/cm^3 for both of them Nevertheless, we suppose that for the assessment of the lid and bottom dose rate, a sensitivity analysis with respect to the modeling of fittings should be performed Each participant is urged to estimate the influence of different modeling on the top and bottom results The description of the computational methods should contain the geometrical modeling of the cask cavity region

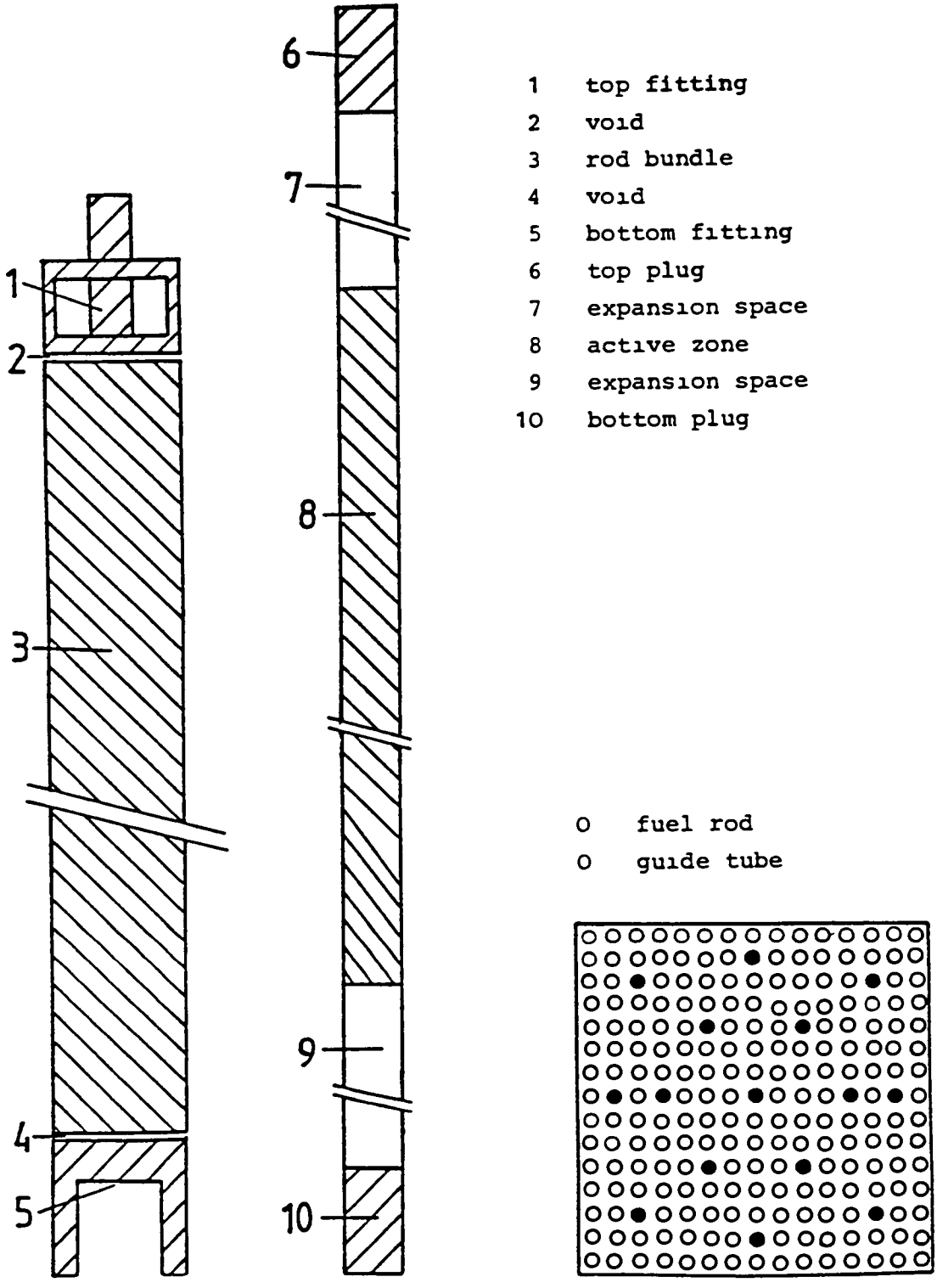

Fig A 5 Cross section view of assembly and single rod arrangement of fuel rods and guide tubes

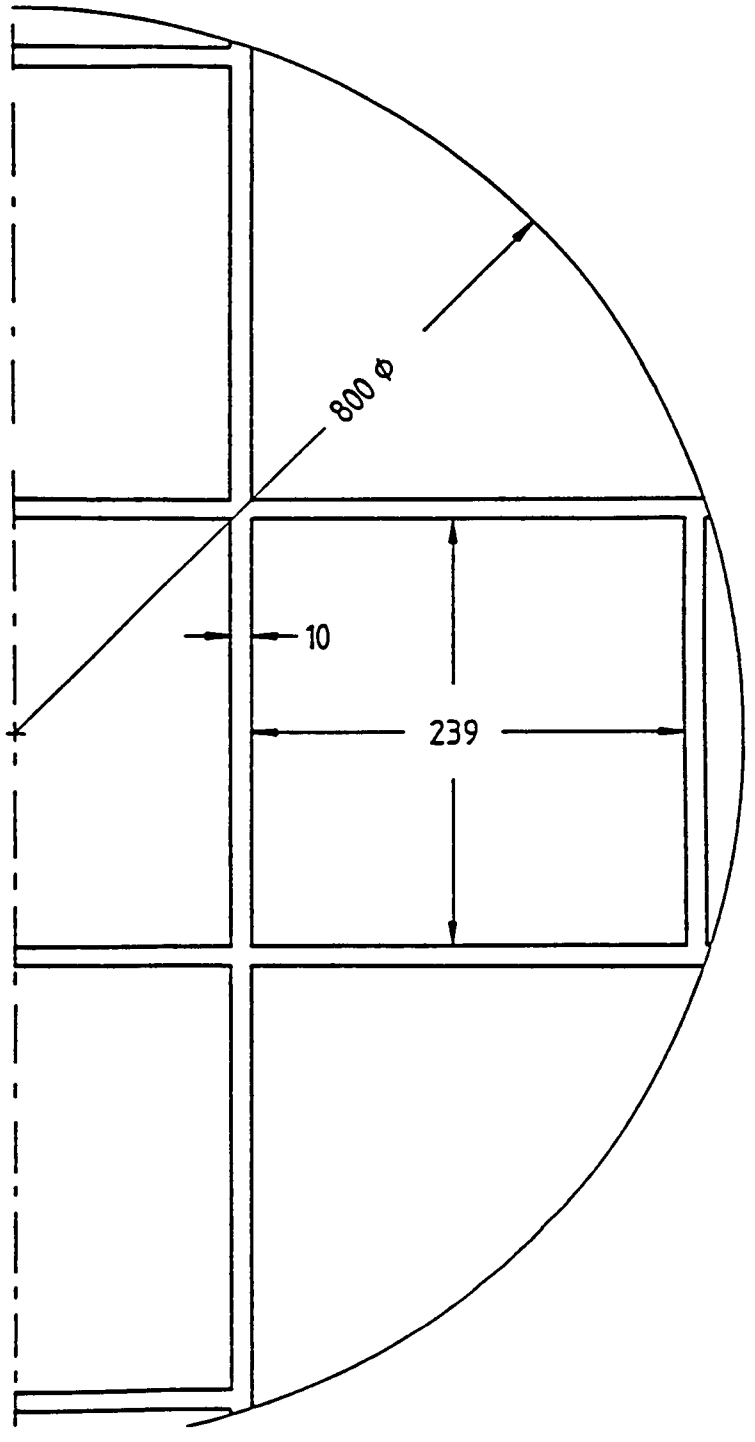

Fig A 6 Construction of basket (dimensions given in mm)

Table A 10 Characteristics of model problem 4, case a[a]

Material Assignment	
Region	Material[b]
Fuel region	Detailed basket with 5 fuel assemblies (See Figs A 5 and A 6) Dry
Top fitting	1 4541, $\rho = 1\ 01$ g/cm^3
Bottom fitting	1 4541, $\rho = 1\ 01$ g/cm^3
Sidewall	1 4541
Cask bottom	1 4541
Cask lid	1 4313
Cooling fins	See Fig A 3
Neutron shield	Polyethylene Location as shown in Fig A 1

Source Description	
Source characteristic	Volume distributed fixed source
Total source strength	$1\ 0 \times 10^9$ n/s $5\ 0 \times 10^{16}$ g/s (Subcritical neutron multiplication not to be taken into account)
Energy distribution	See Table A 19
Spatial distribution	Constant in the active zone of fuel rod zero otherwise

[a]For dimensions, see Table A 14
[b]See Table A 18

Table A 11 Characteristics of model problem 4, case b[a]

Material Assignment	
Region	Material[b]
Fuel region	Detailed basket with 5 fuel assemblies (See Figs A 5 and A 6) Voids totally filled with water (T = 20°C, ρ = 1 0 g/cm^3
Top fitting	1 4541, ρ = 1 01 g/cm^3
Bottom fitting	1 4541, ρ = 1 01 g/cm^3
Sidewall	1 4541
Cask bottom	1 4541
Cask lid	1 4313
Cooling fins	See Fig A 3
Neutron shield	Polyethylene Location as shown in Fig A 1

Source Description	
Source characteristic	Volume distributed fixed source
Total source strength	1 0 × 10^9 n/s 5 0 ×10^{16} g/s (Subcritical neutron multiplication not to be taken into account)
Energy distribution	See Table A 19
Spatial distribution	Constant in the active zone of fuel rod, zero otherwise

[a]For dimensions, see Table A 14
[b]See Table A 18

MODEL PROBLEM 5
CYLINDRICAL IRON CASK WITH ADDITIONAL NEUTRON SHIELD SOURCE TO BE CALCULATED BY THE USER

Model problem 5 is the starting point of a new phase of the shielding benchmark problem dealing with source term related problems It is only a first proposal to start the discussion The experiences from the first (geometrical) problems and the particular requests of the participants should lead to adequate modifications to the following model problems

Model problem 5 consists of a cylindrical iron cask with detailed construction of a basket including five fuel assembly positions Additional neutron shield is added as referred to for model problem 2, case a For the sake of simplicity, cooling fins are omitted Instead of a predefined source, the irradiation history of the fuel assemblies is given, including all necessary operational reactor data The burnup along the active zone of the fuel rods is assumed to be axially varying Activation of construction steels in the neutron flux of the reactor is to be neglected

A description of the model characteristics is given in Table A 12 Basket and fuel assembly are described in Tables A 15 and A 16, respectively

Table A 12 Characteristics of model problem 5[a] [b]

Material Assignment	
Region	Material[c]
Source region	Detailed basket (see Fig A 6) 5 fuel assemblies (see Fig A 5)
Sidewall	Cast iron
Cask bottom	Cast iron
Cask lid	1 4313
Cooling fins	None
Neutron shield	Polyethylene Location as shown in Fig A 1

[a]For dimensions, see Table A 14

[b]Source to be calculated by the participants using composition of fresh UO_2 fuel, irradiation history, reactor data, and axial burnup variation, as listed in Table A 17

[c]See Table A 18

MODEL PROBLEM 6
AS MODEL PROBLEM 5 USING MIXED OXIDE FUEL

Model problem 6 is identical with model problem 5 except that the fuel to be irradiated is assumed to be mixed oxide fuel as referred to in Table A 17 A full description of the model characteristics is provided in Table A 13

Table A 13 Characteristics of model problem 6[a] [b]

Region	Material Assignment Material[c]
Source region	Detailed basket (see Fig A 6) 5 fuel assemblies (see Fig A 5)
Sidewall	Cast iron
Cask bottom	Cast iron
Cask lid	1 4313
Cooling fins	None
Neutron shield	Polyethylene Location as shown in Fig A 1

[a]For dimensions, see Table A 14

[b]Source to be calculated by the participants using composition of fresh MOX fuel, irradiation history, reactor data, and axial burnup variation, as listed in Table A 17

[c]See Table A 18

TABLES AND FIGURES OF GENERAL INTEREST

Table A 14 Dimensions of cask body

Cavity (circular cross section)	
Diameter	80 cm
Height	450 cm
Cask body (circular cross section)	
Outer diameter	
without cooling fins	156 cm
including cooling fins	180 cm
Total height	530 cm
Thickness of sidewall	38 cm
Thickness of bottom	38 cm
Thickness of lid	42 cm
Azimuthal cooling fins	
Number	35
Height	12 cm
Top width	2 cm
Bottom width	5 cm
Spacing	13 cm
Location	Midplane of the first fin on the top level of cask cavity

Table A 15 Characteristics of basket

Number of fuel assembly positions	5
Material	1 4541
Total weight	1043 kg
Total height	440 cm
Thickness of structure sheets	1 0 cm
Basket phase	None
Position of basket inside the cask	Resting on the cask base
Position of fuel assemblies inside the basket	Resting on the cask base centrally positioned within the compartments

Table A 16 Characteristics of model fuel assembly[a] [b]

Total assembly length	445 cm
Width over flats	23 0 cm
Total rod length	393 cm
Length of active zone	342 cm
lower rod plug	1 8 cm
bottom expansion space	31 4 cm
top expansion space	16 0 cm
upper rod plug	1 8 cm
Height of bottom fitting	23 0 cm
top fitting	27 0 cm
Void between bottom fitting and rod	1 0 cm
Void between top fitting and rod	1 0 cm
Total number of rod positions	225
fuel rods	210
control rods	15
Pitch (square lattice)	1 53 cm
Pellet outer diameter	0 969 cm
Cladding inner diameter	1 00 cm
outer diameter	1 15 cm
Guide tube inner diameter	1 25 cm
outer diameter	1 40 cm

Materials and weights per assembly

	Material[c]	Weight/Assembly (kg)
Fuel	UO_2	513 7
Fuel cladding	Zr 4	135 9
Guide tube	Zr 4	11 9
Lower rod plug	1 4541	0 74
Upper rod plug	1 4541	0 74
Expansion spaces	Void	—
Bottom fitting[d]	1 4541	12 3
Top fitting[d]	1 4541	14 4

[a] As used in model problems 4–6

[b] For further details, see Fig A 5

[c] Material composition listed in Table A 18

[d] For the first step, the fitting mass should be homogenized over the fitting length (effective steel density $\rho = 1\ 01\ g/cm^3$)

Table A 17 Composition of fresh fuel of model assembly[a] [b]

Isotope	UO_2 fuel (wt %)	MOX fuel (wt %)
U 234	0 01	0 01
U 235	2 86	0 59
U 236	0 12	0 10
U 238	85 15	83 95
Pu 238	–	0 01
Pu 239	–	2 70
Pu 240	–	0 64
Pu 241	–	0 12
Pu 242	–	0 02
O	rest	rest

Irradiation History

Time (days)	Specific power (kW/kg hevimet)	Burnup (MWd/kg hevimet)
300	32 0	9 6
40	0 0	9 6
300	26 0	17 4
40	0 0	17 4
300	38 0	28 8
40	0 0	28 8
300	37 3	40 0
Cooling time	2 y	

Axial Burnup Distribution

Rod position (cm) From	To	Peaking[d]	Rod position (cm) From	To	Peaking[d]
0	10	0 42	170	180	1 23
10	20	0 60	180	190	1 21
20	30	0 78	190	200	1 19
30	40	0 92	200	210	1 16
40	50	1 04	210	220	1 14
50	60	1 15	220	230	1 11
60	70	1 21	230	240	1 08
70	80	1 27	240	250	1 04
80	90	1 29	250	260	1 00
90	100	1 33	260	270	0 94
100	110	1 33	270	280	0 88
110	120	1 32	280	290	0 78
120	130	1 31	290	300	0 68
130	140	1 29	300	310	0 56
140	150	1 28	310	320	0 44
150	160	1 26	320	330	0 31
160	170	1 25	330	342	0 18

As used in model problems and 6

[b] Dimensions materials and weights as specified in Table A 16

[c] Operational data of model reactor coolant pressure 160 bar average temperature 300 C average boron content 450 ppm

[d] Defined as local burnup/average burnup

Table A 18 Composition of materials used

Material	Total density (g/cm^3)	Element	Content (wt %)
1 4541	7 8	Mn	2 0
		Cr	18 0
		Ni	10 0
		Fe	rest
1 4313	7 7	Mn	1 5
		Cr	12 5
		Ni	4 0
		Fe	rest
Cast iron	7 0	C	3 25
		Si	1 4
		Ni	1 1
		Fe	rest
Polyethylene	0 91	C	85 6
		H	14 4
Epoxi cast resin	1 25	C	76 3
		H	6 7
		O	17 0
Zr 4	6 5	Zr	97 9
		Sn	1 6
		Fe	0 5
Homogeneous source (dry)	1 97	U 235	1 6
		U 238	49 1
		O	6 1
		Zr 4	16 6
		1 4541	26 6
Homogeneous source (wet)	2 81	U 235	1 1
		U 238	34 4
		O	4 3
		Zr 4	11 6
		1 4541	18 6
		water	30 0

Table A 19 Energy spectrum of neutron and gamma radiation source

Neutrons – continuous spectrum according to following formula

$$s(E) = A \exp(B\,E) \quad \sinh(C\,E)^{\frac{1}{2}}$$

A = 0 451
B = 1 035
C = 2 29

Gammas – discrete lines according to following

Energy (MeV)	Source strength (s^{-1})
0 6	2 53 E16[a]
0 7	2 32 E16
1 0	6 95 E14
1 3	5 50 E14
1 7	6 15 E12
2 1	2 70 E14
2 4	2 54 E12
2 8	1 32 E12

[a]Read as $2\,53 \times 10^{16}$

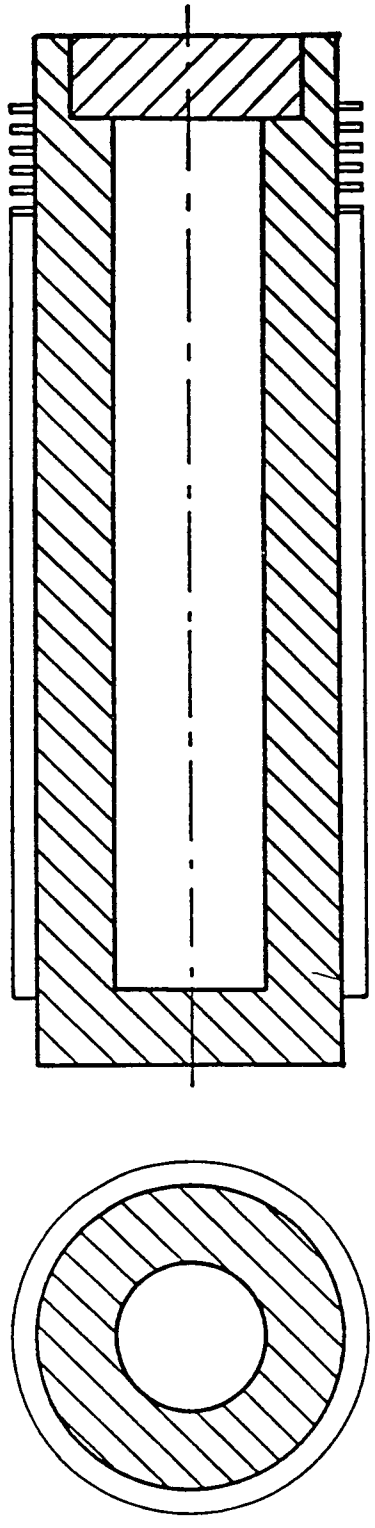

Fig A 7 Cross section view of prototypic cask

INTERNAL DISTRIBUTION

1 C W Alexander
2 S M Bowman
3–7 M C Brady
8–12 B L Broadhead
13 J A Bucholz
14 S N Cramer
15 H L Dodds
16 H R Dyer
17 M B Emmett
18 W W Engle
19 D E Fields
20 N M Greene
21 O W Hermann
22 C M Hopper
23 D T Ingersoll
24 W C Jordan
25 F B K Kam
26 B L Kirk
27 S B Ludwig
28 A P Malinauskas
29 K J Notz
30 J V Pace
31 C V Parks
32 L M Petrie
33 R T Primm
34 R R Rawl
35 J P Renier
36 W A Rhoades
37 J W Roddy
38 R W Roussin
39 T H Row
40 J C Ryman
41 C H Shappert
42 L B Shappert
43 C O Slater
44 J S Tang
45 D K Trubey
46 R M Westfall
47 G E Whitesides/R P Leinius
48 R Q Wright
49–50 Laboratory Records Department
51 Laboratory Records, ORNL–RC
52 Document Reference Section
53 Central Research Library
54 ORNL Patent Section

EXTERNAL DISTRIBUTION

55 A F Avery, AEE Winfrith, Reactor Physics Division, Bldg B 21, Dorchester, GB Dorset DT2 8DH, United Kingdom
56 L Ball, U S Department of Energy, EG&G Idaho, P O Box 1625, Idaho Falls, ID 83415
57 J Boshoven, GA Technologies, Inc , P O Box 85608, San Diego, CA 92186 9784
58 R Chapman, U S Department of Energy, EG&G Idaho, P O Box 1625, Idaho Falls, ID 83415
59 R Collier, U S Department of Energy Oak Ridge Operations Office, P O Box 2001, Oak Ridge, TN 37831
60 J M Creer, Battelle Pacific Northwest Laboratory, P O Box 999, Richland, WA 99352
61 W Danker, Office of Civilian Radioactive Waste Management, U S Department of Energy, Washington, DC 20545
62 R K Disney, Westinghouse Electric Corp , P O Box 158, Madison, PA 15663
63 Division of Engineering, Mathematics and Geosciences, U S Department of Energy, Washington, DC 20545
64 E Easton, Transportation Branch, Office of Nuclear Material Safety & Safeguards, U S Nuclear Regulatory Commission, MS WF1, Washington, DC 20555

65 F P Falci, Manager, Nuclear Materials Transportation R&D, U S Department of Energy, EM 51, Washington, DC 20545
66 L Fischer, Lawrence Livermore National Laboratory, P O Box 808, Livermore, CA 94550
67 M Fisher, U S Department of Energy, 785 DOE Place, Idaho Falls, ID 83402
68 W M Frei, Office of Civilian Radioactive Waste Management, U S Department of Energy, RW 231, Washington, DC 20545
69 M Garcia, Transportation Branch, Office of Nuclear Material Safety & Safeguards, U S Nuclear Regulatory Commission, MS WF1, Washington, DC 20555
70 G W Gardes, Transportation Branch, Office of Nuclear Material Safety & Safeguards, U S Nuclear Regulatory Commission, MS WF1, Washington, DC 20555
71 H Geiser, Wissenschaftlich Technische Ingenieurberatung GMBH, Mozartstrasse 13, 5177 Titz Rodingen, Federal Republic of Germany
72 C Gertz, U S Department of Energy, Nevada Operations Office, Waste Project Office, P O Box 98518, Las Vegas, NV 89193
73 A U Gewehr, Gesellschaft fur Reaktorsicherheit, Forschunsselaende, D 8046 Garching bei Munchen, Federal Republic of Germany
74–78 R E Glass, Sandia National Laboratories, Division 6322, P O Box 5800, Albuquerque, NM 87185
79 G Gualdrini, ENEA TIB/FICS, C R E "E Clementel," Via Mazzini, 2, I 40139 Bologna, Italy
80 L A Hassler, Babcock and Wilcox, 3315 Old Forest Road, P O Box 10935, Lynchburg, VA 24506 0935
81 C Heeb, Battelle Pacific Northwest Laboratory, P O Box 999, Richland, WA 99352
82 J S Hendricks, Los Alamos National Laboratory, P O Box 1663, Los Alamos, NM 87545
83 G F Hohnstreiter, Sandia National Laboratories, Division 6322, P O Box 5800 Albuquerque NM 87185
84 J E Hoogenboom, Delft University Technology, Mekelweg 15, 2629JB Delft, The Netherlands
85 J F Jaeger, Eidgenoessisches Institut fur Reaktorforschung, CH 5303 Wuerenlingen, Switzerland
86 U Jenquin, Battelle Pacific Northwest Laboratory, P O Box 999, Richland, WA 99352
87 M Jenson, U S Department of Energy, EG&G Idaho, P O Box 1625, Idaho Falls, ID 83415
88 C Kouts, Office of Civilian Radioactive Waste Management, U S Department of Energy, Washington, DC 20545
89 W Lake, Office of Civilian Radioactive Waste Management, U S Department of Energy, RW 33, Washington, DC 20545
90 R Lambert, EPRI, P O Box 10412, Palo Alto, CA 94303
91 W C Lattin, U S Department of Energy, Idaho Operations Office Idaho Falls, ID 83402
92 J F Leonard, U S Department of Energy, MS EH 321, Washington, DC 20545
93 A Luksic, Battelle Pacific Northwest Laboratory, P O Box 999, Richland, WA 99352

94 R E Luna, Sandia National Laboratories, Division 6320, P O Box 5800, Albuquerque, NM 87185
95 C Marotta, Private Consultant, 1504 Columbia Ave , Rockville, MD
96 M Mason, Transnuclear, Two Skyline Drive, Hawthorne, NY 10532 2120
97 N B McLeod, E R Johnson Associates, 10461 White Granite Drive, Oakton, VA 22124
98 W Mings, U S Department of Energy, 785 DOE Place, Idaho Falls, ID 83402
99 N Moon, U S Department of Energy, Office of Civilian Radioactive Waste Management, RW 231, Washington, DC 20545
100 T Nguyen, U S Department of Energy, Office of Civilian Radioactive Waste Management, RW 233, Washington, DC 20545
101 Office of Assistant Manager, Energy Research and Development, U S Department of Energy, Oak Ridge Operations, P O Box 2002, Oak Ridge, TN 37831
102 N L Osgood, Transportation Branch, Office of Nuclear Material Safety & Safeguards, U S Nuclear Regulatory Commission, MS WF1, Washington, DC 20555
103 O Ozer, EPRI, P O Box 10412, Palo Alto, CA 94303
104 R W Peterson, Battelle Columbus Laboratories, 505 King Avenue, Columbus, OH 43201
105 F Prohammer, Argonne National Laboratory, 9700 S Cass Avenue, Argonne, IL 60439
106 A Renard, Belgonucleaire, 25 rue du Champ de Mars, B 1050, Brussels, Belgium
107 J P Roberts, Office of Nuclear Material Safety & Safeguards, U S Nuclear Regulatory Commission, MS WF1, Washington, DC 20555
108 J N Rogers, Division 8324, Sandia National Laboratories, Livermore, CA 94550
109 T L Sanders, Sandia National Laboratories, Division 6323, P O Box 5800, Albuquerque, NM 87185
110–114 E Sartori, NEA Data Bank, 91191 Gif sur Yvette Cedex, France
115 S Tanaka, Department of Reactor Engineering, JAERI, Tokai Mura, Naka gun, IBARAKI KEN 319 11, Japan
116 J Thornton, Duke Power Co , P O Box 33189, Charlotte, NC 28242
117 A H Wells, Nuclear Assurance Corporation, 5720 Peachtree Parkway, Norcross, GA 30092
118 W Weyer, Wissenschaftlich Technische, Ingenieurberatung GMBH, Mozartstrasse 13, 5177 Titz Rodingen, Federal Republic of Germany
119 B White, Transportation Branch, Office of Nuclear Material Safety & Safeguards, U S Nuclear Regulatory Commission, MS WF1, Washington, DC 20555
120 M L Williams, LSU Nuclear Science Center, Baton Rouge, LA 70803
121 R F Williams, EPRI, P O Box 10412, Palo Alto, CA 94303
122 C J Withee, Transportation Branch, Office of Nuclear Material Safety & Safeguards, U S Nuclear Regulatory Commission, MS WF1, Washington, DC 20555
123 H Worle, U S Department of Energy, EG&G Idaho, P O Box 1625, Idaho Falls, ID 83415
124 W Y Yoon, EG&G Idaho, P O Box 1625, Idaho Falls, ID 83415
125–134 Office of Scientific and Technical Information, U S Department of Energy, P O Box 62, Oak Ridge, TN 37831